



## **ALCONPAT International**

### **Founders members:**

Liana Arrieta de Bustillos – **Venezuela**  
Antonio Carmona Filho - **Brazil**  
Dante Domene – **Argentina**  
Manuel Fernández Cánovas – **Spain**  
José Calavera Ruiz – **Spain**  
Paulo Helene, **Brazil**

### **Board of Directors International:**

#### **President of Honor**

Angélica Ayala Piola, **Paraguay**

#### **President**

Carmen Andrade Perdriz, **Spain**

#### **Managing Director**

Pedro Castro Borges, **Mexico**

#### **Executive Secretary**

José Iván Escalante García, **Mexico**

#### **Technical Vice President**

Enio Pazini Figueiredo, **Brazil**

#### **Administrative Vice President**

Luis Álvarez Valencia, **Guatemala**

#### **Manager**

Paulo Helene, **Brazil**

## **Revista ALCONPAT**

### **Editor in Chief:**

Dr. Pedro Castro Borges  
Centro de Investigación y de Estudios Avanzados del Instituto  
Politécnico Nacional, Unidad Mérida (CINVESTAV IPN –  
Mérida)  
Merida, Yucatan, **Mexico**

### **Co-Editor in Chief:**

Dr. Fernando Branco  
IST - Universidad de Lisboa  
Lisboa, **Portugal**

### **Executive Editor:**

Dr. José Manuel Mendoza Rangel  
Universidad Autónoma de Nuevo León, Facultad de Ingeniería  
Civil  
Monterrey, Nuevo Leon, **Mexico**

### **Associate Editors:**

Dr. Manuel Fernandez Canovas Universidad  
Politécnica de Madrid. Madrid, **Spain**

Ing. Raúl Husni

Facultad de Ingeniería Universidad de Buenos Aires. Buenos  
Aires, **Argentina**

Dr. Paulo Roberto do Lago Helene  
Universidade de São Paulo.  
São Paulo, **Brazil**

Dr. José Iván Escalante García  
Centro de Investigación y de Estudios Avanzados del  
Instituto Politécnico Nacional (Unidad Saltillo) Saltillo,  
Coahuila, **Mexico**.

Dr. Mauricio López.  
Departamento de Ingeniería y Gestión de la Construcción,  
Escuela de Ingeniería,  
Pontificia Universidad Católica de Chile  
Santiago de Chile, **Chile**

Dra. Oladis Troconis de Rincón Centro de Estudios de  
Corrosión Universidad de Zulia  
Maracaibo, **Venezuela**

Dr. Fernando Branco Universidad  
Técnica de Lisboa  
Lisboa, **Portugal**

Dr. Pedro Garcés Terradillos  
Universidad de Alicante  
San Vicente, **Spain**

Dr. Andrés Antonio Torres Acosta  
Instituto Mexicano del Transporte / Universidad Marista de  
Querétaro  
Querétaro, **Mexico**

Dr. Luiz Fernández Luco  
Universidad de Buenos Aires – Facultad de Ingeniería –  
INTECIN  
Buenos Aires, **Argentina**

**JOURNAL OF THE LATIN-AMERICAN ASSOCIATION  
OF QUALITY CONTROL, PATHOLOGY AND RECOVERY  
OF CONSTRUCTION**

<http://www.revistaalconpat.org>

We present the third issue of the ninth year of the ALCONPAT journal with great satisfaction.

The aim of the journal is to publish case studies within the scope of the Association, namely quality control, pathology and recovery of constructions, including basic and applied research, reviews and documentary research.

This V9N3 issue begins with a work from **Mexico**, where Jorge Uruchurtu Chavarín et. al. evaluated the effect of the Nopal mucilage on the electrochemical properties of concrete. Three concentrations of this additive were designed with a Nopal-water ratio of 1: 1, 1: 2 and 1: 3. Compression tests were performed after 28 days of curing. The samples were evaluated for 270 days through various electrochemical techniques such as: open circuit potential (OCP), electrochemical noise (EN) and linear polarization resistance (LPR). Their results indicated a decrease in compressive strength with an increase in mucilage concentration. The onset of steel corrosion was delayed, and the corrosion rate was lower for samples with Nopal mucilage. The preservation of this additive can be a challenge to analyze, but its use has a great impact on concrete and the environment.

In the second work, from **Brasil**, Mateus Henrique de Souza and Rafael Alves de Souza developed and analyzed polymeric repair mortars composed of vinyl copolymer, PVA (polyvinyl acetate) and SBR (styrene-butadiene). They performed tests for the determination of compression and tensile strengths by diametral compression. In addition, they determined the adherent strength between the repair and the concrete by means of a tensile test by diametral compression. Among the materials tested, it was noted that the material modified by SBR had the best performance, especially in relation to adhesion to concrete. In general, the results showed that the studied mortars modified by the polymers can meet the function of repair material.

The third work of this issue is from **México**, where R. Visairo-Méndez et. al. determined whether the durability index is affected by three sizes of specimens evaluated for repair mortar. They made 5 x 5 cm cubes, 5 x 10 cm and 10 x 20 cm cylinders for each type of mortar. They found that certain indices (WER, TVC and CS) do not depend on the geometry of the specimen. However, the UPV results showed a difference between cubes and cylinders of 10 x 20 cm greater than 17.5%. The results of  $\epsilon_{\text{eff}}$  presented a very interesting difference between the cubes and the 5 x 10 cm cylinders. The authors recommended restricting the height of specimens to a standard value.

In the fourth article, from **Brasil**, Fernando Júnior Resende Mascarenhas and Roberto Chust Carvalho analyzed the fatigue service life of the longitudinal reinforcement in reinforced concrete bridge beams considering the real number of heavy vehicles with 2 to 6 axles on a road section in the state of São Paulo, Brazil. They used theoretical models in a structural system of bridges with two beams doubly supported in sections of 10, 15 and 20 meters. For the determination of the efforts they used the Ftool software and in the estimation of the service life to fatigue the accumulated damage. At the end, it was verified that the lifetime to fatigue of the longitudinal reinforcement varies according to the size of the section, being that in the three analyzed bridges the service life to fatigue is less than 30 years.

The fifth work, by Francisco Roger Carneiro Ribeiro et. al, from **Brazil** present an application of the methodology of the GUT Matrix (Gravity, Urgency, Tendency) in the analysis of the pathological manifestations in buildings, having as examples three historical constructions of the historical center of Sobral, Ceará, Brazil. The investigation was conducted with on-site inspections, photographic registration, mapping of damages and application of the method. The results generated the priority graphs that represent the order for the treatment of each damage in each building. It was possible to conclude that the applied method can be used as an important building maintenance management tool through the prioritization of resolution of the most serious problems, and directly contributes to the preservation and security of historical heritage.

The sixth work in this issue is written by Alberto Hernández Oroza and Rafael González Hernández from **Cuba**, who make a diagnosis of the deterioration of a reinforced concrete building located in Old Havana, Cuba, built in 1906. Due to the years of exploitation and lack of maintenance, the property presents concrete detachments and cracks in almost all structural elements. To evaluate the service life, they carried out studies of apparent resistivity of concrete, chemical tests to quantify the levels of free chloride and sulfate, potential tests, sectional losses of the bars, extractions of concrete specimens and visual analysis of the present lesions. The obtained results showed that although the property shows an advanced deterioration, it can be rehabilitated being possible to extend its service life.

The article that closes this edition is from **Brazil**, where Lara Monalisa Alves dos Santos et. al., present the characteristics and evaluation of a roof system of one of the buildings of the University of Brasília - DF. They analyzed the main anomalies in the roof systems and systematized the intervention priority, with the purpose of correlating it with the corrective measures. The limiting factors for the inspection of the structures were accessibility, as well as the lack of intervention projects. The results obtained indicated that the main anomalies found in the systems are related to the lack of maintenance. The study also brings, as a contribution, indications and technical recommendations for the resolution of situations.

We are confident that the articles in this issue will constitute an important reference for those readers involved with questions of evaluations and characterizations of materials, elements and structures. We thank the authors participating in this issue for their willingness and effort to present quality articles and meet the established times.

On behalf of the Editorial Board

A handwritten signature in black ink, appearing to read 'Pedro Castro Borges', written over a circular stamp or mark.

Pedro Castro Borges  
Editor in Chief



## CONTENT

### Página

### BASIC RESEARCH

**Y. Díaz-Blanco, C. Menchaca-Campos, C. I. Rocabrundo-Valdés, J. Uruchurtu-Chavarín:** Natural additive (nopal mucilage) on the electrochemical properties of concrete reinforcing steel. 260 - 276

**M. H. de Souza, R. A. de Souza:** Analysis of compost repair mortars by vinyl copolymer, PVA, and SBR. 277 – 287

**R. Visairo-Méndez. A. A. Torres-Acosta. R. Alvarado-Cárdenas:** Specimen size effect on the durability indexes determination for cement-based materials. 288 - 302

### APPLIED RESEARCH

**F. Jr. R. Mascarenhas. R. Chust Carvalho:** Fatigue service life of longitudinal reinforcement bars of reinforced concrete beams based on the real heavy traffic. 303 - 319

**I. C. Braga, F. S. Brandão, F. R. C. Ribeiro, A. G. Diógenes:** Application of GUT Matrix in the assessment of pathological manifestations in heritage constructions. 320 - 335

### STUDY CASES

**A. H. Oroza, R. G. Hernández:** Diagnostic of damage in a building of the early twentieth century in Havana. Case study. 336 - 349

**L. M. A. Santos, L. F. Andrade, C. H. A. F. Pereira:** Inspection and evaluation of roofing systems: a case study. 350 - 363

## Natural additive (nopal mucilage) on the electrochemical properties of concrete reinforcing steel

Y. Díaz-Blanco<sup>1</sup> , C. Menchaca-Campos<sup>1</sup> , C. I. Rocabruno-Valdés<sup>2</sup> ,  
J. Uruchurtu-Chavarín<sup>1\*</sup> 

\*Contact author: [juch25@uaem.mx](mailto:juch25@uaem.mx)

DOI: <http://dx.doi.org/10.21041/ra.v9i3.429>

Reception: 29/07/2019 | Acceptance: 21/08/2019 | Publication: 30/08/2019

### ABSTRACT

In this investigation the effect of Nopal mucilage on the electrochemical properties of concrete was evaluated. Three concentrations of this additive were designed with a Nopal-water ratio of 1:1, 1:2 and 1:3. Compressive tests were performed after 28 days of curing. Specimens were evaluated for 270 days through various electrochemical techniques such as: Open Circuit Potential (OCP), Electrochemical Noise (EN) and Linear Polarization Resistance (LPR). Results indicate a decrease in compressive resistance in samples with Nopal mucilage at 28 days. The onset of steel corrosion was delayed and the corrosion rate was lower for samples with Nopal mucilage. The conservation and storage of this additive before being used in concrete can be a challenge to analyze.

**Keywords:** Nopal mucilage; reinforcing concrete; electrochemical techniques; corrosion.

**Cite as:** Díaz-Blanco, Y., Menchaca-Campos, C., Rocabruno-Valdés, C. I., Uruchurtu-Chavarín J. (2019), "Natural Additive (Nopal Mucilage) on the Electrochemical Properties of Concrete Reinforcing Steel", Revista ALCONPAT, 9 (3), pp. 260 – 276, DOI: <http://dx.doi.org/10.21041/ra.v9i3.429>

<sup>1</sup> Centro de Investigación en Ingeniería y Ciencias Aplicadas (CIICAP), Instituto de Investigación en Ciencias Básicas y Aplicadas (IICBA), Universidad Autónoma del Estado de Morelos, Cuernavaca, México.

<sup>2</sup> Centro Nacional de Investigación y Desarrollo Tecnológico (CENIDET), Tecnológico Nacional de México (TecNM), Cuernavaca, México.

### Legal Information

Revista ALCONPAT is a quarterly publication by the Asociación Latinoamericana de Control de Calidad, Patología y Recuperación de la Construcción, Internacional, A.C., Km. 6 antigua carretera a Progreso, Mérida, Yucatán, 97310, Tel.5219997385893, [alconpat.int@gmail.com](mailto:alconpat.int@gmail.com), Website: [www.alconpat.org](http://www.alconpat.org)

Responsible editor: Pedro Castro Borges, Ph.D. Reservation of rights for exclusive use No.04-2013-011717330300-203, and ISSN 2007-6835, both granted by the Instituto Nacional de Derecho de Autor. Responsible for the last update of this issue, Informatics Unit ALCONPAT, Elizabeth Sabido Maldonado, Km. 6, antigua carretera a Progreso, Mérida, Yucatán, C.P. 97310.

The views of the authors do not necessarily reflect the position of the editor.

The total or partial reproduction of the contents and images of the publication is strictly prohibited without the previous authorization of ALCONPAT Internacional A.C.

Any dispute, including the replies of the authors, will be published in the second issue of 2020 provided that the information is received before the closing of the first issue of 2020.

## **Influencia de un aditivo natural (mucílago de nopal) en las propiedades electroquímicas del acero de refuerzo del concreto**

### **RESUMEN**

En esta investigación se evaluó el efecto del mucílago de Nopal sobre las propiedades electroquímicas del concreto. Se diseñaron tres concentraciones de este aditivo con una relación Nopal-agua de 1:1, 1:2 y 1:3. Las pruebas de compresión se realizaron a los 28 días de curado. Las muestras se evaluaron durante 270 días a través de diversas técnicas electroquímicas como: Potencial a Circuito Abierto (OCP), Ruido Electroquímico (EN) y Resistencia a la Polarización Lineal (LPR). Los resultados indican una disminución de la resistencia a la compresión en muestras con mucílago de Nopal a los 28 días. El inicio de la corrosión se retrasó y la velocidad de corrosión fue menor para las muestras con mucílago de Nopal. La conservación y el almacenamiento de este aditivo antes de usarse en el concreto puede ser un desafío para analizar.

**Palabras clave:** mucílago de nopal; hormigón armado; técnicas electroquímicas; corrosión.

## **Influência de um aditivo natural (mucilagem nopal) nas propriedades eletroquímicas do aço de reforço de concreto**

### **RESUMO**

Nesta investigação, avaliou-se o efeito da mucilagem de Nopal sobre as propriedades eletroquímicas do concreto. Três concentrações deste aditivo foram desenhadas com uma relação Nopal-água de 1: 1, 1: 2 e 1: 3. Os testes de compressão foram realizados após 28 dias de cura. As amostras foram avaliadas por 270 dias através de várias técnicas eletroquímicas, tais como: Potencial de Circuito Aberto (OCP), Ruído Eletroquímico (EN) e Resistência à Polarização Linear (LPR). Os resultados indicam uma diminuição na resistência à compressão em amostras com mucilagem de Nopal aos 28 dias. O início da corrosão do aço foi retardado e a taxa de corrosão foi menor nas amostras com mucilagem de Nopal. A preservação e armazenamento deste aditivo antes de ser usado em concreto pode ser um desafio para analisar.

**Palavras-chave:** Mucilagem de pera espinhosa; concreto armado; técnicas eletroquímicas; corrosão.

## **1. INTRODUCTION.**

Corrosion of reinforcing steel in concrete structures exposed to environments contaminated with chlorides is the most common cause of premature deterioration (Hansson, 1984; Pech-Canul and Castro, 2002). The above leads to large economic losses as well as the reduction of the useful life of the structures (Valipour et. al., 2014). In recent decades, numerous investigations have been carried out in this field to analyze the causes and characteristics of this phenomenon and provide solutions to this important pathology of concrete. Normally a good quality concrete keeps the steel protected due to its high alkalinity, in addition the concrete cover acts as a physical barrier that prevents the access of aggressive agents from the surrounding environment (Hansson, 1984). These properties are lost at an early age, so the use of natural materials or additives that improve the properties of concrete and extend its useful life is a very important aspect to consider.

Currently the additives form an integral part of the components in cement-based mixtures (Ramírez-Arellanes et. al., 2012). However, despite the effectiveness of synthetic additives to improve the different properties of concrete, these are highly polluting. In that sense, the

investigation of natural additives from plants and their use in concrete are becoming more and more relevant.

The *Opuntia* genus belongs to the Cactaceae family and is also known as cactus pear plant (Sáenz et. al., 2004). One of the main uses of the Cactaceae family is directly related to the production of mucilage. The stems and leaves secrete a viscous liquid, which is a gum or hydrocolloid, mainly composed of polysaccharides. Polysaccharides are composed of long chains of monosaccharide units, resulting in polymeric carbohydrate molecules (Zhang et.al., 2019). This complex carbohydrate has potential uses as an additive for several industrial products (Sáenz et. al., 2004). It has been used as a water purifier, as an additive in lime mortars to improve its adhesion, as well as an additive capable of modifying the properties in mortars both in the fresh and hardened state (León-Martínez et. al., 2010). Its use in concrete varies according to the properties to be modified, such as: workability, aspects such as paste homogeneity, as well as the setting time of the mixture (Zhang et. al., 2019). Also, it is considered a potential source of industrial hydrocolloids with many application in the food industry (Cárdenas et. al., 1997; Sáenz et. al., 2004; León-Martínez et. al., 2010).

*Opuntia ficus-indica*, is a native plant of Mexico that grows in arid and semi-arid areas. Currently its cultivation for commercial reasons has spread to countries such as Italy, the United States, Chile and Argentina (Torres-Acosta, 2007; Martínez-Molina et. al., 2015). In Mexico, this plant is called Nopal and is a great source of food for the general population, as well as for livestock. Since ancient times, the gel produced by this cactus has been used to paint and cover adobe walls, as well as for the maintenance and preservation of churches and historic buildings in Latin America (Chandra et. al., 1998; Torres-Acosta and Martínez-Madrid, 2005; Torres-Acosta, 2007).

Different studies agree that the compounds present in the Nopal mucilage are very varied, being able to find proteins, as well as different types and compositions of polysaccharides (Chandra et. al., 1998). In general, the carbohydrate composition in the mucilage contains varying proportions of l-arabinose, d-galactose, l-rhamnose and d-xylose as the main sugar units (León-Martínez et. al., 2011). Some natural polymers are capable of modifying specific properties of cementitious materials during construction (Peschard et al., 2004). Some properties of cement mortars in the fresh state can be improved with the addition of water-soluble polymers. The cement mixtures modified with these polymers have a high water retention than ordinary mortars. This behavior is mainly due to the hydrophilic parts of the polymers fixing the water molecules in the fresh mixture, preventing drying by evaporation and absorption in the surrounding porous material (Knapen and Van Gemert, 2009).

Ramírez-Arellanes et. al. (Ramírez-Arellanes et. al., 2012) analyzed the effect of Nopal mucilage in cement paste; determining that the setting times increased with the addition of this natural additive. Also, they reported that there were changes in microscopy of mixtures with mucilage. Other authors report that the sizes of calcium hydroxide crystals are reduced (Chandra et. al., 1998) and in the presence of water soluble polymers the microstructure of the concrete is modified (Peschard et. al., 2004; Knapen and Van Gemert, 2009).

Other preliminary findings suggest that small concentrations of Nopal gel could be useful as a corrosion inhibitor for reinforcing steel in chloride-contaminated mortar. There was an improvement in the durability of the Nopal gel specimens, due to an increase in polarization resistance and a decrease in corrosion-induced cracking (Martínez-Molina et. al., 2015).

This present research focuses on the study of Nopal mucilage as a modifying additive for the electrochemical properties of reinforced concrete. In that regard, the objective of this investigation is to provide a solution that minimizes the damages caused by the corrosion of the reinforcing steel, this being the pathology that most affects the reinforced concrete structures. An important parameter of the analysis is to determine the corrosion rate of the reinforcing steel with the addition of different concentrations of Nopal mucilage and analyze its effect over time.



## 2. EXPERIMENTAL PROCEDURE.

### 2.1 Nopal mucilage extraction.

The cactus leaves that were used had a fresh state of preservation and were free of spines. To proceed with the extraction of the Nopal mucilage, the following procedure was carried out: i) the cleaning of the leaves was carried out to eliminate traces of dust and other residues, ii) the leaves were cut into pieces of 1cm x 1cm to extract the gel as much as possible and iii) the pieces were mixed with water to obtain three concentrations of mucilage in a Nopal-water weight ratio of 1: 1, 1: 2 and 1: 3, seen on Figure 1.

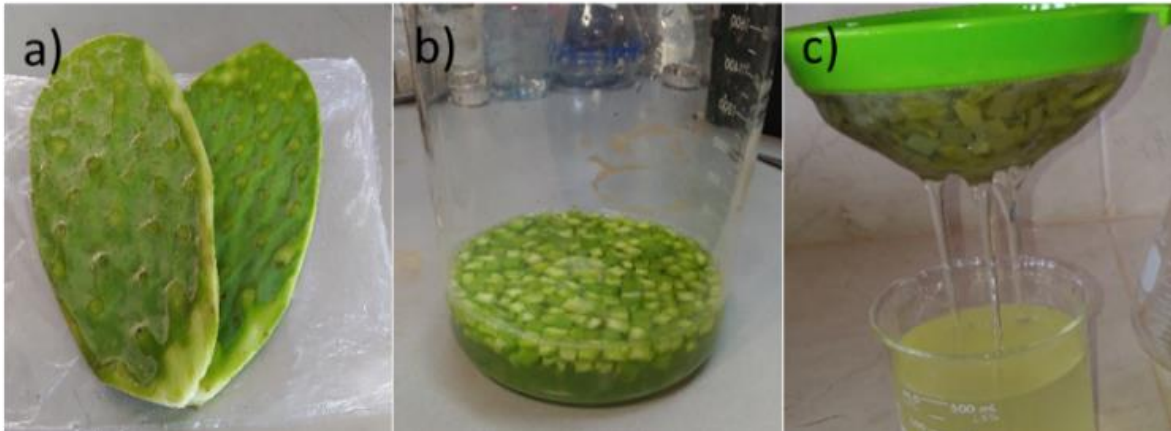


Figure 1. a) Fresh cactus leaves, b) Prickly pear cactus mixed with water y c) Filtration process of Nopal mucilage.

The extraction of the Nopal mucilage was carried out by two methods, which are described below. Maceration at room temperature, in which each Nopal mixture with water was allowed to macerate for 48 hours for later use in the concrete. After this time the solution began to acquire a darker tone and a certain smell of decomposition, as other authors affirm (Chandra et. al., 1998). The following extraction method was maceration applying temperature in this case the Nopal and water mixtures were placed on a grill applying a temperature of 95 degrees Celsius for 10 minutes. Then it was allowed to standstill for 24 hours, at which time the solution was incorporated into the concrete. In both extraction methods before incorporating the Nopal mucilage into the concrete the solution was filtered.

### 2.2 Design of concrete mixes.

The concrete mixes were designed using a CPC30R cement (Type II ASTM-C-150) taking into account a characteristic strength of 250 kg/cm<sup>2</sup>. The water/cement ratio used was 0.45 for each of the mixtures made. River sand was used as a fine aggregate and the coarse aggregate from crushed stone had a maximum size of 20 mm. The reinforcing steel formed by 3/8 inch grade 42 and the corrugated bars had no surface treatment. The proportions for concrete mixtures are shown in Table 1.

Table 1. Concrete mixture ratio for each cylindrical sample (CS) and prismatic sample (PS).

Materials	Amount of materials per sample													
	CO		CO+1-1N		CO+1-2N		CO+1-3N		CO+1-1NT		CO+1-2NT		CO+1-3NT	
	CS	PS	CS	PS	CS	PS	CS	PS	CS	PS	CS	PS	CS	PS
Cement (kg)	0.041	0.231	0.041	0.231	0.041	0.231	0.041	0.231	0.041	0.231	0.041	0.231	0.041	0.231
Sand (kg)	0.081	0.452	0.081	0.452	0.081	0.452	0.081	0.452	0.081	0.452	0.081	0.452	0.081	0.452
Gravel (kg)	0.127	0.711	0.127	0.711	0.127	0.711	0.127	0.711	0.127	0.711	0.127	0.711	0.127	0.711
Water (l)	0.019	0.105	-	-	-	-	-	-	-	-	-	-	-	-
Nopal mucilage (l)	-	-	0.019	0.105	0.019	0.105	0.019	0.105	0.019	0.105	0.019	0.105	0.019	0.105

The specimens were designed with a 30 mm of concrete cover between the edge of the bars and the sides of the cube. Therefore, the specimens were 7 cm wide, 10 cm long and 10 cm high, and the exposed area of the steel bars in contact with the concrete was 18 cm<sup>2</sup>, as seen in Figure 2. Each steel bar was coated with adhesive tape on the mortar-air interface as described by other authors (González et. al., 2004; Caré and Raharinaivo, 2007; Poursaee, 2010).

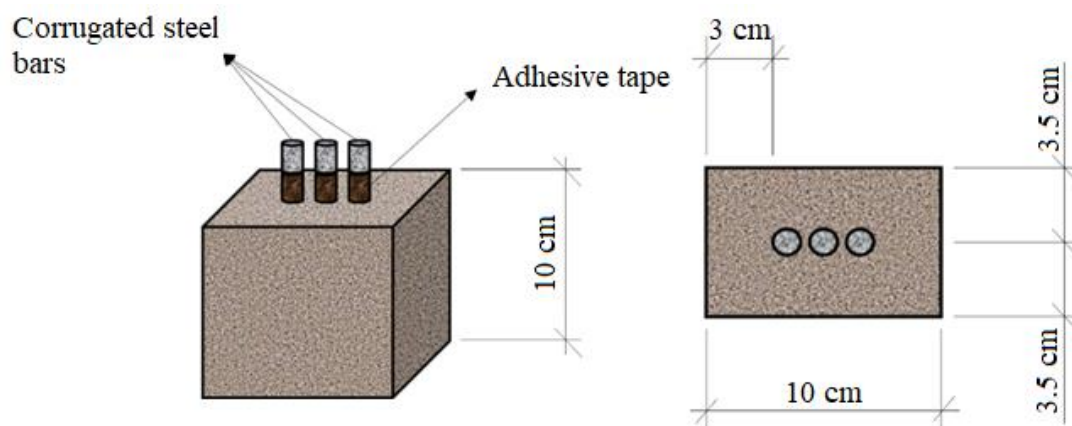


Figure 2. Dimensions of concrete samples.

The preparation of the mixtures was carried out at room temperature inside the laboratory. Once all the solid elements were mixed, the Nopal mucilage was added according to the concentration obtained. Only water was added to the control sample, in the rest of the specimens the water was replaced by the Nopal mucilage. After 24 hours of fabrication, the samples were placed in water for 28 days, time of which the curing of concrete was carried out. After that, they remained partially submerged for the rest of the test period in a 3% sodium chloride solution, simulating a marine environment. The distance between the upper edge of the samples and the solution was maintained around 2 cm.

The first electrochemical tests were started after 24 hours of mixing the materials and for the next 270 days. All tests were performed keeping the specimens in the curing solution at the beginning and then in the sodium chloride solution. The techniques used to analyze the electrochemical behavior of reinforcing steel were the following: Open Circuit Potential, Electrochemical Noise and Linear Polarization Resistance.

Table 2 shows the nomenclature used to identify each sample with the different concentrations of Nopal mucilage, as well as the control sample.

Table 2. Identification of the samples.

Samples	Nopal-water weight ratio	Extraction method	Nomenclature
1	----	No Nopal mucilage (CO)	CO
2	1:1	Maceration at room temperature (N)	CO+1-1N
3	1:2	Maceration at room temperature (N)	CO+1-2N
4	1:3	Maceration at room temperature (N)	CO+1-3N
5	1:1	Maceration applying temperature (NT)	CO+1-1NT
6	1:2	Maceration applying temperature (NT)	CO+1-2NT
7	1:3	Maceration applying temperature (NT)	CO+1-3NT

### 2.3 Compression resistance technique.

The Compression Resistance technique is one of the most widely used tools in the analysis of the mechanical properties of concrete. Three concrete samples were designed for each concentration of Nopal mucilage, including samples without mucilage. The compression resistance test was performed 28 days after the curing process of all specimens, while remaining wet. Cylindrical specimens were designed from PVC pipes with a height / diameter ratio equal to 2, with the following dimensions: 4.3 cm of diameter and 8.6 cm of height. The specimens were scaled, taking into account that in each step of this project it was ensured to guarantee the lowest consumption of energy and materials. The parameters were defined according to ASTM C39 (Dúran-Herrera et. al., 2012; Rahmani et. al., 2013).

### 2.4 Parameters of electrochemical techniques.

#### 2.4.1 Open circuit potential technique.

The Open Circuit Potential technique is one of the most widely used tools for the analysis of reinforced concrete structures (Morozov et. al., 2013). The measurement of Open Circuit Potential was carried out against a Saturated Calomel Electrode (SCE). In this case, a measurement of the steel electrodes of each specimen was made. The final value obtained was the average of the three measurements. The first reading was taken 24 hours after the samples were made, and weekly measurements were made for a period of 270 days. For this, a multimeter was used connecting one terminal to the working electrode and the other to the reference electrode of Calomel. To measure the Open Circuit Potential, the reference electrode was placed inside the curing solution and the saline solution, as close as possible to the working electrodes. It was taken into account that the tip of the calomel reference electrode was separated from the bottom of the solution container. Table 3 shows the ranges of corrosion potential values for reinforced concrete structures and the corrosion probability criteria according to ASTM C876 (Morris et. al., 2002; Pérez-Quiroz et. al., 2008).

Table 3. Corrosion probability criteria for reinforcing steel related to the measurement of Open Circuit Potential (OCP).

Open circuit potential (OCP) values (mV vs. SCE)	Corrosion probability criteria
> -125	10% risk of corrosion
-126 to -275	Intermediate corrosion risk
< -276	90% risk of corrosion

### 2.4.2 Electrochemical noise techniques.

Corrosion processes such as: generalized and localized corrosion, stress corrosion cracking, as well as passivation phenomena, generate spontaneous fluctuations in the electrode's free corrosion potential (Gusmano et. al., 1997). An ACM Instruments Auto ZRA potentiostat was used to analyze the electrochemical noise of all samples. The readings for each test were 1024 data with a sampling rate of one data per second. In addition, the standard method of analysis of three nominally identical electrodes was used (Cottis, 2001).

One of the most important advantages offered by this electrochemical technique is that its application does not imply any artificial alteration of the system during the test time (Legat et. al., 2004). A parameter widely used in the analysis of the electrochemical noise signal is noise resistance ( $R_n$ ), defined as the ratio of standard deviations of potential and current noise, according to equation (Bing et. al., 2007):

$$R_n = \frac{\sigma_v}{\sigma_i} \quad (1)$$

where,  $\sigma_v$  is the standard deviation of potential noise and  $\sigma_i$  is the standard deviation of current noise. A linear trend removal of the time series of potential and current was performed.

Some authors have analyzed the relationship between noise resistance ( $R_n$ ) and polarization resistance ( $R_p$ ), concluding that they can be considered equivalent for many systems (Aballe et. al., 2001; Girija et. al., 2007).

### 2.4.3 Linear polarization resistance technique.

The Linear Polarization Resistance technique is a very versatile tool frequently used for the electrochemical studies of reinforcement steel embedded in concrete (Andrade et. al., 2001). One of its main advantages is that it allows to determine the kinetics of the corrosive process. According to other studies, a voltage signal was applied in the range of  $\pm 20$  mV over the corrosion potential ( $E_{corr}$ ), a current signal being recorded as a response (Poursaee, 2010). For the measurement of the Linear Polarization Resistance a sweep rate of 10 mV/min was applied. In addition, the reference electrode and graphite counter electrode were placed inside the curing solution and saline solution. Both electrodes were placed next to each other and as close as possible to the working electrodes. The polarization resistance can be determined through the expression (2), established as the slope of the polarization curve around the corrosion potential,  $E_{corr}$  (Andrade and Alonso, 1996; Morris et al., 2002):

$$R_p = \frac{\Delta E}{\Delta I} \quad (2)$$

where  $R_p$  is the polarization resistance ( $\Omega$ ),  $\Delta I$  is change in current (A) and  $\Delta E$  is change in potential (V) (Poursaee, 2010). According to the equation (3) proposed by Stern-Geary, it is possible to determine the corrosion rate of the reinforcing steel through a constant of proportionality B. This equation states that the current density  $I_{corr}$  is inversely proportional to the  $R_p$  (Hansson, 1984; Morris et. al., 2002):

$$i_{corr} = \frac{B}{R_p} \quad (3)$$

The ranges of corrosion rate values in terms of the useful life of reinforcing steel in concrete are shown in Table 4 (Andrade and Alonso, 1996).

Table 4. Intervals of corrosion rate related to the degree of corrosion of the steel in the concrete in terms of useful life.

Corrosion current $I_{corr}(\mu A/cm^2)$	CR (mm/y)	Condition of the rebar
$I_{corr} < 0.1$	$< 0.001$	Negligible.
$I_{corr} 0.1 - 0.5$	0.001-0.005	Low to moderate corrosion.
$I_{corr} 0.5 - 1.0$	0.005-0.010	Moderate to high corrosion.
$I_{corr} > 1.0$	$> 0.010$	High corrosion rate.

From the  $I_{corr}$  values, the efficiency of the Nopal mucilage as a corrosion inhibitor of the reinforcing steel in concrete was determined, according to the following equation (Díaz-Cardenas et al., 2017):

$$I.E. (\%) = \left[ \frac{I_{corr} - I'_{corr}}{I_{corr}} \right] * 100 \quad (4)$$

where: I.E. is the efficiency of the inhibitor,  $I_{corr}$  is the corrosion current density ( $\mu A/cm^2$ ) without inhibitor and  $I'_{corr}$  is the corrosion current density ( $\mu A/cm^2$ ) with inhibitor.

### 3. RESULTS AND DISCUSSION.

#### 3.1 Compression strength.

Table 5 shows the average values of compressive strength after 28 days of concrete curing.

Table 5. Average values of compressive strength after 28 days.

Samples	Compressive strength (kg/cm <sup>2</sup> )
CO	248.9
CO+1-1N	223.5
CO+1-2N	234.9
CO+1-3N	246.5
CO+1-1NT	225.8
CO+1-2NT	234.6
CO+1-3NT	244.1

As can be seen, there are no significant differences in compression resistance values, regardless of the method of extracting the Nopal mucilage. On the other hand, as can be seen after 28 days, all samples with Nopal mucilage maintain compression resistance values lower than the control sample. This is due to the fact that the Nopal mucilage traps water and that decreases the hydration rate of the cement at early ages, due to the hydrophilic part of the polymers present in the mucilage fix the water molecules in the fresh mixture (Knapen and Van Gemert, 2009). For samples with a concentration 1-3 of Nopal mucilage, there was a decrease in resistance between 2.4 and 4.8 kg/cm<sup>2</sup>, however, for concentration 1-1 ratio of mucilage, the decrease in compression resistance remained between 23.3 and 25.4 kg/cm<sup>2</sup> respect to the control samples. Some authors describe a similar trend and show that the presence of polysaccharides in the mucilage solution are the main causes of this behavior (Chandra et. al., 1998). It is also known that Nopal mucilage as a natural additive in concrete is able to delay cement setting (Peschard et. al., 2004). However, according to Chandra et. al. (Chandra et. al., 1998) in the long term, the cactus mucilage favors the increase in compression resistance, exceeding the control sample values.

### 3.2 Open circuit potential.

The corrosion potential values for all samples with Nopal mucilage are detailed in Figure 3.

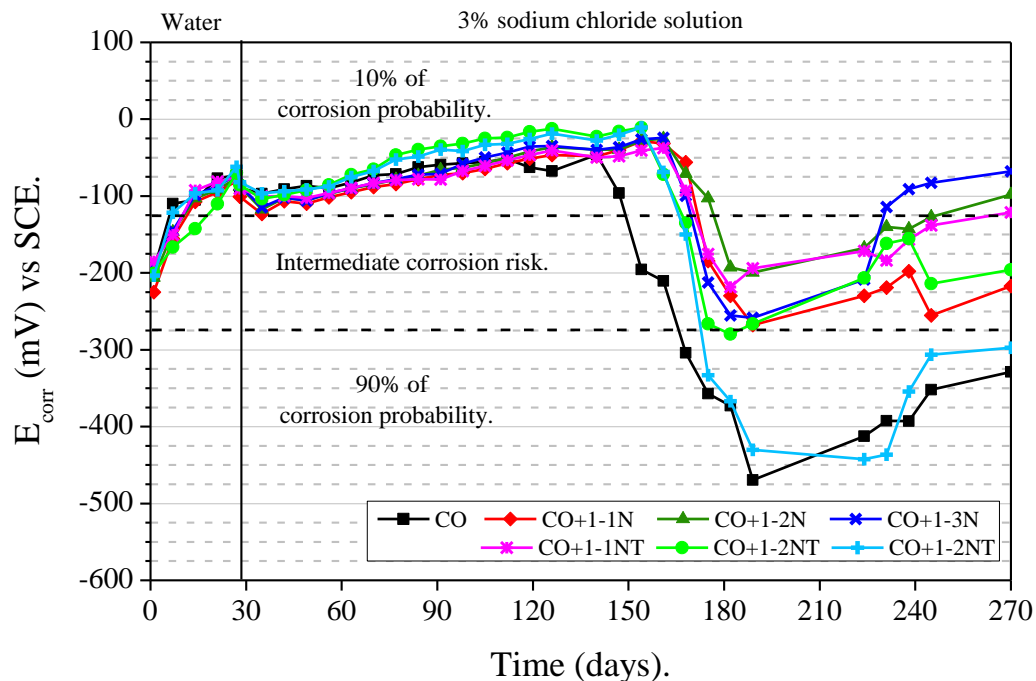


Figure 3. Behavior of corrosion potential values ( $E_{\text{corr}}$ ) with time.

During the concrete curing process, it is clear that the potential of all samples acquires very noble values, between -90 and -50 mV. These values remain in the range of a 10% probability of corrosion (Pérez-Quiroz et. al., 2008). The high alkalinity, as well as the presence of moisture and oxygen in the concrete pore network, are factors that influence these potential values. Under these conditions, the steel develops an oxides passive layer of compact and waterproof (Hansson, 1984). All samples with Nopal mucilage, have a drop in their values and reach the range of intermediate corrosion risk. Possibly, due to the presence of chloride ions on the surface of the steel, localized corrosion occurs and consequently the breakdown of the passive layer (Caré and Raharinaivo, 2007). Although with the advance of the exposure period, the ideal conditions of the concrete seem to be maintained and the potential values are gradually recovered, approaching more noble potential values, between -210 and -60 mV. Unlike the control sample that reaches values close to -500 mV with a probability of corrosion of 90%. The CO+1-3N sample showed the best behavior with very noble values of potential, around 60 mV at 270 days of testing.

Various factors influence the behavior of the Nopal mucilage specimens. Cactus gel acts as a cementing retarding additive (Zhang et. al., 2019). In addition, it is able to retain moisture for a longer period of time, because the polysaccharides have a water retention character and decrease the speed of drying of the concrete (Chandra et. al., 1998). Therefore, the process of micro-cracking of concrete is reduced, a phenomenon that takes place especially in hot climates (Zhang et. al., 2019).

### 3.3 Electrochemical noise.

As an example, the following time series shows the current fluctuations of the samples with Nopal mucilage obtained by maceration at room temperature, see Figure 4 and Figure 5.

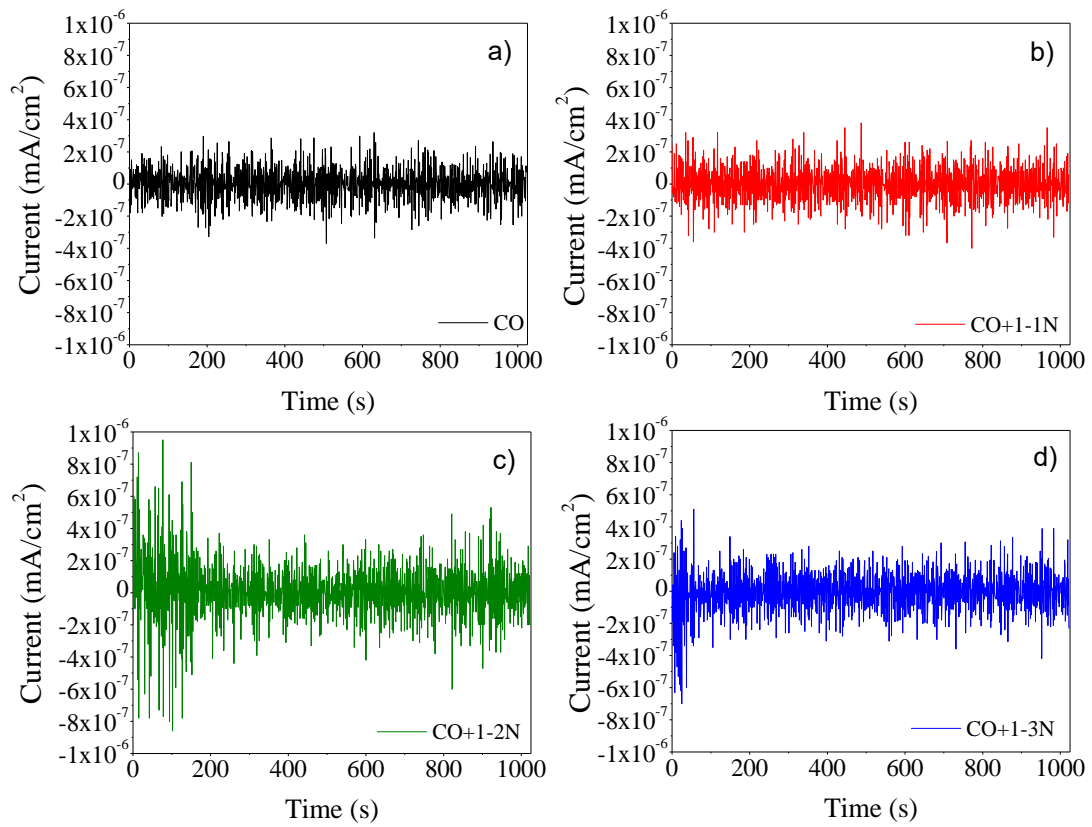


Figure 4. Time series of current at 28 days of concrete curing for the following samples: a) CO, b) CO+1-1N, c) CO+1-2N and d) CO+1-3N.

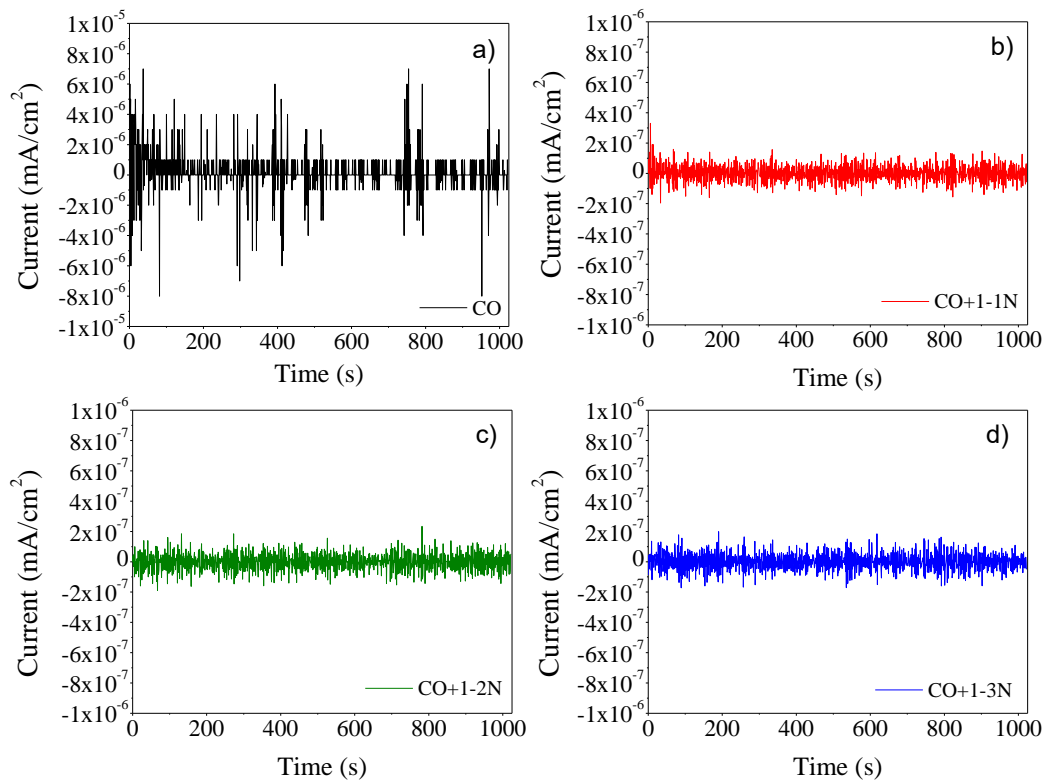


Figure 5. Time series of current at 161 days of concrete curing for the following samples: a) CO, b) CO+1-1N, c) CO+1-2N and d) CO+1-3N.

After 28 days of concrete curing, all current time series show a similar behavior with fluctuations that reach values of up to  $2 \times 10^{-7}$  mA/cm<sup>2</sup>. These low current values are indicative of a passivation state in the reinforcing steel. The passive layer of steel evolves over time (Hansson, 1984) and through this technique these small changes in current values can be detected (Gusmano et al., 1997; Cottis, 2001). Only CO+1-3N sample has some transients with values of up to  $8 \times 10^{-7}$  mA/cm<sup>2</sup>. With the advance of the exposure time to the aggressive environment, a significant change in the behavior of the time series for the CO sample can be seen. In general, a change in the values of current time series of up to an order of magnitude is observed, with some transients reaching values of up to  $8 \times 10^{-6}$  mA/cm<sup>2</sup>. This behavior can be associated to the presence of chloride ions on the surface of the steel, which cause the rupture of the oxide layer (Hansson, 1984). On the other hand, the samples with Nopal mucilage for day 161 show a decrease in the current values, and no abrupt changes are observed. This is an indication that the steel passivation steel is maintained as well as the conditions for it to remain in that state.

Figure 6 shows the noise resistance values determined from the standard deviation values of voltage and current of the analyzed time series.

At the beginning of the tests, a progressive increase in  $R_n$  is observed. These results show that the cactus mucilage does not adversely affect the curing process of concrete and guarantees the conditions for the reinforcing steel to develop a passive film. After 150 days of testing, the control sample shows a fall in  $R_n$  values close to  $2 \times 10^4 \Omega \cdot \text{cm}^2$ , with significant fluctuations in their values. This behavior indicates that the onset of corrosion consists of a series of severe localized events (Legat et. al., 2004).

At the end of the test period all samples with Nopal, keep values greater than  $1 \times 10^5 \Omega \cdot \text{cm}^2$ , with the exception of the CO+1-3NT sample, which maintained a slightly higher performance respect to the control sample. In contrast, the CO+1-3N sample reached values greater than  $4 \times 10^5 \Omega \cdot \text{cm}^2$  significantly improving the electrochemical properties of reinforced concrete. This response evidences part of the advantages offered by this Nopal gel, as it not only acts as a retarder of setting concrete, but also as an additive that can improve the electrochemical response of reinforcing steel, delay the onset and active spread of corrosion in reinforcing steel (Martinez-Molina et. al., 2015).

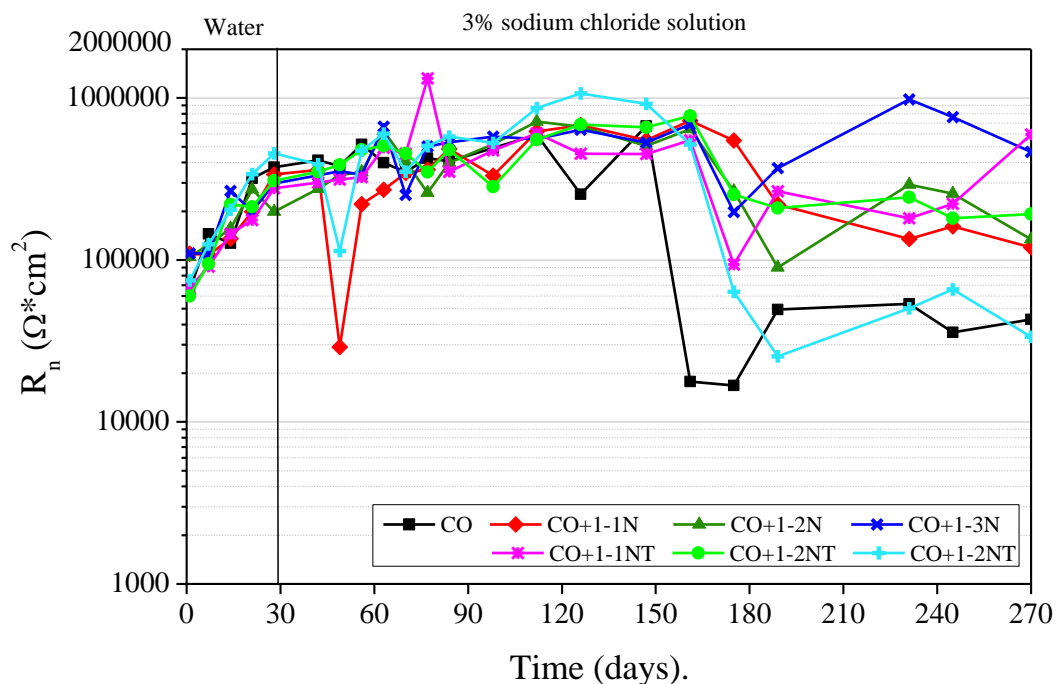


Figure 6. Behavior of noise resistance ( $R_n$ ) values with time.



### 3.4 Linear Polarization Resistance.

In Figure 7 it can be observe the  $R_p$  values obtained from linear polarization resistance technique.

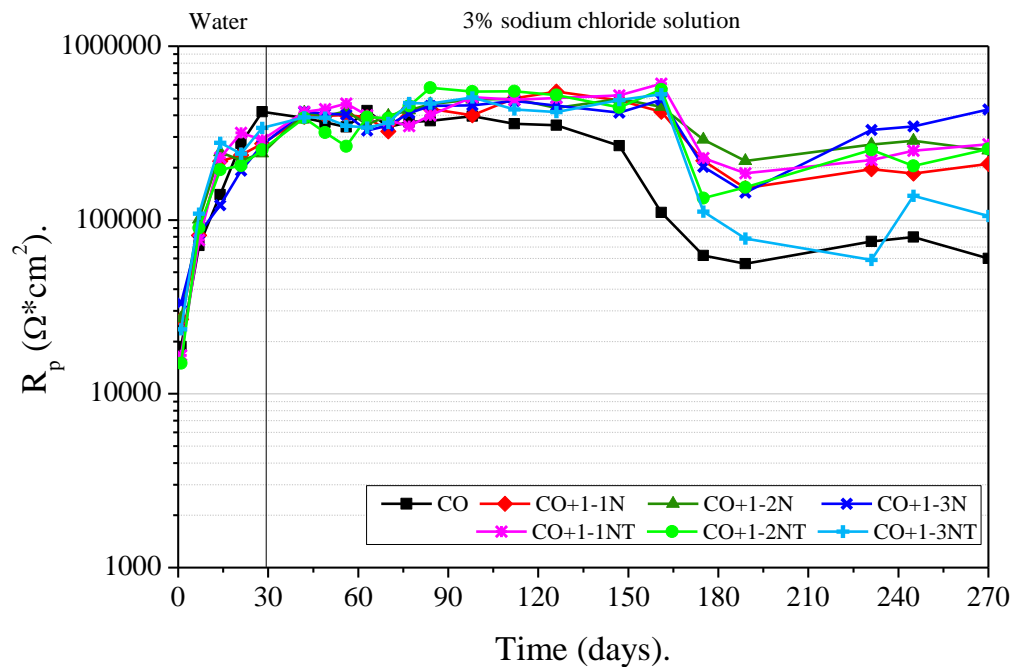


Figure 7. Behavior of polarization resistance ( $R_p$ ) values with time.

In general, it can be seen that these results show a similar trend to noise resistance values. The good performance of the Nopal mucilage within the concrete matrix is evident, because despite presenting a drop in  $R_p$  values after 150 days of exposure to the aggressive environment, progressively the resistance of all samples increases at the end of the trial period.

A very important property that influences the behavior described by the samples with Nopal mucilage is its high viscosity, a parameter that improves the workability of the mixture as well as the homogeneity of the concrete (Knapen and Van Gemert, 2009; León-Martínez et. al., 2014). Some studies affirm that certain natural polymers (polysaccharides) present in the Nopal mucilage, react with the cement compounds forming complexes that reduce the porosity in concrete, mainly because they are smaller compounds (Chandra et. al., 1998; Ramírez-Arellanes et. al., 2012).

A linear correlation was made from the  $R_n$  and  $R_p$  results of all samples, as shown in Figure 8.

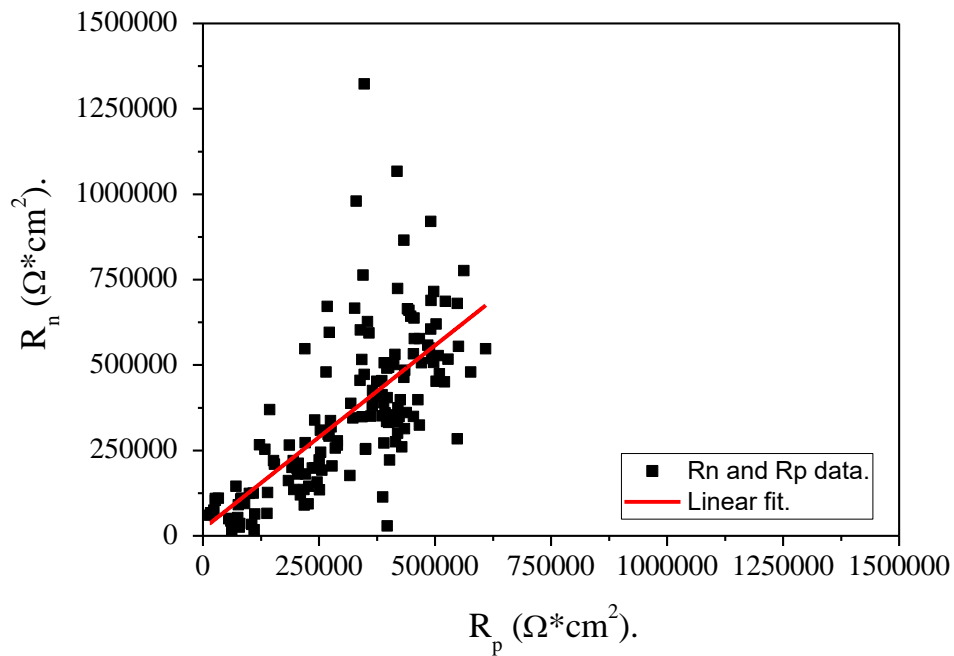


Figure 8. Correlation between the  $R_n$  and  $R_p$  values of all samples.

From this analysis a correlation coefficient with a value of 0.695 was obtained. This value indicates a reasonable correlation between the results of both electrochemical techniques (Kearns et al., 1996), taking into account that a value of zero indicates that there is no correlation and a value of one indicates a very good correlation. This result confirming that both techniques are equivalent and suitable for the electrochemical study of reinforcing steel in concrete. In fact, many studies of the electrochemical behavior of reinforcing steel in particular with the use of these techniques have been reported in the literature (Andrade et. al., 2004; Legat et. al., 2004; Bing et. al., 2007; Poursaee, 2010).

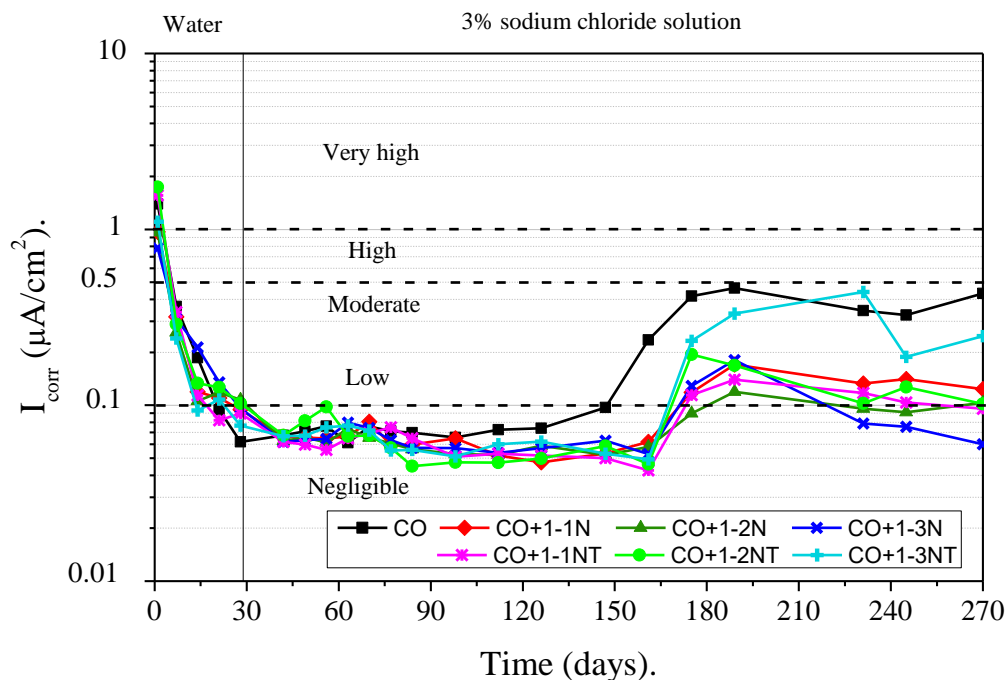


Figure 9. Behavior of corrosion rate ( $I_{corr}$ ) values with time.

The corrosion rate is inversely proportional to the Linear Polarization Resistance values from which the  $I_{\text{corr}}$  was determined for all samples (Andrade and Buják, 2013). According to some researches the proportionality factor (constant B) varies from 13 to 52 mV. In this study on the analysis of the corrosion rate of the reinforcing steel in concrete, a value of  $B = 26$  mV was applied (Andrade et. al., 2004). All corrosion rate values in terms of current density are shown in Figure 8. During the curing process of concrete, a rapid decrease in  $I_{\text{corr}}$  values can be observed until values below  $0.1 \mu\text{A}/\text{cm}^2$  are reached in the negligible corrosion speed range (Andrade and Alonso, 1996). At these values, steel possibly already developed a state of passivity due to the presence of oxygen, moisture and a highly alkaline medium (Hansson, 1984). With the advance of the exposure time to the aggressive medium all samples with mucilage maintain very low  $I_{\text{corr}}$  values. This behavior, as stated by other studies, is possibly due to the fact that this natural additive is capable of reducing the diffusion coefficient of chlorides, caused by an increase in the viscosity of the solution of the concrete pores (Ramírez-Arellanes et. al., 2012).

At the end of the test period, samples with Nopal mucilage maintained corrosion rate values between  $0.1$  and  $0.2 \mu\text{A}/\text{cm}^2$ , except for the CO+1-3N sample, which maintained values lower than  $0.08 \mu\text{A}/\text{cm}^2$  in the range of negligible corrosion rate (Andrade and Alonso, 1996) These indicated that the Nopal mucilage not only improves the electrochemical properties of steel, but also that in the presence of chlorides it can keep the reinforcing steel protected for a longer time (Martinez-Molina et. al., 2015). On the contrary, the control sample is maintained in the range of moderate corrosion rate.

Table 6 shows the values of corrosion current density and Nopal mucilage efficiencies reached at the end of the test period. As can be seen, the highest efficiency of Nopal mucilage inhibitor was 86% for the CO+1-3N sample, with a 1-3 concentration of Nopal mucilage extracted by maceration at room temperature for 48 hours.

Table 6. Electrochemical parameters obtained after 270 days of testing.

Samples	$I_{\text{corr}}$ ( $\mu\text{A}/\text{cm}^2$ )	I.E. (%)
CO	0,432	-
CO+1-1N	0,124	71
CO+1-2N	0,103	76
CO+1-3N	0,060	86
CO+1-1NT	0,095	78
CO+1-2NT	0,102	77
CO+1-3NT	0,247	43

#### 4. CONCLUSIONS.

This research work was aimed at the study of the electrochemical properties of reinforcing steel in concrete with the addition of Nopal mucilage. An analysis was made from three concentrations of Nopal mucilage taken up by two extraction methods. The favorable effect of this natural additive was appreciated by restricting the onset of corrosion and protecting the reinforcing steel.

The conclusions are as follows:

For the samples with the Nopal mucilage concentration 1-3, the highest compression resistance values were achieved, taking into account that this natural additive acts as a retardant of the setting of the concrete.

From the open circuit potential, the favorable effect of the Nopal mucilage was appreciated as an additive that can delay the corrosion of reinforcing steel in concrete. The CO+1-3N sample reached very noble potential values at the end of the trial period, being the most favorable dosage.

During the concrete curing process, all samples exhibited a similar behavior and a rapid increase in the noise resistance ( $R_n$ ) and the polarization resistance ( $R_p$ ) values were observed. It can be affirmed that the Nopal mucilage within the concrete matrix maintains the ideal conditions for the steel to acquire a state of passivation.

All samples with Nopal mucilage showed the highest  $R_n$  and  $R_p$  values with respect to the control sample for a longer period of time. A reasonable correlation coefficient was obtained between both electrochemical results from  $R_n$  y  $R_p$ , with a value of 0.695.

The Nopal mucilage was able to delay the onset of corrosion in concrete and maintain a corrosion rate between negligible and low until the end of the test period.

The mixture that presented the best electrochemical behavior was CO+1-3N, with an efficiency of 86% for the concentration of Nopal mucilage of 1:3, obtained by maceration at 48 hours without cooking at 95° Celsius.

## 5. ACKNOWLEDGEMENTS.

CONACyT (Consejo Nacional de Ciencia y Tecnología de México).

## 6. REFERENCES.

- Aballe, A., Bautista, A., Bertocci, U. and Huet, F. (2001), ‘*Measurement of the noise resistance for corrosion applications*’, Corrosion. 57(1):35–42. doi: <https://doi.org/10.5006/1.3290327>
- Andrade, C., Keddani, M., Nóvoa, X. R., Pérez, M. C., Rangel, C. M. and Takenouti, H. (2001), ‘*Electrochemical behaviour of steel rebars in concrete: influence of environmental factors and cement chemistry*’, Electrochimica Acta. 46: 3905–3912. doi: [https://doi.org/10.1016/S0013-4686\(01\)00678-8](https://doi.org/10.1016/S0013-4686(01)00678-8)
- Andrade, C., Alonso, C., Gulikers, J., Polder, R., Cigna, R., Vennesland Ø., Salta, M., Raharinaivo, A. and Elsener, B. (2004), ‘*Test methods for on-site corrosion rate measurement of steel reinforcement in concrete by means of the polarization resistance method*’, Materials and Structures/Materiaux et Constructions. 37(273):623–643. doi: <https://doi.org/10.1617/13952>
- Andrade, C. and Alonso, C. (1996), ‘*Corrosion rate monitoring in the laboratory and on-site*’, Construction and Building Materials. 10(5):315–328. doi: [https://doi.org/10.1016/0950-0618\(95\)00044-5](https://doi.org/10.1016/0950-0618(95)00044-5)
- Andrade, C. and Buják, R. (2013), ‘*Effects of some mineral additions to Portland cement on reinforcement corrosion*’, Cement and Concrete Research. 53:59–67. doi: <https://doi.org/10.1016/j.cemconres.2013.06.004>
- Bing, Z., Jian-Hua L., Rong-Gang H., Rong-Gui D. and Chang-Jian L. (2007), ‘*Study on the corrosion behavior of reinforcing steel in cement mortar by electrochemical noise measurements*’, Electrochimica Acta. 52(12):3976–3984. doi: <https://doi.org/10.1016/j.electacta.2006.11.015>
- Cárdenas, A., Higuera-Ciapara, I. and Goycoolea, F. M. (1997), ‘*Rheology and Aggregation of Cactus (Opuntia ficus-indica) Mucilage in Solution*’, Journal of the Professional Association for Cactus Development. 2:152–159.
- Caré, S. and Raharinaivo, A. (2007), ‘*Influence of impressed current on the initiation of damage in reinforced mortar due to corrosion of embedded steel*’, Cement and Concrete Research. 37(12):1598–1612. doi: <https://doi.org/10.1016/j.cemconres.2007.08.022>
- Chandra, S., Eklund, L. and Villarreal, R. R. (1998), ‘*USE OF CACTUS IN MORTARS AND CONCRETE*’, Cement and Concrete Research. 28(1):41–51.
- Cottis, R. A. (2001), ‘*Interpretation of Electrochemical Noise Data*’, Corrosion. 57(3):265–285.
- Díaz-Cardenas, M. Y. Valladares-Cisneros, M. G., Lagunas-Rivera, S., Salinas-Bravo, V. M.,

- Lopez-Sesenes, R. and Gonzalez-Rodríguez, J. G. (2017) '*Peumus boldus extract as corrosion inhibitor for carbon steel in 0.5 M sulfuric acid*', Green Chemistry Letters and Reviews, 10(4): 257–268. doi: <https://doi.org/10.1080/17518253.2017.1369167>
- Dúran-Herrera, A., De-León, R., Juárez, C. A. and Valdez, P. (2012), *Mucilago de nopal como reductor de retracción en concreto auto-consolidable*, ANAIS DO 54o CONGRESSO BRASILEIRO DO CONCRETO - CBC2012 – 54CBC, (Brazil), pp. 1-18.
- Girija, S., Kamachi Mudali, U., Khatak, H. S. and B. Raj, (2007), '*The application of electrochemical noise resistance to evaluate the corrosion resistance of AISI type 304 SS in nitric acid*', Corrosion Science. 49:4051–4068. doi: <https://doi.org/10.1016/j.corsci.2007.04.007>
- González, J. A., Miranda, J. M. and Feliu, S. (2004), '*Considerations on reproducibility of potential and corrosion rate measurements in reinforced concrete*', Corrosion Science. 46:2467–2485. doi: <https://doi.org/10.1016/j.corsci.2004.02.003>
- Gusmano, G., Montesperelli, G., Pacetti, S., Petitti, A. and D'Amico, A. (1997), '*Electrochemical Noise Resistance as a Tool for Corrosion Rate Prediction*', Corrosion. 53(11):860–868. doi: <https://doi.org/10.5006/1.3290271>
- Hansson, C. M. (1984), '*Comments on electrochemical measurements of the rate of corrosion of steel in concrete*', Cement and Concrete Research. 14(4):574–584. doi: [https://doi.org/10.1016/0008-8846\(84\)90135-2](https://doi.org/10.1016/0008-8846(84)90135-2)
- Kearns, J. R., Scully, J. R., Roberge, P. R., Reichert, D. L. and Dawson, J. L. (1996), *STP 1277. Electrochemical Noise Measurement for Corrosion Applications*, ASTM International. Edited by J. Kearns et al. 100 Barr Harbor Drive, West Conshohocken, PA 19428-2959. doi: <https://doi.org/10.1520/STP1277-EB>
- Knapen, E. and Van Gemert, D. (2009), '*Cement hydration and microstructure formation in the presence of water-soluble polymers*', Cement and Concrete Research. 39:6–13. doi: <https://doi.org/10.1016/j.cemconres.2008.10.003>
- Legat, A., Leban, M. and Bajt, Ž. (2004), '*Corrosion processes of steel in concrete characterized by means of electrochemical noise*', Electrochimica Acta. 49:2741–2751. doi: <https://doi.org/10.1016/j.electacta.2004.01.036>
- León-Martínez, F. M., Rodríguez-Ramírez, J., Medina-Torres, L. L., Méndez Lagunas, L. L. and Bernad-Bernad, M. J. (2011), '*Effects of drying conditions on the rheological properties of reconstituted mucilage solutions (Opuntia ficus-indica)*', Carbohydrate Polymers. 84:439–445. doi: <https://doi.org/10.1016/j.carbpol.2010.12.004>
- León-Martínez, F. M., Cano-Barrita, P. F. de J., Lagunez-Rivera, L. and Medina-Torres, L. (2014), '*Study of nopal mucilage and marine brown algae extract as viscosity-enhancing admixtures for cement based materials*', Construction and Building Materials. 53:190–202. doi: <https://doi.org/10.1016/j.conbuildmat.2013.11.068>
- León-Martínez, F. M., Méndez-Lagunas, L. L. and Rodríguez-Ramírez, J. (2010), '*Spray drying of nopal mucilage (Opuntia ficus-indica): Effects on powder properties and characterization*', Carbohydrate Polymers. 81(4):864–870. doi: <https://doi.org/10.1016/j.carbpol.2010.03.061>
- Martinez-Molina, W., Torres-Acosta, A., Hernández-Leos, R., Alonso-Guzman, E., Mendoza-Pérez, I. and Martínez-Peña, I. (2015), '*The inhibitive properties of Nopal slime on the corrosion of steel in chloride-contaminated mortar*', Anti-Corrosion Methods and Materials. 63(1):65–71. doi: <https://doi.org/10.1108/acmm-05-2014-1381>
- Morozov, Y., Castela, A. S., Dias, A. P. S. and Montemor, M. F. (2013), '*Chloride-induced corrosion behavior of reinforcing steel in spent fluid cracking catalyst modified mortars*', Cement and Concrete Research. 47:1–7. doi: <https://doi.org/10.1016/j.cemconres.2013.01.011>
- Morris, W., Vico, A., Vazquez, M. and De Sanchez, S. R. (2002), '*Corrosion of reinforcing steel evaluated by means of concrete resistivity measurements*', Corrosion Science. 44(1):81–99. doi: [https://doi.org/10.1016/S0010-938X\(01\)00033-6](https://doi.org/10.1016/S0010-938X(01)00033-6)

- Pech-Canul, M. A. and Castro, P. (2002), ‘Corrosion measurements of steel reinforcement in concrete exposed to a tropical marine atmosphere’, *Cement and Concrete Research*. 32(3):491–498. doi: [https://doi.org/10.1016/S0008-8846\(01\)00713-X](https://doi.org/10.1016/S0008-8846(01)00713-X)
- Pérez-Quiroz, J.T., Terán, J., Herrera, M.J., Martínez, M. and Genescá, J. (2008), ‘Assessment of stainless steel reinforcement for concrete structures rehabilitation’, *Journal of Constructional Steel Research*. 64:1317–1324. doi: <https://doi.org/10.1016/j.jcsr.2008.07.024>
- Peschard, A., Govin, A., Grosseau, P., Guilhot, B. and Guyonnet, R. (2004), ‘Effect of polysaccharides on the hydration of cement paste at early ages’, *Cement and Concrete Research*. 34:2153–2158. doi: <https://doi.org/10.1016/j.cemconres.2004.04.001>
- Poursae, A. (2010), ‘Potentiostatic transient technique, a simple approach to estimate the corrosion current density and Stern-Geary constant of reinforcing steel in concrete’, *Cement and Concrete Research*. 40(9):1451–1458. doi: <https://doi.org/10.1016/j.cemconres.2010.04.006>
- Rahmani, E., Dehestani, M., Beygi, M. H A, Allahyari, H. and Nikbin, I. M. (2013), ‘On the mechanical properties of concrete containing waste PET particles’, *Construction and Building Materials*. 47:1302–1308. doi: <https://doi.org/10.1016/j.conbuildmat.2013.06.041>
- Ramírez-Arellanes, S., Cano-Barrita, P. F. de J., Julián-Caballero, F. and Gómez-Yañez, C. (2012), ‘Propiedades de durabilidad en concreto y análisis microestructural en pastas de cemento con adición de mucílago de nopal como aditivo natural’, *Materiales de Construcción*. 62(307):327–341. doi: <https://doi.org/10.3989/mc.2012.00211>
- Sáenz, C., Sepúlveda, E. and Matsuhiro, B. (2004), ‘Opuntia spp mucilage’s: A functional component with industrial perspectives’, *Journal of Arid Environments*. 57:275–290. doi: [https://doi.org/10.1016/S0140-1963\(03\)00106-X](https://doi.org/10.1016/S0140-1963(03)00106-X)
- Torres-Acosta, A. A. (2007), ‘Opuntia-Ficus-Indica (Nopal) mucilage as a steel corrosion inhibitor in alkaline media’, *Journal of Applied Electrochemistry*. 37(7):835–841. doi: <https://doi.org/10.1007/s10800-007-9319-z>
- Torres-Acosta, A. A. and Martínez-Madrid, M. (2005), ‘Mortar improvements from Opuntia Ficus Indica (Nopal) and Aloe Vera Additions’, *Inter American Conference on Non-Conventional Materials and Technologies in Ecological and Sustainable Construction*. IAC-NOCMAT, Rio de Janeiro (Brazil), pp. 655-664.
- Valipour, M., Shekarchi, M. and Ghods, P. (2014), ‘Comparative studies of experimental and numerical techniques in measurement of corrosion rate and time-to-corrosion-initiation of rebar in concrete in marine environments’, *Cement and Concrete Composites*. 48:98–107. doi: <https://doi.org/10.1016/j.cemconcomp.2013.11.001>
- Zhang, H., Feng, P., Li, L. and Wang, W. (2019), ‘Effects of starch-type polysaccharide on cement hydration and its mechanism’, *Thermochimica Acta*. 678:1-9. doi: <https://doi.org/10.1016/j.tca.2019.178307>

## Analysis of compost repair mortars by vinyl copolymer, PVA, and SBR

M. H. de Souza<sup>1\*</sup> , R. A. de Souza<sup>1</sup> 

\*Contact author: [mateushsouza@outlook.com](mailto:mateushsouza@outlook.com)

DOI: <http://dx.doi.org/10.21041/ra.v9i3.330>

Reception: 09/07/2019 | Acceptance: 27/05/2019 | Publication: 30/08/2019

### ABSTRACT

This work has as its objective the development and analysis of compostable polymeric mortars using vinyl copolymer, PVA (polyvinyl acetate) and SBR (styrene-butadiene). Tests were carried out to determine the compressive and diametral compression tensile strengths. In addition, the adhesive strength between the repair and the concrete was determined by means of a diametral compression traction test. Among the materials tested, it was noticed that the material modified by SBR had the best performance, especially with respect to the adhesion to the concrete. In general, the results show that modified polystyrene hair hairs can be used to repair material.

**Keywords:** repair, polymer mortar, pathological manifestations, repair mortar, adhesion strength.

**Cite as:** de Souza, M. H., de Souza, R. A. (2019), “Analysis of compost repair mortars by vinyl copolymer, PVA, and SBR”, Revista ALCONPAT, 9 (3), pp. 277 – 287, DOI: <http://dx.doi.org/10.21041/ra.v9i3.330>

<sup>1</sup> Universidade Estadual de Maringá, Brasil.

### Legal Information

Revista ALCONPAT is a quarterly publication by the Asociación Latinoamericana de Control de Calidad, Patología y Recuperación de la Construcción, Internacional, A.C., Km. 6 antigua carretera a Progreso, Mérida, Yucatán, 97310, Tel.5219997385893, [alconpat.int@gmail.com](mailto:alconpat.int@gmail.com), Website: [www.alconpat.org](http://www.alconpat.org)

Responsible editor: Pedro Castro Borges, Ph.D. Reservation of rights for exclusive use No.04-2013-011717330300-203, and ISSN 2007-6835, both granted by the Instituto Nacional de Derecho de Autor. Responsible for the last update of this issue, Informatics Unit ALCONPAT, Elizabeth Sabido Maldonado, Km. 6, antigua carretera a Progreso, Mérida, Yucatán, C.P. 97310.

The views of the authors do not necessarily reflect the position of the editor.

The total or partial reproduction of the contents and images of the publication is strictly prohibited without the previous authorization of ALCONPAT Internacional A.C.

Any dispute, including the replies of the authors, will be published in the second issue of 2020 provided that the information is received before the closing of the first issue of 2020.

## **Análise de argamassas de reparo compostas por copolímero vinílico, PVA e SBR**

### **RESUMO**

Este trabalho teve por objetivo desenvolver e analisar argamassas poliméricas de reparo compostas por copolímero vinílico, PVA (acetato de polivinila) e SBR (estireno-butadieno). Foram realizados ensaios para a determinação das resistências à compressão e tração por compressão diametral. Além disso, determinou-se a resistência aderente entre o reparo e o concreto por meio de um ensaio de tração por compressão diametral. Entre os materiais testados, notou-se que o material modificado por SBR teve o melhor desempenho, sobretudo com relação à aderência ao concreto. De modo geral, os resultados mostraram que as argamassas modificadas pelos polímeros estudados podem atender à função de material de reparo.

**Palavras-chave:** reparo; argamassa polimérica; manifestações patológicas; argamassa de reparo; resistência à aderência.

## **Análisis de morteros de reparación compuestos por copolímero vinílico, PVA y SBR**

### **RESUMEN**

Este trabajo tuvo por objetivo desarrollar y analizar morteros poliméricos de reparación compuestas por copolímero vinílico, PVA (acetato de polivinilo) y SBR (estireno-butadieno). Se realizaron ensayos para la determinación de las resistencias a la compresión y tracción por compresión diametral. Además, se determinó la resistencia adherente entre la reparación y el hormigón por medio de un ensayo de tracción por compresión diametral. Entre los materiales probados, se notó que el material modificado por SBR tuvo el mejor desempeño, sobre todo con relación a la adherencia al concreto. En general, los resultados mostraron que los morteros modificados por los polímeros estudiados pueden atender a la función de material de reparación.

**Palabras clave:** reparación; mortero de polímeros; manifestaciones patológicas; mortero de reparación; resistencia a la adherencia.

## **1. INTRODUCTION**

Despite the advances in technologies in the construction industry, in many cases, there is a lack of there are still many quality poor-quality concrete structures. This fact may affect the performance and useful life of these constructions (Geiker, 2012). In this way, it is therefore necessary to understand the constructive failures in concrete structures and the mechanisms that lead to the deterioration of the concrete these structures. With further the knowledge of the failures that occur in the concrete structures, it is necessary to proceed with technical interventions can be carried out that, aiming to improve their performance and the useful life of the structures.

There are currently products on the market, there are products that help to solve the pathological manifestations of construction. However, the same material can be marketed in order to as a remedy for structural problems of with quite different properties. For concrete structures, if the properties of substrate and repair materials have different values, are incompatible and may occur. In this way, the repair can be compromised (Helene, 1992). In short, the incompatibility incompatibilities between the repair materials and the substrates can generate future problems with the repair service (Luković et al., 2012). In this way Therefore, one must it is necessary to understand the differences between polymer mortars in order to use them efficiently.



The contributions given to mortars by the addition of polymeric adhesives allow repairs to concrete structures to be more effective in their application. When polymer additives are added, the properties of adhesion, plasticity, cohesion, flexibility, impermeability, and durability are improved, and in this way, it becomes possible to perform several types of repair (Soufi et al., 2016).

Among the properties required for a mortar used for repairing concrete structures, adhesion is one of the most important. In most cases of rupture in repairs, most cases, the fracture is located in the transition zone between new and old materials (Ueda et al., 2011). In this way Therefore, the adhesion between the different cementitious materials can be considered to depend mainly on the rigidity, cleanliness, and roughness of the substrate (Espeche and León, 2011).

The verification of the adherence adhesion capacity between the materials can be carried out by indirect traction techniques where. In these situations, direct traction loads are not applied. However, the adhesion values are obtained by equations that relate items such as applied load, test body geometry, among and other factors. Tensile tests on diametral compression bending and traction are examples of tests that refer to indirect traction (Espeche and León, 2011).

The diametral compression tensile test is commonly used to determine the tensile strength of composite cement materials. This test, also known as the "Brazilian test," has guidelines described by national standard NBR 7222 of 2011, and has been verified as being applicable to. Thus, in view of the conditions of the test, the applicability of this test was verified for the verification of adhesion between two different materials.

This same method was used for the analysis of binding between new materials and old materials, and a study for recovery of structures (Espeche and León, 2011). Figure 1 illustrates the assay performed.  $P_u$  represents the load applied linearly on the test body, and  $\sigma_x$  and  $\sigma_y$  represent the tensions on the horizontal (x) and vertical (y) axisaxes, respectively.

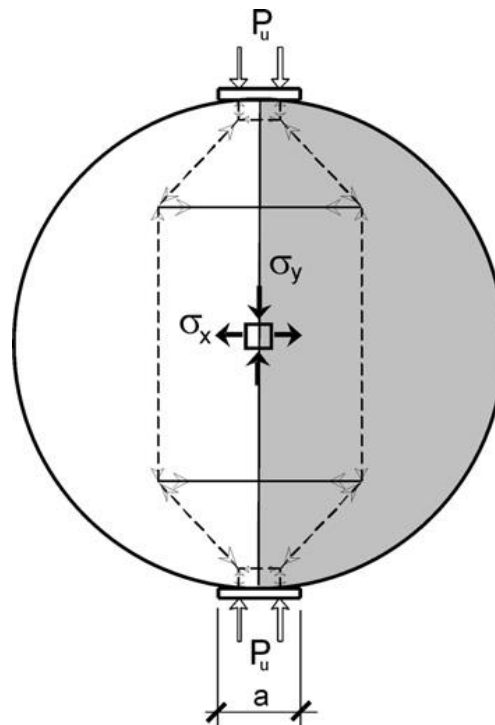


Figure 1. Representation of loading and stress distribution in the determination of traction by diametral compression.

Other studies using the same test method have been conducted to determine the adhesion of pavement repair materials (Alanazi et al., 2016). The same procedure was used by different authors to analyze the adhesion of a material composed of rubber (styrene-butadiene) (Sprinkel and Ozyildirim, 2000).

The operation of the test consists of the application of diametrically opposed loads and the verification of the traction in the same plane, as shown in Figure 1. In this way, tensions will occur in the plane of connection between the materials. Using these, it is possible to determine the bond strength between the parts.

As the repair usually deals with elements of different ages, it is necessary to evaluate the bonding tension between the materials (Espeche and León, 2011), and the quality of bonding can be classified according to five classes: excellent, very good, good, regular, and poor (Sprinkel and Ozyildirim, 2000). These bond quality levels are related to the bond strength between the materials, as shown in Table 1.

Table 1. Quality of the adhesion resistance between the repair and the substrate.

Quality of adhesion	Adhesion strength (MPa)
Excellent	$\geq 2,1$
Very good	1,7 - 2,1
Good	1,4 - 1,7
Regular	0,7 - 1,4
Bad	0 - 0,7

This work is based on the analysis of the properties of acrylic-based polymer mortars; styrene-butadiene (SBR), vinylic copolymer, and polyvinyl acetate (PVA). The polymers were added to the reference mortar, which was composed of one part of cement to three parts of sand. The analysis was based on its mechanical strength and adhesive strength, which were tested by diametral compression tensile tests, following the proposal of Espeche and León (2011), in a transition plane between the materials (concrete and polymer mortar).

The importance of this work is associated with the analysis of each polymer material and its efficiency. Through this work, it will be possible to perform the repair of concrete structures using only cement, sand, and a polymeric adhesive. In addition, their ability to perform repairs on different substrate properties will be analyzed based on a theoretical basis for guided repair materials, similar to the studies by Helene (1992).

## 2. MATERIALS AND EXPERIMENTAL PROGRAM

In order to verify the results and analyze the impact of the polymers on the mortars, a reference mortar was created. This material was composed of the same ratio of cement and sand (one part cement to three parts sand, by mass) used in the polymer mortars. However, the reference mortar did not contain any polymer additives. Industrial sand of fine particle size ( $<600 \mu\text{m}$ ), Portland cement of type CP II Z 32, and water were used to create the mortar.

Three types of polymeric adhesives were used for the preparation of the repair mortars: vinylic copolymer, PVA, and SBR. Table 2 presents some properties of the adhesive materials used in this work.

Table 2. Properties of the polymeric adhesives used in the repair mortars.

Basic composition	pH	Density (kg/l)
Vinylic copolymer	4-5	1,02
Polyvinyl acetate - PVA	4-6	1,05
Styrene-butadiene - SBR	6-8	1,0

Source: Vedacit Impermeabilizantes® (2017); Sika® (2015); TekBond® (2015).

The polymers studied were included in the blend together with the kneading water as indicated by the manufacturers. The volume ratios of polymer to water (polymer:water) used were 1:2 for vinylic copolymer, 1:3 for PVA, and 1:4 for SBR.

In order to obtain a mortar with thixotropic properties, sufficient kneading water was used only to allow the molding of beads by hand without any gloss on the surface, since gloss on the surface would indicate in principle excess water (Souza and Ripper, 1998).

In order to maintain the same thixotropic property, which was evaluated qualitatively, the proportion of cement and sand was maintained and the amount of kneading water of the mortars was varied. Thus, the water/cement mass ratios (total kneading water equal to the amount of water plus the amount of polymer) used were 0.52 for vinylic copolymer, 0.42 for PVA, and 0.38 for SBR.

The mortar characterization was performed by molding cylindrical specimens measuring 5 cm in diameter and 10 cm in height. These specimens were tested for compression and diametral compression traction. In addition to these mechanical properties, the bond strengths of these materials to concrete were verified through test bodies composed of concrete and mortar of 10 cm in diameter and 20 cm in height. In this way, diametral compression tensile tests of cylindrical test specimens composed of concrete and mortar were carried out, as shown in Figure 2. The guidelines of ABNT NBR 7222 of 2011 were followed to evaluate the adhesion between different materials, as used by Espeche and León (2011), Alanazi et al. (2016), and Radhakrishna et al. (2012).



Figure 2. Test specimen to evaluate adhesion between concrete and repair mortar.

Concrete specimen halves were initially molded. To obtain the substrate, a concrete trait that is common in construction sites was used, with an average resistance of approximately 25 MPa. After 28 days' minimum cure of the concrete, water saturation of the surface and filling of the cylindrical specimen (10 cm × 20 cm) with the repair material were performed. The filling was carried out with manual densification of the layers.

The adhesion between the parts of the specimen (Figure 2) was evaluated in two ways. The first method was to evaluate the adhesion of the new material to the old one only with the saturation of the bonding surface between the materials. The other method sought to evaluate the bond between the materials in the presence of an epoxy-based adhesion bridge. This application has the function of improving the adhesion between the concrete material, as well as the saturation of the surface with water.

The verification of the adherent strength was performed by means of diametrical compression (Figure 3 - B), which was performed in diametrically opposite lines, in the specimen (Figure 3 - A). By obtaining the breaking load, it was possible to calculate the bond strength between concrete and mortars by means of ABNT NBR 7222 of 2011.



Figure 3. (A) Test body used to determine the adhesion between the repair and the concrete; (B) Test to determine the adhesion between the repair and concrete by diametral compression.

For each mortar, four test specimens (5 cm × 10 cm) were tested for compressive strength, four (5 cm × 10 cm) for tensile strength, four (10 cm × 20 cm) for bond strength without bridge adhesion strength, and four (10 cm × 20 cm) for adherent bond strength.

The failure of the material was considered by the rupture in the plane of connection between the materials, which was subjected to a diametrically opposite loading, according to the guidelines of Norm NBR 7222 of 2011 that define diametral compression traction. The failure initially stabilizes the applied load and, subsequently, separates the repair materials and substrate. The loading application is automated, and it is interrupted when the material breaks. At this point, failure of the repair material is considered to have occurred.

### 3. RESULTS

The results obtained for mechanical resistances for the repair mortars and reference mortar are presented in Table 3. The results refer to the compressive and tensile strengths of the mortars and the adhesion strengths between the mortar and concrete.

Table 3. Mechanical resistance of repair and reference mortars.

Mechanical properties		Reference	Vinylic copolymer	PVA	SBR
Compressive strength	Minimal resistance (MPa)	17,55	16,99	12,22	15,08
	Maximum resistance (MPa)	21,31	20,93	15,89	17,93
	Average resistance (MPa)	19,34	19,72	14,5	16,74
	Standard deviation (MPa)	1,55	1,86	1,98	1,48
Tensile strength	Minimal resistance (MPa)	1,90	1,66	1,50	2,27
	Maximum resistance (MPa)	1,09	1,91	1,68	3,31
	Average resistance (MPa)	2,00	1,75	1,57	2,83
	Standard deviation (MPa)	0,09	0,11	0,09	0,43
Bond strength – Without adhesion bridge	Minimal resistance (MPa)	0,28	0,56	0,41	0,71
	Maximum resistance (MPa)	0,77	0,68	0,78	0,90
	Average resistance (MPa)	0,50	0,61	0,65	0,80
	Standard deviation (MPa)	0,25	0,05	0,21	0,80
Bond strength – With adhesion bridge	Minimal resistance (MPa)	0,73	1,11	1,33	1,64
	Maximum resistance (MPa)	1,22	1,60	1,59	2,09
	Average resistance (MPa)	1,04	1,38	1,44	1,91
	Standard deviation (MPa)	0,22	0,23	0,11	0,19
Note: For all assays, four (4) test bodies were used.					

When analyzing the results presented in Table 3, it can be observed that the polymer mortars tested in this work present improvements over the reference mortar in some properties, while in other properties they show lower values than the reference mortar. The results are presented graphically in Figure 4.

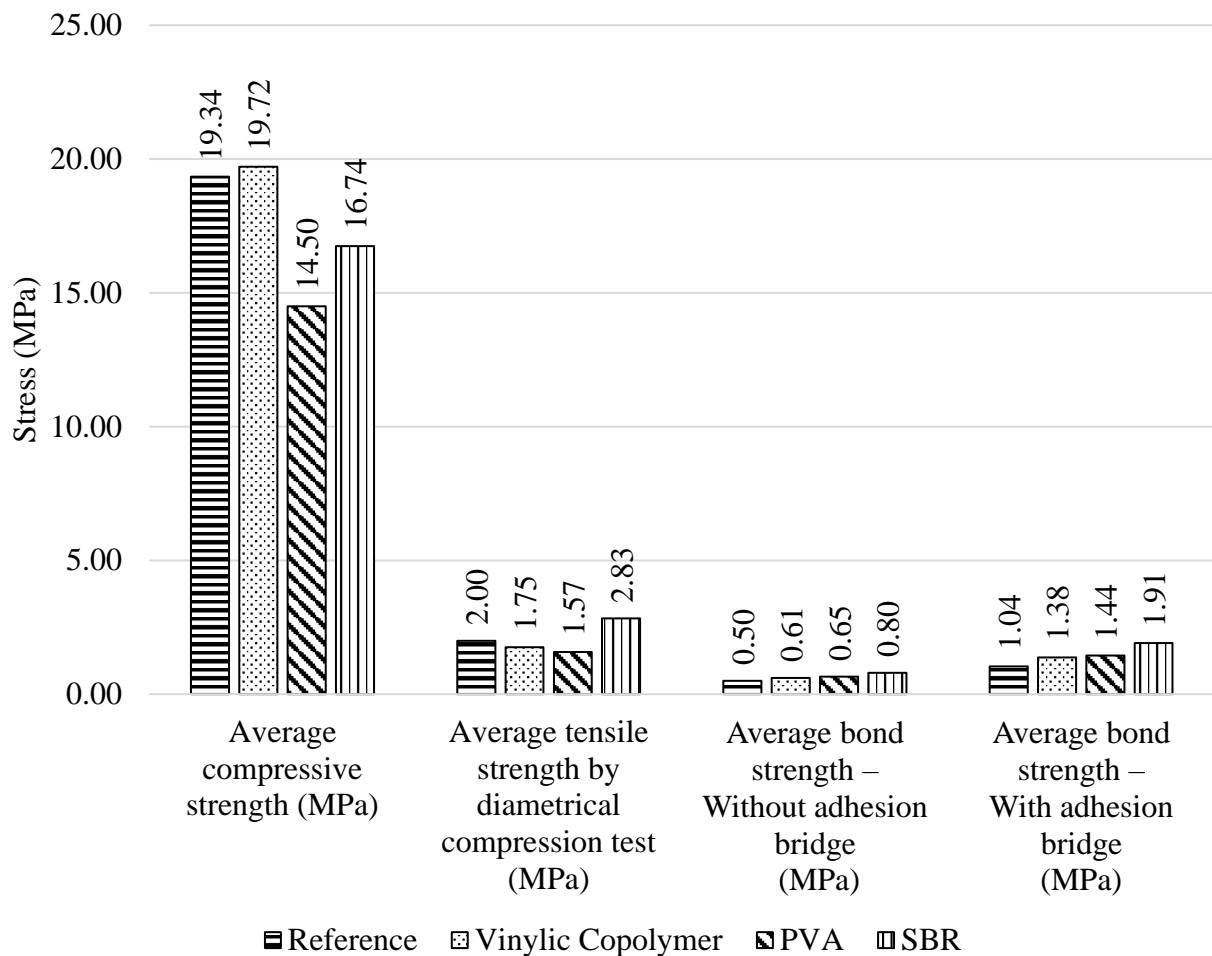


Figure 4. Mechanical resistance of repair and reference mortars.

The results obtained for compression show that the mortar modified with vinylic copolymer has a small increase in the resistance compared to the reference, as shown in Figure 4. Among the other polymeric materials, a reduction of the average resistance for the SBR-modified mortar is observed, as predicted in the literature (Ukrainczyk and Rogina, 2013). The lowest results for compressive strength were recorded for mortar composed of PVA.

For the diametral compression tensile strength, the results showed that the SBR-modified mortar has a higher tensile strength than the other materials tested. The other materials tested (mortars composed of vinylic copolymer and PVA) obtained lower results than those of the reference. An improvement of the repair material was therefore observed when using the SBR base polymeric adhesive.

The results of the verification of the adhesion strength between the mortar and the concrete, in cases with and without the presence of an adhesion bridge, are shown in Figure 4. From the results obtained (Figure 4) the presence of polymer components may contribute to the adhesion between different materials.

In the first case, without the adhesion bridge, the composite material with sbr presented better results. This shows that the presence of SBR base adhesives in mortars contributes to the adhesion of the repair to the substrate (Ukrainczyk and Rogina, 2013). The other materials were also improved in adherence, if compared to the reference, however, the results were lower than the SBR. In the first analysis, an adhesion obtained for the material composed of SBR is configured as regular, since it presents values higher than 0.7 MPa (Sprinkel and Ozyildirim, 2000).

When analyzing the results for the adhesion resistance between the repair and substrate in the presence of an adhesion bridge, it was observed that there is a contribution from the bridge. In general, when comparing the results for bridgeless and bridged adhesion, an increase of more than 100% in resistance in the presence of the adhesive material can be observed. These values show the influence of the adhesion bridge in repair situations.

The material that obtained the highest values was composed of SBR. In this evaluation, the lowest result was related to the reference material. It was noticed that the presence of polymers in the mortars contributes directly to the adhesion, with or without an adhesion bridge. "Very good" behavior was observed for the material composed of SBR, as it presents an adhesion strength value between 1.7 and 2.1 MPa (Sprinkel and Ozyildirim, 2000). The mortar composed of PVA presents "good" behavior, since its result is between 1.4 and 1.7 MPa. On the other hand, the reference mortar presents "regular" behavior, since its adherent strength is between 0.7 and 1.4 MPa.

After verification of the rupture planes between the concrete and the repair material, as shown in Figure 5, it can be observed that the loading may have obeyed the plane of union between both materials.

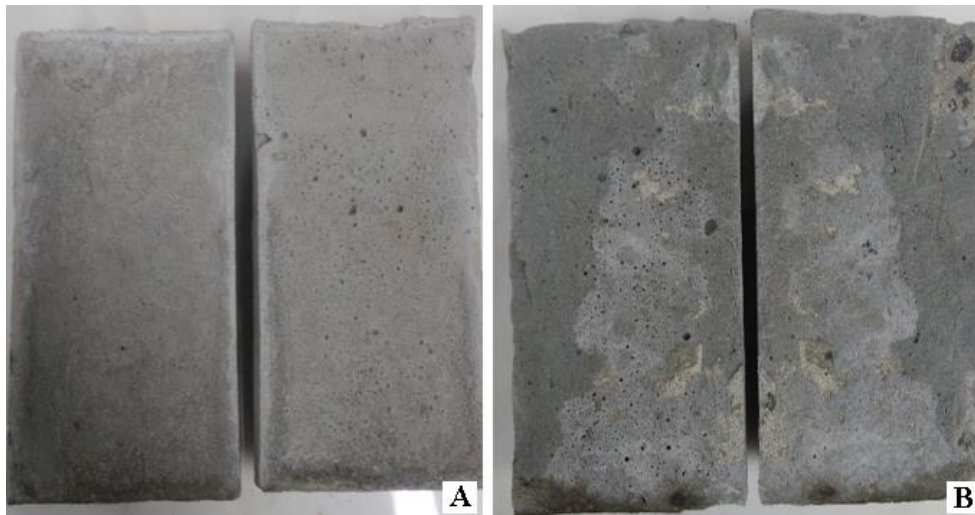


Figure 5. (A) Plan of rupture of a test specimen tested in adhesion without an adhesion bridge; (B) Plan of rupture of a test specimen tested in adhesion with an adhesion bridge.

In the first situation, without the adhesion bridge (Figure 5 - A), it was observed that the two halves separated perfectly. In other words, there was no presence of mortar in the concrete half or the presence of concrete in the middle of the mortar. This is an indication that the plane of rupture is more brittle than the resistances of the two materials. This assertion is corroborated by the values of the results, presented in Table 3. In other words, the properties of the polymeric materials do not confer great adhesion resistance between cementitious materials.

In cases where an epoxy-based adhesion bridge was used (Figure 5 - B), it was observed that there was the presence of concrete parts next to half of the mortar and parts of the mortar next to the concrete half. This may indicate that the adhesion strength is improved by the adhesion bridges. It is possible to verify this numerically from the data in Table 3. It was observed that the failure occurs in part of the bonding material, with a perfect separation between the two materials, and in another part it was observed that one of the two bonded materials failed. It was considered that the same situation did not occur in the absence of an adhesion bridge. By observing the results, it was considered that the presence of the bridge contributed to the adherent properties between the materials.

## 4. CONCLUSIONS

From the results obtained in the laboratory and their respective analyses, it was concluded that the physical and mechanical properties of the mortars used in structural repairs can be improved by the presence of polymeric components. The following highlights are presented from the research carried out:

- a) Vinylic copolymer: The mortar modified with vinylic copolymer showed an increase in the compressive strength, traction, and adhesion between the concrete and repair, relative to the reference;
- b) PVA: The base repair material PVA showed an increase in its adhesion to the reference. However, the values of compression and traction were lower than those of the reference material. In the analysis of the results, it was possible to observe a relationship between the composite mortars composed of vinylic copolymer and PVA. Both are vinyl-based, however, the best results were recorded for the vinylic copolymer, with a small unfavorable difference in the adhesive capacity;
- c) SBR: Among the materials tested, the mortar modified with SBR presented the best results, mainly with respect to the adhesion to the substrate. The compressive strength was lower than the reference. However, for the other analyzed properties, the material showed good behavior.

Regarding the adhesion of the tested materials, two analyses can be performed. In the first, which is related to the application of the repair material on a saturated surface, it was observed that there was an average improvement in the results of approximately 30% with respect to the reference mortar.

In the presence of the epoxy-based adhesion bridge, an improvement in adhesion strength values of at least 120% relative to the saturated surface was noted. From these results, it was observed that the use of the adhesion bridge allows the binding capacity between the materials to be considered from "good" to "very good". This shows that the presence of a bonding material between the repair and substrate is advisable in order to ensure an efficient adhesion interface.

## 5. ACKNOWLEDGMENTS

The authors would like to thank CAPES for their financial support, as well as the Graduate Program in Urban Engineering of the State University of Maringá for the availability of physical space and equipment for conducting tests.

## 6. REFERENCES

- Alanazi, H., Yang, M., Zhang, D., Gao, Z. (2016), *Bond strength of PCC pavement repairs using metakaolin-based geopolymer mortar*. Cement and Concrete Composites. 65: 75-82. <https://doi.org/10.1016/j.cemconcomp.2015.10.009>
- Associação Brasileira de Normas Técnicas. (2011) *NBR 7222: Concreto e argamassa — Determinação da resistência à tração por compressão diametral de corpos de prova cilíndricos*. Rio de Janeiro.
- Espeche, A. D., León, J. (2011), *Estimation of bond strength envelopes for old-to-new concrete interfaces based on a cylinder splitting test*. Construction and Building Materials. 25: 1222–1235. <https://doi.org/10.1016/j.conbuildmat.2010.09.032>
- Geiker, M. R. (2012), *On the importance of execution for obtaining the designed durability of reinforced concrete structures: Construction of durable concrete structures*. Materials and corrosion. 63:1114 -1118. <https://doi.org/10.1002/maco.201206754>



- Helene, P. R. D. L. (1992), “*Manual para reparo, reforço e proteção de Estruturas de Concreto*”. PINI, São Paulo, Brasil.
- Luković, M., Ye, G., Van Breugel, K. (2012), “*Reliable concrete repair: A critical review*”. 14th International Conference Structural Faults and Repair. Edinburgh, Scotland, UK.
- Radhakrishnan, R., Syam Prakash, V., Prasad Varma Thampan, C. K. (2012), *Performance of Styrene Butadiene Rubber as a Concrete Repair Material in tropical climate*. International Journal of Advancements in Research & Technology, Volume 1, Issue 6, pp. 1-5, ISSN 2278-7763
- Soufi, A., Mahieux, P. Y., Ait-Mokhtar, A. (2016), *Influence of polymer proportion on transfer properties of repair mortars having equivalent water porosity*. Materials and Structures. 49: 383–398. <https://doi.org/10.1617/s11527-014-0504-3>
- Souza, V. C. M. D., Ripper, T. (1998), “*Patologia, Recuperação e Reforço de Estruturas de Concreto*”. PINI, São Paulo, Brasil.
- Sprinkel, M. M., Ozyildirim, C. (2000), *Evaluation of high performance concrete overlays placed on Route 60 over Lynnhaven Inlet in Virginia*. Charlottesville, EUA.
- Ueda, H., Tamai, Y., Kudo, T. (2011), *Evaluation of the Durability of Cement-based Repair Materials*. Railway Technical Research Institute. 52: 92-96. <https://doi.org/10.2219/rtriqr.52.92>
- Ukrainczyk, N., Rogina, A. (2013), *Styrene–butadiene latex modified calcium aluminate cement mortar*. Cement & Concrete Composites. 41: 16–23. <https://doi.org/10.1016/j.cemconcomp.2013.04.012>

## Specimen size effect on the durability indexes determination for cement-based materials

R. Visairo-Méndez<sup>1\*</sup>  A. A. Torres-Acosta<sup>2</sup>  R. Alvarado-Cárdenas<sup>1</sup> 

\*Contact author: [rvisairom@gmail.com](mailto:rvisairom@gmail.com)

DOI: <http://dx.doi.org/10.21041/ra.v9i3.381>

Reception: 18/01/2019 | Acceptance: 02/08/2019 | Publication: 30/08/2019

### ABSTRACT

In this project is required to determine if there is any result variation in durability indexes due to size effect in sizes of mortar specimens. Cubes 5 x 5 cm, 5 x 10 cm and 10 x 20 cm cylinders for each mortar type were considered. It was found that in certain indexes (WER, TVC, and CS) results did not depend on specimen's geometry. Nonetheless, UPV index result presented differences up to 17.5 % between the cubes and the 10 x 20 cm cylinders.  $\epsilon_{eff}$  index result showed an interesting difference between the cubes and the 5 x 10 cm cylinders used in full length. Therefore, it is recommended to restrict the height of the specimen to a standard value.

**Keywords:** mortar; durability; size; performance.

**Cite as:** Visairo-Méndez, R., Torres-Acosta, A. A., Alvarado-Cárdenas, R. (2019), "Specimen size effect on the durability indexes determination for cement-based materials", Revista ALCONPAT, 9 (3), pp. 288 – 302, DOI: <http://dx.doi.org/10.21041/ra.v9i3.381>

<sup>1</sup> Dirección de Investigación y Posgrado, Facultad de Ingeniería, Universidad Autónoma de Querétaro, Santiago de Querétaro, México.

<sup>2</sup> Escuela de Ingeniería y Ciencias, Campus Querétaro, Instituto Tecnológico de Estudios Superiores de Monterrey, Santiago de Querétaro, México.

### Legal Information

Revista ALCONPAT is a quarterly publication by the Asociación Latinoamericana de Control de Calidad, Patología y Recuperación de la Construcción, Internacional, A.C., Km. 6 antigua carretera a Progreso, Mérida, Yucatán, 97310, Tel.5219997385893, [alconpat.int@gmail.com](mailto:alconpat.int@gmail.com), Website: [www.alconpat.org](http://www.alconpat.org)

Responsible editor: Pedro Castro Borges, Ph.D. Reservation of rights for exclusive use No.04-2013-011717330300-203, and ISSN 2007-6835, both granted by the Instituto Nacional de Derecho de Autor. Responsible for the last update of this issue, Informatics Unit ALCONPAT, Elizabeth Sabido Maldonado, Km. 6, antigua carretera a Progreso, Mérida, Yucatán, C.P. 97310.

The views of the authors do not necessarily reflect the position of the editor.

The total or partial reproduction of the contents and images of the publication is strictly prohibited without the previous authorization of ALCONPAT Internacional A.C.

Any dispute, including the replies of the authors, will be published in the second issue of 2020 provided that the information is received before the closing of the first issue of 2020.

## Efecto del tamaño de los especímenes en la determinación de los índices de durabilidad para materiales base cemento

### RESUMEN

En este proyecto se requiere determinar si índices de durabilidad son afectados por tres tamaños de especímenes evaluados de mortero de reparación. Se elaboraron cubos de 5 x 5 cm, cilindros de 5 x 10 cm y de 10 x 20 cm para cada tipo de mortero. Se encontró que ciertos índices (WER, TVC y CS) no dependen de la geometría del espécimen. Sin embargo, los resultados de UPV presentaron una diferencia entre cubos y cilindros de 10 x 20 cm mayor a 17.5 %. Los resultados de  $\epsilon_{\text{eff}}$  presentaron una diferencia muy interesante entre los cubos y los cilindros de 5 x 10 cm. Se recomienda restringir la altura de los especímenes a un valor estándar.

**Palabras clave:** mortero; durabilidad; tamaño; comportamiento.

## Efeito do tamanho da amostra na determinação dos índices de durabilidade de argamassas base cimento

### RESUMO

Em este projeto é necessário determinar se os índices de durabilidade são afetados por três tamanhos de amostras avaliadas para argamassa de reparo. Cilindros de 5 x 5 cm, 5 x 10 cm e 10 x 20 cm para cada tipo de argamassa foram considerados. Verificou-se que em determinados índices (WER, TVC e CS) os resultados não dependiam da geometria da amostra. No entanto, o resultado do índice de UPV apresentou diferenças de até 17,5% entre os cubos e os cilindros de 10 x 20 cm. O resultado do índice  $\epsilon_{\text{eff}}$  mostrou uma diferença interessante entre os cubos e os cilindros de 5 x 10 cm. Nestes casos, recomenda-se restringir a altura da amostra a um valor padrão.

**Palavras-chave:** argamassa; durabilidade; tamanho; comportamento.

## 1. INTRODUCTION

Concrete structures exposed to aggressive environments (urban, marine, industrial, or combinations of them) develop premature damage during their service life (< 10 years after being built and put into service). Typical deterioration manifestations are cracks and rust stains on the concrete's surface and may reach even more marked deterioration process by the delamination of the concrete cover if the corrosion of reinforcement or prestressing steel is not stopped. This pathology is quite common today in concrete structures; it is usually because they are not designed with durability criteria, but instead on mechanical strength only. (Torres et. al., 2002; Torres and Castro, 2013; Calado et. al., 2015; Mendoza-Rangel et. al., 2016).

### 1.1. Durability design

Concrete durability is the concrete's capability to sustain physical, chemical, biological and climatic effects as established by national and international regulations. The service life is defined as the period of time in which the structure is put into service until it needs to be repaired, rehabilitated, or reinforced, due to some type of damage that could cause aesthetic reduction or compromise the safety of its occupants (users). In this way, the fact that a structure has fulfilled its service life implies that its aesthetics or safety conditions must be restored through corrective maintenance, and not necessarily assume that the structure is about to collapse, as it is erroneously defined in certain instances. (Troconis et. al., 1997; Shi et. al., 2012; Mendoza-Rangel et. al., 2016).

A durable structure is one which service life can be longer than 50 years, and in countries where concrete technology has evolved rapidly, the design service lives could reach between 80 to 100 years. Using concrete's material selection criteria based on ambient aggressiveness, the process of designing concrete structures with durability criteria begins. Once the selected materials that could be used for concrete manufacturing, the next step is the design of the same structure by mechanical loading strength. Knowing the cement type, the mineral additions that could be used in the design mix, the amount of the cementitious content, and the water/cement ratio (w/c), structural engineers could forecast the compressive strength of the designed mix. This could allow structures to protect their service lives for over 80 years, thus avoiding costly repairs during their service lifespan. Another alternative of durability design could be through durability indexes as it has been investigating recently. (Torres et. al., 2002; Helene et. al., 2003; Solís et. al., 2012; Mendes et. al., 2018).

## 1.2. Construction of durable concrete structures

In the supervision and quality control of durable concrete, the manufacture, transport, placement, consolidation and curing, dosing, and concrete cover compliance of the elements to be manufactured, should be closely monitored. In the case of the concrete's manufacture and dosage for durable mixtures, it is the obligation of the contractor and/or external supervisor to extract concrete cores in strategic elements to determine that the concrete already placed and hardened, meets the performance requirements of the projected durability. By this methodology, the owner assures that the materials used in the contracted construction are indeed quite durable. This need to verify that the concrete placed in the structural elements complies with the performance requested in the design is due to the fact that: performing these tests in standardized cylinders, manufactured by laboratories or accredited specialists for their manufacture, could not reflect what is actually being placed in the different concrete elements of the work. (Helene et. al., 2003; Torres and Castro, 2018).

## 1.3. Durability index tests

Concrete durability performance has been evaluated from physical and mechanical laboratory tests. The most commonly used are: wet electrical resistivity (WER), ultrasonic pulse velocity (UPV), total void content (TVC), Effective Porosity ( $\epsilon_{\text{eff}}$ ), and compressive strength (CS). All experimental values obtained from these tests are commonly known as durability indexes (Table 1). Such tests are regularly performed either in a field laboratory, or in a quality control/quality assurance (QC/QA) laboratory from the supervision company. Also, correlations between indexes had been made considering CS, WER and Water Capillary Absorption test (WCA) (Medeiros-Junior et. al., 2019). The methodology followed to characterize the durability (or obtain the durability indexes) of concrete mixtures before and during the construction work use specimens from various dimensions and shapes. (Troconis et. al., 1997; Mejía et. al., 2018).

The well-known thematic project DURAR (Troconis et. al., 1997) indicates the height of the specimens should be <50 mm in some tests but the contact area could be variable. Typically, such sampling, are either cubes or cylinders with side dimensions from five to 30 cm. For example, typical cube dimensions are of 5 x 5 cm, 10 x 10 cm, or 15 x 15 cm; typical cylinder dimensions are 5 x 10 cm, 10 x 20 cm, and 15 x 30 cm. These variable shapes and dimensions may vary the durability index results obtained if the performance test has restrictions on the specimen dimensions, as observed in the literature with some mechanical testing affected by the dimension of the specimen (Bazant and Planas, 1997; Bazant, 2000). This dimension effect on the materials mechanical performance is defined as the size effect law (SEL), in which materials such as concrete with aggregate sizes quite large in dimension, may produce different mechanical performance depending on the specimen size used for testing. Hence, the objective of this investigation is to

present an experimental program in order to determine if the durability index tests (WER, UPV, TVC,  $\epsilon_{\text{eff}}$ , and CS) are affected by the specimen shape and dimension.

Table 1. Durability index levels (Troconis et. al., 1997)

Durability Index Test	Low performance	Intermediate performance	High performance
WER, k $\Omega$ -cm	< 10	10 – 50	> 51
UPV, km/s	< 2.9	3 – 4	> 4.1
TVC, %	> 15	10 - 15	< 10
$\epsilon_{\text{eff}}$ , %	> 10	5 - 10	< 5
CS; MPa	< 30	30 - 50	> 51

## 2. EXPERIMENTAL PROCEDURE

### 2.1. Materials

In order to determine if the shape and dimensions of the specimens affect the durability indexes, the present investigation discard the possible effect on the size of the aggregate, thus mortar (cement, water, sand) instead of concrete (cement, water, sand, gravel) was used as the tested material.

The mortars were defined in accordance with the durability indexes: low, intermediate and high performance (called N2, N1 and MR, and SR in this investigation). These variations on the mortar’s mixture were considered to review if were also affected by the variables evaluated.

For the mortars N1 and N2 the cement used was the so called CPC cement (Mexican name for Type I Portland cement with some unknown fillers to decrease the Clinker content; no specifications of the cement were provided by the manufacturer) according to NMX-C-414-ONNCCE-1999. The sand used was silica from a mine bank, mesh size number 89, as per ASTM C33 - 2003. The cement:sand proportions by weight used to fabricate the tested mortars was 1:2.75. The mixture proportions of the mortar mixtures used are described in Table 2.

Table 2. Mixture proportion of low (N2) and intermediate (N1) performance mortars

Material	N2 [l / m <sup>3</sup> ]	N1 [l / m <sup>3</sup> ]
Cement	128.04	186.24
Water	322.67	322.67
Sand	549.29	491.09

For mortars MR and SR were used two commercial trademarks, and were provided with certain dosage protected, thus no detailed information was obtained from the manufacturers.

The information from the MR mortar was that contains propylene fibers, but the manufacturer did not provide information on the fiber size nor the content. The MR mortar fabrication was performed following the manufacturer’s specifications written on the product’s bag: 190 ml of water per kilogram of product, providing 9.5 l of water per 50 kg bag. Both, dry product and water were prepared in a mortar mixer, waiting until the mixture was fully homogenized before placing it into a 5 x 5 cm cube or 5 x 10 or 10 x 20 cm cylinder molds. The physical properties of the product obtained by the manufacturer are listed in Table 3.

The information provided for SR mortar was: CPC cement (without concentration defined), marble quarry sand, low water-to-cement (w/c) ratio (< 0.35), 3rd generation water reducer based on polycarboxilates (powder presentation integrated in the dry mixture). The product arrived in closed

plastic buckets (20 l) and only tap water needed to be added in a mortar mixer (not allowed to be mix by hand, based on manufacturer recommendations).

Table 3 Physical characteristics for MR mortar provided by manufacturer

Physical characteristic	Description	Description
Dry volumetric mass	1,413 kg / m <sup>3</sup>	-
Hardened volumetric mass	1,690 kg / m <sup>3</sup>	-
Compressive strength	16.0-18.0 MPa at 1 day	35.0-45.0 MPa at 28 days
Flexure strength	9.5-9.7 MPa at 1 day	11.0-12.0 MPa at 28 days
Tensile strength	3.2-4.0 MPa at 1 day	40.0-46.0 MPa at 28 days

## 2.2. Specimen dimensions

For this investigation, three dimensions were selected for mortar specimens: 5 x 5 cm cubes (cube), 5 x 10 cm cylinders (Cyl-5), and 10 x 20 cm cylinders (Cyl-10). For N1 and N2 mortars, the mixtures were prepared in order to obtain 15 cubes, four 5 x 10 cm cylinders (small), and nine 10 x 20 cm (large) cylinders. The specimens obtained of the mortars MR and SR were the same amount of cubes (15) and small cylinders (4), the remaining mortar was used to fill molds to obtain 10 x 20 cm cylinders. All the amount of specimens obtained are presented in Table 4.

Table 4. Amount of specimens elaborated in this investigation

Type of mortar	Cube 5 x 5 cm	Cyl. 5 x 10 cm	Cyl. 10 x 20 cm
Low performance	15	4	9
Intermediate performance	15	4	9
Intermediate performance	15	4	15
High performance	15	4	22

For some tests, the large cylinders were cut for the method defines a special specimen height ( $\leq 5$  cm). There were a total of four specimens of this type for each cylinder (named SI-10).

## 2.3. Wet Electrical Resistivity (WER) index

Determining the WER involves a simple technique that quickly measures the value of a concrete, and also it is cost effective, given the low cost of the required equipment. The specimen was removed from the curing chamber (hence the name WER), wet sponges placed on either end, and metal plates (normally a corrosion-resistant metal such as stainless steel or bronze) placed on either end touching the sponges. Afterwards the voltage was transmitted through the two plates and the resulting ionic current was measured. The voltage equipment to measure the current values were used to calculate the electrical wet resistance (WR) between the plates, that is, the resistance of the mortar specimen. The mortar was measured by using a commercial Resistance Meter following NMX-C-514-ONNCCE-2016 standard procedure (in kilo ohms, k $\Omega$ ). The resulting value was multiplied by a cell constant dividing the specimen area (A) by its length (L): 5 cm for cubes, 1.96 cm for small cylinders, and 3.93 cm for big cylinders. Figure 1 represents this test.

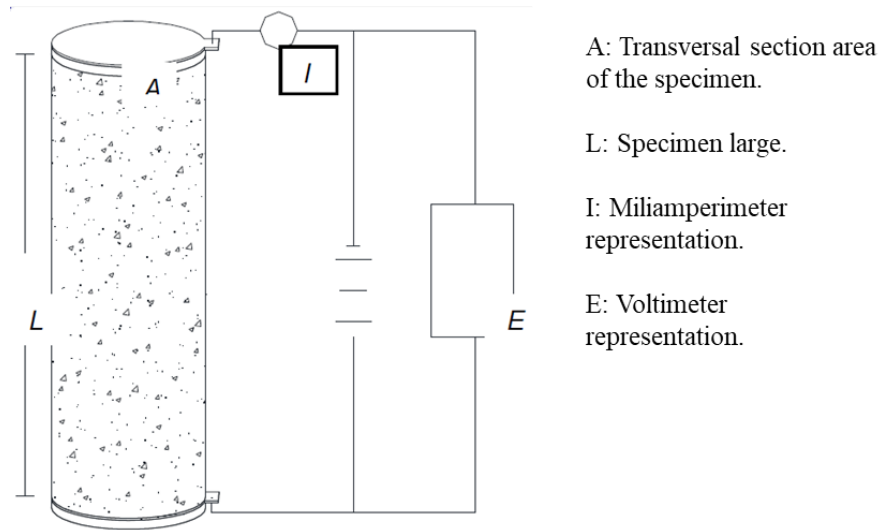


Figure 1. Representation of WER test

#### 2.4. Ultrasonic Pulse Velocity (UPV) index

The UPV technique, an indirect method to determine the homogeneity of cement based materials, was used to estimate another physical property of the mortar cubes (Troconis et. al., 1997). In this method, an emitter sends an ultrasonic pulse that travels through the material until reaching a receptor. The distance between the emitter to the receiver was divided by the elapsed time for which the wave travelled from both transducers is known as UPV. After performing the electrical resistance testing, the same specimens were used to carry out the UPV technique. The UPV was measured by using a commercial ultrasonic pulse velocity tester. The procedure followed was in accordance to ASTM C597 - 2002 and project DURAR (Troconis et. al., 1997). Figure 2 represents this test.



Figure 2. Equipment used for UPV test

#### 2.5. Total Void Content (TVC) index

The TVC was measured following the ASTM C642 - 1997 procedure. After drying at 50 °C (122 °F) until constant mass (from 20 to 35 days), an initial measurement was taken and designated as dry mass ( $m_D$ ). The cubes were then placed in a high humidity plastic container and measurements were taken constantly until reaching constant mass, when a final saturated mass ( $m_S$ )

was recorded. The water-saturated specimens were weighed inside the water to measure saturated-submerged mass ( $m_{SS}$ ). The TVC (%) was estimated with the equation (1):

$$TVC (\%) = \frac{100 \cdot (m_S - m_D)}{m_S - m_{SS}} \quad (1)$$

Since the method defines specimen height  $\leq 5$  cm, specimen used in this test needed additional preparation by slicing the large cylinders, to 5 cm deep slices approximately. This type of specimen was called SI-10 in this investigation.

## 2.6. Effective Porosity ( $\epsilon_{eff}$ ) index

This index is obtained as a result of the Water Capillary Absorption test (WCA). In order to determine the capillary absorption of the mortar, the specimens were tested following the Fagerlund technique (Troconis et. al., 1997; ASTM C1585, 2004). This technique is the basis of the Swedish standard using four coefficients to describe mortar and concrete capillary absorption kinetics: water penetration resistance ( $m$ ), capillary absorption coefficient ( $k$ ), effective porosity ( $\epsilon_{eff}$ ), and capillary absorption ( $S$ ). The same pre-conditioning was conducted in order to obtain 5 cm height specimens (SI-10) for the large cylinder shapes.

The specimens were dried at 50 °C (108 °F) and  $< 30$  % R.H. until a constant mass was achieved and subsequent drying in a desiccator. The cubes were then covered with a sealing material (wax) on four of their six faces, and the cylinders and slices at their curved perimeter, leaving the top and bottom faces uncovered. After recording the initial dry mass with wax cover ( $W_0$ ) the specimens were placed inside a flat-bottomed container ( $22 \pm 4$  °C [ $97 \pm 18$  °F] and  $\sim 100$  % R.H.), making sure that the water level was reached between 3 and 5 mm (0.1 and 0.2 in.) deep. The water used for the small cylinders was contaminated with 3.5 % of chloride ions (by water mass). All the specimens were kept inside their recipient and the water level was daily monitored to maintain it at the same mark level (avoiding water loss due to evaporation, or specimens water absorption).

The change in mass of the mortar specimen per exposed unit area ( $(W_t - W_0) / A$ ) was then registered once a day, five days a week, during the first two months. Afterwards three measurements per week were recorded for the next three months. Finally, the measurements were taken once per week until the testing experimental period ended.

The absorption coefficients were calculated on the basis of the following equations (Troconis et. al., 1997):

$$m [sec \cdot m^{-2}] = t_n \cdot z^{-2} \quad (2)$$

$$k [kg \cdot m^{-2} \cdot sec^{-1/2}] = (W_t - W_0) \cdot A^{-1} \cdot t^{-1/2} \quad (3)$$

$$\epsilon_{eff} [\%] = 0.001 \cdot k \cdot m^{-1/2} \quad (4)$$

$$S [m \cdot sec^{-1/2}] = m^{-1/2} \quad (5)$$

where coefficient  $k$  can be evaluated as the slope of the linear region of graph  $(W_t - W_0) / A$  as a function of  $t^{1/2}$ ; the  $m$  coefficient can be determined by calculating the time  $t_n$  required for water to get to the top face of the probe (i.e., when  $z = 10$  cm [4 in.] for small cylinders).

## 2.7. Compressive Strength (CS) index

The cubes and cylinders were tested up to the failure limit under compression by a procedure in accordance to ASTM C109/C109M - 2002. The tests were performed by using a Universal Servo



Hydraulic Testing Machine (nominal maximum capacity of 500 kN [112.4 kips]). The loading rate was  $\sim 0.25$  MPa/sec [36.26 psi/sec]. A PC computer interfaced to the testing machine stored the output of the testing machine (maximum load) automatically.

### 3. RESULTS AND DISCUSSIONS

For a better interpretation, the results are presented as an average of three specimens per conditioning: mortar type, shape (cube or cylinder) and dimension.

#### 3.1. Wet Electrical Resistivity (WER) index

The concept of electrical resistivity is a parameter which indicates the interconnection between pores in granular (i.e. soils) and porous materials. In porous materials, such as mortar or concrete, the electrical resistivity depends on the degree of pore saturation and, to a lesser extent, on paste hydration or the presence of dissolved salts in an aqueous phase (Troconis et. al., 1997). Figure 3 presents the average WER vs. time data from the three mortar types (average value of at least from three specimens per mixture, shape and dimension). The performance of mortar MR was variable between N1 and N2 parameters. It was decided to compare conventional mortars N1 and N2 vs. commercial mortar SR.

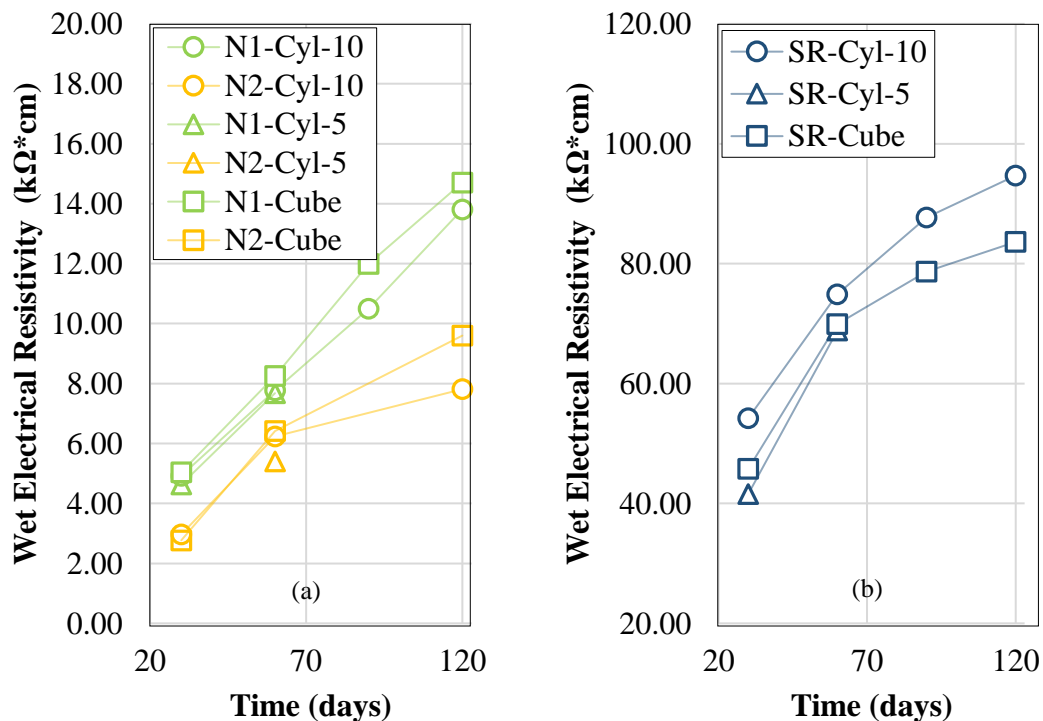


Figure 3. Average WER vs. time experimental values: (a) low (N2) and intermediate (N1) performance mortars; (b) high performance mortar (SR)

As in Figure 3, similar WER index performance was observed in all tested mortars: WER index increased with time. It is also observed from same figure that the different specimen shapes (cube vs. cylinder) and dimensions, did not affect the average WER results obtained using the direct method (NMX-C-514-ONNCCE, 2016), thus supporting the idea to measure WER regardless of specimen geometry but using a length dimension  $L \geq 5$  cm.

Comparing the performance of the three types of mortar testes, low performance mortar N2 increased with time and started to follow an asymptotic curve, reaching average WER index values of about 9 k $\Omega$ -cm very close to the target value in Table 1. In the case of intermediate performance mortar N1, the average WER index data continued increasing with time, which means that the cement was still hydrating and the porosity was still decreasing. The average WER index values obtained at 120 days reached about 14 k $\Omega$ -cm, which is quite close to the lower limit established in Table 1.

Finally, the average WER index data obtained with high performance mortar SR followed a nonlinear behavior after 60 days and, at 120 days of monitoring, the value reached was about 90 k $\Omega$ -cm, but it was still increasing at a low pace than at the beginning of the monitoring time. The value obtained at 120 days surpassed the 51 k $\Omega$ -cm value defined as the lower limit of such high performance mortars.

In a recent investigation (Mejía et. al., 2018), it is also observed that the commercial mortars are in the same range despite the size of specimen corresponding to an intermediate performance. The lowest mortar corresponds to a low performance with an average  $\pm 6$  k $\Omega$ -cm at 120 days.

### 3.2. Ultrasonic Pulse Velocity (UPV) index

The UPV index performance vs. time is observed in Figure 4. For this performance index the material evaluated was only the high performance mortar SR. This was because the other mortars were not considered for this index evaluation due to a specimen shortage.

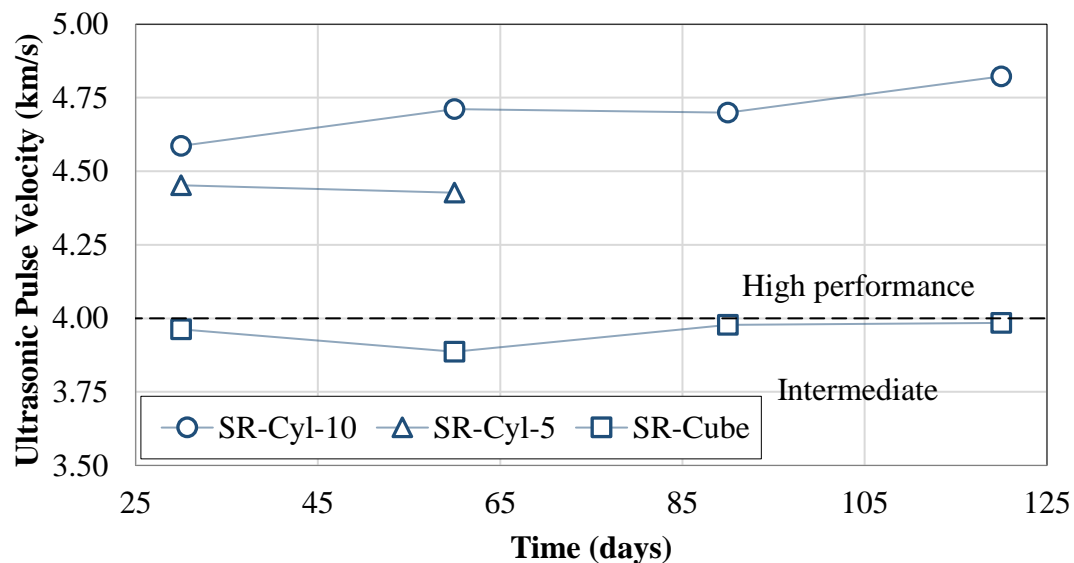


Figure 4. Average UPV vs. time experimental values for high performance mortar (SR)

As observed, UPV index maintained almost constant during the experimental time (from 25 to 120 days). But the UPV values for the three different dimensions were different between them, showing smaller values when 5 cm cubes were used as specimens (~3.95 km/s), followed by the values obtained with 5 x 10 cm cylinders (~4.44 km/s), and finally by the 10 x 20 cm UPV results (~4.70 km/s).

Based on the evaluation criteria for UPV index in Table 1, SR stayed at high performance mortar if the specimen length  $L \geq 10$  cm. If the specimen's length is less than 10 cm, same SR mortar shifted to an intermediate performance mortar.

The difference between the 5 x 5 cm cube and the 5 x 10 cm cylinder was about 12.4 %, and in regards to the 10 x 20 cm was about 19.0 %. Based on the present results and according to the

Table 1, it is recommended that the UPV index needs to be measured using long enough specimens ( $L \geq 10$  cm), because the small ones could produce measurement errors. This could be a consequence of the components of the commercial trademark mortar because the cylinders, that are bigger than the cubes, presented a better performance which means a better hydration of the cement.

In a recent investigation (Mejía et. al., 2018), the results between the size mortars are different too. In their investigation, cubes (5 x 5 x 5 cm) presented high performance. Two of the mortars presented an average of  $\pm 4.2$  km/s at 120 days, but the same mortars in 10 x 20 cm cylinder presented an average of  $\pm 3.85$  km/s at the same age. This could be a consequence of the cement that has been hydrated, if the specimen is small, the voids will disappear and the pulse of the lecture in this test will be quickly.

### 3.3. Total Void Content (TVC) index

Figure 5 presents the results obtained of TVC vs. time for the three different specimen geometries used. For TVC index, the specimens used were full size cubes and small cylinders. The third specimen shapes and dimensions used were 5 cm in height and slices cut from the 10 x 20 cm cylinders (SI-10).

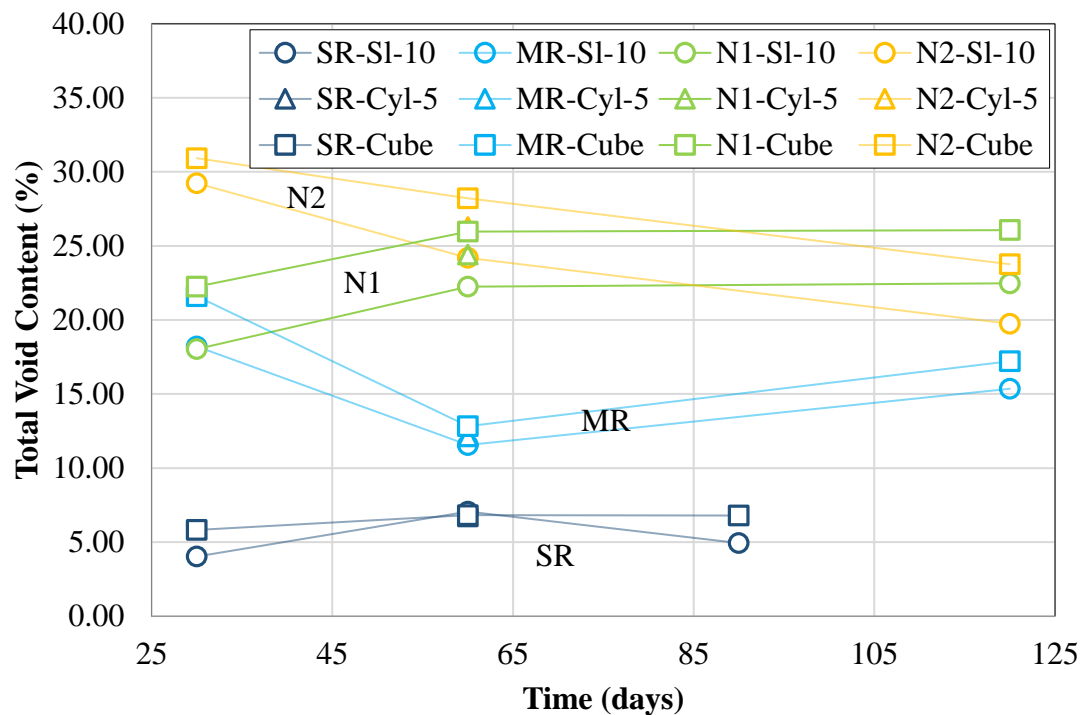


Figure 5. Average TVC index vs. time experimental values for low (N2), intermediate (N1, MR) and high performance (SR) mortars

A decision was taken on this dimension matter because all standardized methods to determine void content on hardened cement-based materials recommend using small specimens, such as 5 x 5 cm cubes or 5 cm slices cut from 10 x 20 cm cylinders. Therefore, it was tried to determine if full size small cylinders (5 x 10 cm) could provide differences in the results obtained.

As observed from Figure 5, low performance mortar N2 average TVC index was similar regardless of specimen shape (cube, cylinder or slice) and dimension, giving after 60 days and up to 120 days experimentation period values of 24.4 % in SI-10, 26.3 % in small cylinders 5 x 10 cm and 27.6 %

in cubes; (in accordance with the Table 1 performance criteria), with differences between specimens' shape and dimension  $\pm 10.5\%$ .

For intermediate performance mortars, N1 and MR, the TVC index results were similar regardless of the specimen shape (cube, cylinder or slice) and dimension, but have some interesting differences between them. Since N1 mortar was prepared as a typical cement-based mortar (cement, water, and sand), its average TVC index performance was quite similar to the low performance mortar (N2), showing values of about 24 % at 120 days, which correspond to low performance values as shown in Table 1.

At the other extreme, the MR mortar presented an average TVC index value of just 16 %, which correspond to performance values in the limit between intermediate and high performance mortar, as defined in Table 1. Finally, the SR mortar show an average TVC index values quite low of 6 % corresponding to the high performance limit presented in Table 1. This mortar also presented similar average TVC index values regardless of the specimen's shape and dimension.

### 3.4. Effective Porosity ( $\epsilon_{eff}$ ) index

The effective porosity performance in time is shown in Figure 6 as per effective porosity average values,  $\epsilon_{eff}$ . Average  $\epsilon_{eff}$  index with time for all mortar tested agreed with typical mortar performance: as curing time increase,  $\epsilon_{eff}$  decreases due to higher hydration degree of the cement paste in the mortar.

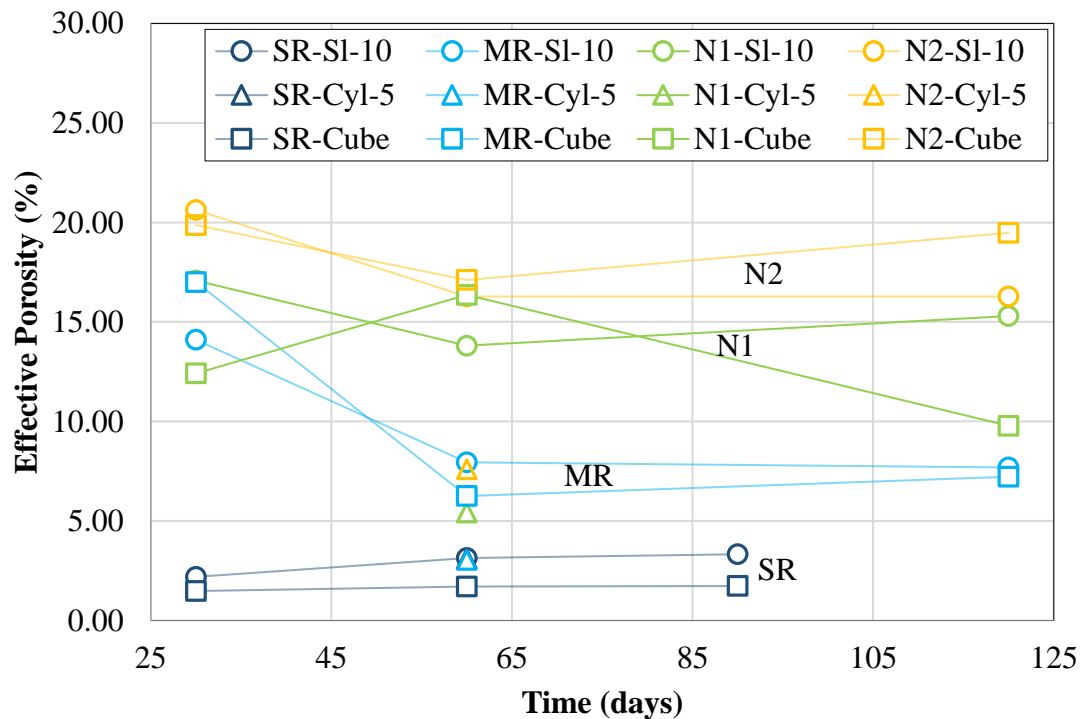


Figure 6. Average  $\epsilon_{eff}$  index vs. time experimental values for low (N2), intermediate (N1, MR) and the high performance (SR) mortars

Figure 6 also shows that the  $\epsilon_{eff}$  value differences between mortar type at 120 days of age: N2's  $\epsilon_{eff}$  between 16 % - 20 %, N1's  $\epsilon_{eff}$  of between 10 % - 16 %, MR's  $\epsilon_{eff}$  of about 7.5 %, and SR's  $\epsilon_{eff}$  of about 2.5 %. Therefore, it was observed that there was no difference on  $\epsilon_{eff}$  index values between N1 and N2, which supports TVC index values obtained (Figure 5). Compared against Table 1 the performance value ranges for this  $\epsilon_{eff}$  index, N1 and N2 index values obtained correspond to a low

performance mortar, the MR index values as intermediate performance mortar, and the SR index values as a high performance mortar.

Regarding the effect of shape and dimension of the specimens on the average  $\epsilon_{\text{eff}}$  index, the MR (intermediate performance) and SR (high performance) mortars did not show any difference between the three different specimens used. Furthermore, the low performance mortars, the N1 and the N2 for this particular index, presented quite some differences in the obtained values depending on the specimen shape and dimension, and in some cases (N1-Cube) an erratic performance (results presented ups and downs in time).

In N1 and N2 mortars the difference between small cylinders and the average of cubes and slices of 10 x 20 cm at 60 days was about 278 % and 220 %, respectively. This could be because the height of the small cylinders is larger than the cubes and the slices. Additionally, it is observed that after 60 days of curing, the 10 cm slices presented higher average  $\epsilon_{\text{eff}}$  index than the cubes, such effect could be due to the fact that the cement reacted faster in smaller specimens than in larger specimens such as 10 x 20 cm cylinders, where the slices were cut. Another possibility is that it could be due to a geometric effect: total volume of the specimen *vs.* its contact area effect on the water solution (cubes and 5 x 10 cm cylinders have this ratio smaller than slices cut from 10 x 20 cm cylinders). Therefore, the  $\epsilon_{\text{eff}}$  index might be affected from specimen shape and dimensions.

### 3.5. Compressive Strength (CS) index

The mechanical strength of the tested mortars was obtained using two specimen dimensions only, cubes and 10 x 20 cm cylinders. The average CS results *vs.* time of testing are exhibited in Figure 7.

In the same figure, the average CS index values obtained from the three different mortars are easily defined. The low performance mortar N2 presented average CS index values about 25 MPa; intermediate mortar N1 and MR show average CS index values of 40 MPa and 50 MPa, respectively; and the high performance mortar SR reached values between 60 MPa and 80 MPa. The average CS index values obtained compared to specimen's shape and dimensions (cube *vs.* 10 x 20 cm cylinder) for N1, N2, and MR mortars are similar: the differences between average values were less than  $\pm 10$  %.

The SR mortar presented an erratic performance of CS index values, as observed in Figure 7. This performance should be investigated in the near future, perhaps it is due to an apparent deficiency on the specimen preparation when the dimensions are large, such as the 10 x 20 cm.

The workability of this commercial available mortar during the mixing is quite low at the beginning, but after 15 minutes of being in the mixer, the mortar transformed in an almost liquid state, remaining like this if mixer is running. Afterwards, pouring of the mortar in the molds did not follow the standardized procedure (NMX-C-514-ONNCCE, 2016) because its highly fluid form, and due the fact that the mortar with the molds needs to be consolidated by a vibrating table. Therefore, additional testing on such specimen preparation with this specialized mortar need to be performed in the near future to get the best results of this material.

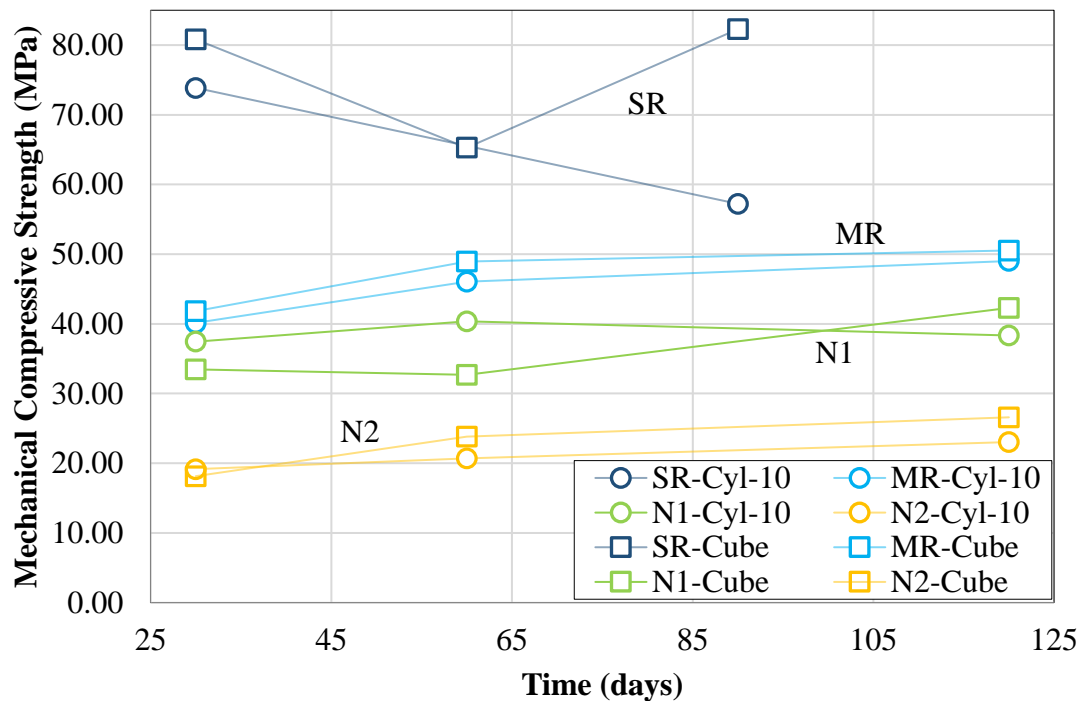


Figure 7. Average CS index vs. time experimental values for low (N2), intermediate (N1, MR) and high performance (SR) mortars

#### 4. CONCLUSIONS

This investigation presents an experimental program to determine if the durability index tests (WER, UPV, TVC, ( $\epsilon_{\text{eff}}$ ), and CS) are affected from specimen shape and dimension. Based on the results obtained, the following conclusions were drawn:

1. Wet electrical resistivity (WER), total void content (TVC), and compressive strength (CS) durability indexes were not affected by specimen's geometry and size.
2. Ultrasonic pulse velocity (UPV) and effective porosity ( $\epsilon_{\text{eff}}$ ) durability indexes were affected by specimen's geometry and size. It is recommended that the UPV index uses specimens with  $L \geq 10$  cm. Yet, in order to determine the  $\epsilon_{\text{eff}}$  index, the specimen height needs to be restricted to  $H \leq 5$  cm, regardless of specimen's shape (cube or slice).

#### 5. ACKNOWLEDGEMENTS

The authors wish to thank Universidad Autónoma de Querétaro (UAQ), Instituto Mexicano del Transporte (IMT), and Universidad Marista de Querétaro (UMQ) for allowing us the use of their laboratory equipment and facilities. We also acknowledge the Graduate Scholarship and financial support of Consejo Nacional de Ciencia y Tecnología (CONACYT) awarded to M.E. Visairo-Méndez. A special acknowledgment: Servicios Integrales (SICGA S.A. de C.V.), Movinco (Movinco S.A. de C.V.), and MasaRoca (MasaRoca S.A. de C.V.) for the provision of the commercial mortar materials.

The opinions and findings in this research are those of the author and not necessarily those of the funding agencies.

## 6. REFERENCES

- ASTM International. (1997), *ASTM C642 Standard Test Method for Density, Absorption, and Voids in Hardened Concrete*. <https://doi.org/10.1520/C0642-97>
- ASTM International. (2002), *C109/C109M Standard Test Method for Compressive Strength of Hydraulic Cement Mortars (Using 2-in, or [50-mm] Cube Specimens)*. [https://doi.org/10.1520/C0109\\_C0109M-02](https://doi.org/10.1520/C0109_C0109M-02)
- ASTM International. (2002), *ASTM C597 Standard Test Method for Pulse Velocity Through Concrete*. <https://doi.org/10.1520/C0597-02>
- ASTM International. (2003), *ASTM C 33 Standard Specification for Concrete Aggregates*. [https://doi.org/10.1520/C0033\\_C0033M-18](https://doi.org/10.1520/C0033_C0033M-18)
- ASTM International. (2004), *ASTM C1585 Standard Test Method for Measurement of Rate of Absorption of Water by Hydraulic-Cement Concretes*. <https://doi.org/10.1520/C1585-04>
- Bazant, Z. P. (2000). Size effect. *International Journal of Solids and Structures*, 37(1-2), 69-80. [https://doi.org/10.1016/S0020-7683\(99\)00077-3](https://doi.org/10.1016/S0020-7683(99)00077-3)
- Bazant, Z. P., Planas, J. (1997), “*Fracture and Size Effect in Concrete and Other Quasibrittle Materials*” CRC press. Florida, United States of America. <https://doi.org/10.1201/9780203756799>
- Calado, C., Camoes, A., Monteiro, E., Helene, P., Barkokébas Jr., B. (2015). Durability Indicators Comparison for SCC and CC in Tropical Coastal Environments. *Materials*. 8:1459-1481. <https://doi.org/10.3390/ma8041459>
- Helene, P., Pereira, F. (Ed.). (2003), “*Manual de Rehabilitación de Estructuras de Hormigón. Reparación, Refuerzo y Protección*”. CYTED XV: F Corrosión/impacto ambiental sobre materiales: Reparación, refuerzo y protección de estructuras de hormigón, Construction Chemicals, Degussa, Sao Paulo, Brazil.
- Medeiros-Junior, R. A., Munhoz, G. S., Medeiros, M. H. (2019), Correlations between water absorption, electrical resistivity and compressive strength of concrete with different contents of pozzolan. *Latin-American Journal of Quality Control, Pathology and Construction Recovery*. 9(2):152-166. <http://dx.doi.org/10.21041/ra.v9i2.335>
- Mejía, M., Torres, A. A., del Valle, A., Vázquez, V. E., Trueba, C., Martínez, M., Lomelí, M. G. (2018), Publicación Técnica 513 - Caracterización física y mecánica por desempeño de morteros de reparación, para su uso en la infraestructura del transporte de la SCT. *Secretaría de Comunicaciones y Transportes, Instituto Mexicano del Transporte, Coordinación de Ingeniería Vehicular e Integración Estructural*.
- Mendes, S. E., Oliveira, R. L., Cremonese, C., Pereira, E., Pereira, E., Medeiros-Junior, R. A. (2018), Electrical resistivity as a durability parameter for concrete design: Experimental data versus estimation by mathematical model. *Construction and Building Materials*. 192:610-620. <https://doi.org/10.1016/j.conbuildmat.2018.10.145>
- Mendoza-Rangel, J. M., Flores-Jarquín, J. M., De Los Santos, E. U., Garcés Terradillos, P. (2016), Durability of sustainable repair mortars exposed to industrial environments. *Latin-American Journal of Quality Control, Pathology and Construction Recovery*. 6(1):41-51. <http://dx.doi.org/10.21041/ra.v6i1.114>
- ONNCCE (1999), *NMX-C-414-ONNCCE-1999 Industria de la Construcción - Cementos Hidráulicos - Especificaciones y Métodos de Prueba*.
- ONNCCE (2016), *NMX-C-514-ONNCCE-2016 Industria de la Construcción - Resistividad Eléctrica del Concreto Hidráulico - Especificaciones y métodos de ensayo*.
- Shi, X., Xie, N., Fortune, K., Gong, J. (2012), Durability of steel reinforced concrete in chloride environments: An overview. *Construction and Building Materials*. 30:125-138. <https://doi.org/10.1016/j.conbuildmat.2011.12.038>

- Solís, R. G., Moreno, E. I., Arjona, E. (2012), Resistencia de concreto con agregado de alta absorción y baja relación a/c. *Latin-American Journal of Quality Control, Pathology and Construction Recovery*. 2(1):21-28. <http://dx.doi.org/10.21041/ra.v2i1.23>
- Torres, A. A., Castro, P. (2013), Corrosion-Induced Cracking of Concrete Elements Exposed to a Natural Marine Environment for Five Years. *Corrosion Engineering Section*. 69(11):1122-1131. <http://dx.doi.org/10.5006/0844>
- Torres, A. A., Castro-Borges, P. (2018), La filosofía para obtener obras de concreto durables. *IC Ingeniería Civil – Estructuras*. I(586):12-15.
- Torres, A., Fabela, M., Vázquez, D., Hernández, J., Martínez, M., Muñoz, A. (2002), Publicación Técnica 204 - Cambios en la rigidez y resistencia a la flexión de vigas de concreto dañadas por corrosión del refuerzo. *Secretaría de Comunicaciones y Transportes, Instituto Mexicano del Transporte, Coordinación de Ingeniería Vehicular e Integridad Estructural*.
- Troconis de Rincón, O., Romero De Carruyo, A., Andrade, C., Helene, P., Díaz, I. (Ed.). (1997), “Manual de inspección, evaluación y diagnóstico de corrosión en estructuras de hormigón armado”. CYTED, XV: B Corrosión/impacto ambiental sobre materiales: Durabilidad de la armadura, Río de Janeiro, Brazil.



## Fatigue service life of longitudinal reinforcement bars of reinforced concrete beams based on the real heavy traffic

F. Jr. R. Mascarenhas<sup>1\*</sup>  R. Chust Carvalho<sup>1</sup> 

\*Contact author: [fer.jr.resende@hotmail.com](mailto:fer.jr.resende@hotmail.com)

DOI: <http://dx.doi.org/10.21041/ra.v9i3.375>

Reception: 18/12/2018 | Acceptance: 15/07/2019 | Publication: 30/08/2019

### ABSTRACT

This paper analyzes the fatigue service life of longitudinal reinforcement in reinforced concrete bridge beams by considering the actual number of heavy vehicles from 2 to 6 axes in a railway in the state of São Paulo, Brazil. Theoretical models with a structural system composed by bridges with two simply supported beams and spans of 10, 15 and 20 meters are used. Ftool is used to determine the internal stresses, and the cumulative damage method in the estimation of the fatigue life. At the end, it is verified that the fatigue service life of the longitudinal reinforcement varies according to the size of the span, and in the three analyzed bridges the fatigue service life is less than 30 years.

**Keywords:** bridges; reinforced concrete; fatigue; service life; beams.

**Cite as:** Mascarenhas, F. Jr. R., Chust Carvalho, R. (2019), “*Fatigue service life of longitudinal reinforcement bars of reinforced concrete beams based on the real heavy traffic*”, Revista ALCONPAT, 9 (3), pp. 303 – 319, DOI: <http://dx.doi.org/10.21041/ra.v9i3.375>

<sup>1</sup> Civil Engineering Graduate Program (PPGECiv), Federal University of São Carlos (UFSCar), Brazil.

### Legal Information

Revista ALCONPAT is a quarterly publication by the Asociación Latinoamericana de Control de Calidad, Patología y Recuperación de la Construcción, Internacional, A.C., Km. 6 antigua carretera a Progreso, Mérida, Yucatán, 97310, Tel.5219997385893, [alconpat.int@gmail.com](mailto:alconpat.int@gmail.com), Website: [www.alconpat.org](http://www.alconpat.org)

Responsible editor: Pedro Castro Borges, Ph.D. Reservation of rights for exclusive use No.04-2013-011717330300-203, and ISSN 2007-6835, both granted by the Instituto Nacional de Derecho de Autor. Responsible for the last update of this issue, Informatics Unit ALCONPAT, Elizabeth Sabido Maldonado, Km. 6, antigua carretera a Progreso, Mérida, Yucatán, C.P. 97310.

The views of the authors do not necessarily reflect the position of the editor.

The total or partial reproduction of the contents and images of the publication is strictly prohibited without the previous authorization of ALCONPAT Internacional A.C.

Any dispute, including the replies of the authors, will be published in the second issue of 2020 provided that the information is received before the closing of the first issue of 2020.

## Vida útil à fadiga da armadura longitudinal de vigas de pontes de concreto armado frente ao tráfego real de veículos pesados

### RESUMO

Este trabalho analisa a vida útil à fadiga da armadura longitudinal em vigas de pontes de concreto armado considerando-se o número real de veículos pesados de 2 a 6 eixos em um trecho rodoviário do estado de São Paulo, Brasil. Utilizou-se modelos teóricos com um sistema estrutural com pontes com duas vigas biapoiadas com vãos de 10, 15 e 20 metros. Para determinação dos esforços emprega-se o software Ftool e na estimativa da vida útil à fadiga o método do dano acumulado. Ao fim, verifica-se que o tempo de vida útil à fadiga da armadura longitudinal varia de acordo com o tamanho do vão, sendo que nas três pontes analisadas a vida de serviço à fadiga é inferior a 30 anos.

**Palavras-chave:** pontes; concreto armado; fadiga; vida útil; vigas.

## Vida útil a la fatiga de la armadura longitudinal de vigas de puentes de hormigón armado frente al tráfico real de vehículos pesados

### RESUMEN

Este documento analiza la vida de servicio a la fatiga del refuerzo longitudinal en vigas de puentes de concreto reforzado considerando el número real de vehículos pesados de 2 a 6 ejes en un tramo de carretera en el estado de São Paulo, Brasil. Se utilizan modelos teóricos en un sistema estructural de puentes con dos vigas doblemente apoyadas en tramos de 10, 15 y 20 metros. Para la determinación de los esfuerzos se utiliza el software Ftool y en la estimación de la vida útil a la fatiga o daño acumulado. Al final, se verifica que el tiempo de vida a la fatiga del refuerzo longitudinal varía según el tamaño del tramo, siendo que en los tres puentes analizados la vida de servicio a la fatiga es inferior a 30 años.

**Palabras clave:** puentes; concreto armado; fatiga; vida útil; vigas.

## 1. INTRODUCTION

Nowak and Fischer (2016, p. 297) state that the traffic infrastructure “not just ensures economic performance and efficiency, but also provides mobility and quality of life to the population, hence decisively contributing to the country’s wealth”.

According to Brazilian National Confederation of Transport (CNT, 2018), the road freight transport in Brazil corresponds to 61.1%, and the transport of people corresponds to 82.8% of the total. Bridges and viaducts are directly affected by the predominance of railway mode transport. Beyond being very important in the transport systems, ensuring the proper functioning and safety of these structures has an impact on the socioeconomic developments of surrounding cities and even of a country (Zhou; Chen, 2018; Bastidas-Arteaga, 2018).

Permanent loads, such as self-weight, and the moving loads, which are represented by the vehicles that commute on those structures, are some of the actions acting on bridges and viaducts. (Schneider; Marx, 2018). The annual number and weigh of the road freight vehicles in Brazilian and worldwide highways have been increasing (Pircher et al., 2011; Han et al., 2015; Deng et al., 2016; Han et al., 2017).

This growth has generated several problems in the constituent elements of bridges and viaducts. Among the structural problems that bridges and viaducts are susceptible, the fatigue needs to be

highlighted (Pimentel et al., 2008; Baroni et al., 2009) because the variability and the regime of moving loads make these structures more likely to suffer from this phenomenon.

Liu and Zhou (2018) confirm what has been presented above, and they advocate that “the research on the fatigue problem of reinforced concrete beams is of great significance to the design, maintenance and reinforcement of bridges” (Liu; Zhou, 2018, p. 3512).

Based on this, using the real and actual traffic data from a highway, the fatigue service life of the longitudinal reinforcement bars of beams of three theoretical reinforced concrete bridges with different span sizes will be estimated. Those bridges will be designed according to the Brazilian Code NBR 7188 using the Brazilian Load Model TB 450, which represents a vehicle with 450 kN of total loading (Brazilian National Standards Organization, ABNT, 2013).

### 1.1 Methodology

As theoretical reference will be used digital scientific articles from journals and congresses in both Portuguese and English languages. Moreover, books, which are references in the area of study, will be used; national and international relevant Codes, such as ABNT NBR 7188:2013, the current Brazilian Code of “Road and pedestrian live loads on bridges, viaducts, footbridges and other structures”, and the Brazilian Code ABNT NBR 6118:2014 - Design of concrete structures — Procedure. The numerical evaluations performed in this research will be made through Analytical Methods using the mathematical equations described in item 2 of this paper. Fatigue life will be determined using the Fatigue Damage Accumulation methodology (Miner's rule), and the bending moments will be determined in the middle span of the reinforced concrete beams using the structural analysis finite element software Ftool (FTOOL, 2008). The choice to use Ftool is because it is a free tool and is widely used in technical and academic projects, either as a pedagogical tool or in the scientific environment.

## 2. FATIGUE

According to NBR 6118, “fatigue is a phenomenon associated with repeated dynamic actions, which can be understood as a process of progressive and permanent modifications of the internal structure of a material subjected to oscillation of stresses resulting from these actions” (ABNT, 2014, p. 193). Habeeba et al. (2015, p. 2561) explain that the “fatigue is a progressive deterioration of a structure by crack growth, due to a series of stress variations (cycles) resulting from the application of repeated loads, such as induced in bridge components under traffic loads and heavy vehicle crossings”, and those cycles can be low or high (Habeeba et al., 2015, p. 2561).

The stress range is given by the difference of the maximum and minimum stresses, and it is expressed by the following equation (1):

$$\Delta\sigma = \sigma_{\max} - \sigma_{\min} \quad (1)$$

Where:  $\Delta\sigma$  is the stress range;  $\sigma_{\max}$  is the maximum stress and  $\sigma_{\min}$  is the minimum stress.

The stress ratio R between the stresses is given by:

$$R = \frac{\sigma_{\min}}{\sigma_{\max}} \quad (2)$$

Among the different methodologies adopted in the fatigue analysis, the principle of linear damage accumulation according to Miner's rule will be used. This methodology will be adopted due to the fact that in the fatigue of bridges occur random (non-uniform) stress cycles (Santos, Pfeil, 2014).

Pimentel et al. (2008) and Wang et al. (2013) state that the cumulative damage in fatigue  $D$  linearly relates the number of cycles experienced  $n$  to the number of cycles required to cause the structural failure  $N$ :

$$D = \sum_{i=1}^k \frac{n_i}{N_i} \quad (3)$$

Where:  $D$  is the cumulative damage;  $n_i$  is the number of experienced cycles;  $N_i$  is the number  $N$  of necessary cycles required to cause the structural failure due to fatigue. Wang et al. (2013, p. 3) explains that  $D$  is “linearly proportional to  $n_i$  to each stress range  $\Delta\sigma_i$ ”

Freitas (2014, p. 24-24) comments that “the use of Fatigue Damage Accumulation Methodology has as main advantage its rigor, due to the absence of conversion and simplification equations”. The author also points out that “when the study focusses on a reduced number of elements, the use of this method can be viable”, as it is the case of this research that analyzes reinforced concrete beams (Freitas, 2014, p. 24-25).

Branco et al. (1999) remark the following conclusions about the results that can be obtained to the cumulative damage  $D$ :

- $D > 1$  – The fatigue life of the analyzed structural element is less than the designed one, so, the structural failure due to fatigue will occur during the stipulated (designed) service life, which requires that measures are taken to delay and or control such a process;
- $D = 1$  – The fatigue life due to fatigue of the analyzed structural element is the designed one;
- $D < 1$  – The fatigue life due to fatigue is higher than the designed one, so the structural member has a fatigue life, or a residual life (RL).

Based on the determination of the cumulative damage, it is possible to determine the fatigue service life (VU):

$$VU = \frac{1}{D} \quad (4)$$

In this context, it is relevant to clarify the concepts of Functional Life and Design Service Life. Branco and Paulo (2012, p. 2) advocate that “the characterization of the life of a bridge must begin by defining its functional life, in other words, the characterization of the intended maximum traffic capacity” during the service life of bridges and viaducts.

The authors also explain that the “service life is frequently less than the structural life of the bridge” and, once the problems start to happen, these structures must undergo a rehabilitation process, “for example, increasing their width or building a new bridge near” that bridge with certain issues, “ensuring the maintenance of the functional quality of the crossing” (Branco, Paulo, 2012, p. 2).

It has been claimed by Branco et al. (2013, p. 5) that the Design Service Life “is associated with the safety conditions and use of the structure, namely ensuring that no collapse, excessive deformation, etc. occur”. Branco and Paulo (2012) indicate that bridges and viaducts used to be designed to have a service life of 50 years, however, nowadays, this lifespan went to 75 years, and in some countries and depending on the significance of the work, from 100 to 120 years. Therefore, the fatigue service life is related to the structural life of the bridge under the fatigue aspect.

The called S-N Curves or Wöhler Curves, which are also used in the fatigue life assessment, are graphical representations that relate the modulus of stress ( $S$ ) to the number of cycles ( $N$ ) required to cause the failure of the material and are plotted from experimental data (Pereira, 2006; Baroni, 2010).

## 2.1 Fatigue of concrete

The Brazilian Code NBR 6118 (ABNT, 2014, p. 192) advocates that the fatigue life assessment of bridges needs to be done using the frequent combination of actions, even though the fatigue phenomenon “is controlled by the accumulation of the deleterious effect of repeated loads”, in other words, by the cumulative damage method. Hence, the frequent combination of actions is given by equation 5:

$$F_{d,ser} = \sum_{i=1}^m F_{gik} + \psi_1 \cdot F_{q1k} + \sum_{j=1}^n \psi_{2j} \cdot F_{qjk} \quad (5)$$

Where:  $F_{d,ser}$  is the design value of the actions to the Service Limit State (SLS);  $F_{gik}$  are the permanent loads;  $F_{q1k}$  is the main living load;  $F_{qjk}$  are the secondary living loads;  $\psi_1$  is the reduction factor of frequent combination;  $\psi_{2j}$  is the reduction factor to the transient combination; moreover,  $\psi_1$  is equal to 0,5 to beams.

Fatigue loads of high intensity, which can cause damage under 20,000 cycles, are not studied by NBR 6118 (ABNT, 2014), and only the actions of medium and low intensity and the number of receptions up to 2,000,000 cycles are addressed by the Brazilian Code. According to the NBR 6118 (ABNT, 2014, p. 193), “for the consideration of the spectrum of actions, it is accepted that those of vehicles with full load up to 30 kN may be excluded in the case of road bridges”.

Schlaflli and Bruhwiler (1998), Ray and Kishen (2014) and Ruiz et al. (2015) hold the position that the mechanic behavior of reinforced concrete elements is closely connected to the reinforcement behavior. Then, the failure of the structure is associated to the failure of the reinforcement that, most of the time, happens under bending moments (Schlaflli; Bruhwiler, 1998, Ray; Kishen; 2014, Ruiz et al., 2015).

Maggi (2004, p. 8) shows that the fatigue of concrete “starts in a microscopic scale, and it is associated to the increase of cracks opening and the stiffness reduction”. Among the factors that influence the fatigue strength of concrete include: “stress range, loads history, material properties, loads frequency, stress gradient and backlash periods” (Maggi, 2004, p. 8).

Zanury et al. (2011) point out that, in a big picture, the repeated cycles acting on a structural member cause stiffness reduction due to excessive cracking and deformation. This loss of stiffness is due to the degradation of concrete in its compressed region and the reduction of the called “tension stiffening”. Junges (2017, p. 91) states that “the term tension stiffening refers to the ability of concrete to carry tensile stresses between cracks due to the transfer of forces from the reinforcement bars to the concrete through adhesion”.

The figure 1 presents the reduction of the tension stiffening as the number of cycles increases, based on tests made by Zanuy et al. (2011). Analyzing this figure, it is possible to highlight two important aspects: as the number of cycles increases, it gets closer to the pure State II; and the gradual reduction of the tension stiffening is due to the loss of adhesion between steel bars and concrete.

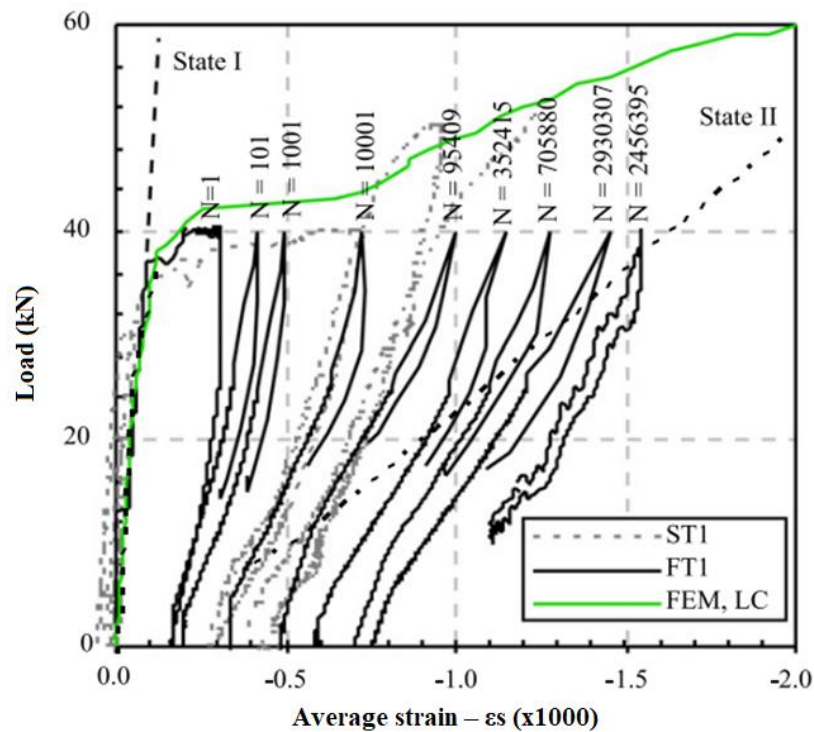


Figure 1. Fatigue failure in a reinforced concrete element (Zanuy et al., 2011)

### 2.1 Fatigue in the reinforcement bar

Schlaflli and Bruhwiler (1998) establish that the fatigue propagation can be divided in two stages. At the first stage the cracks propagation is stable; at second stage it is seen a brittle fracture in the remaining section (Schlaflli; Bruhwiler, 1998). The American Code ACI 215R-74 affirms that the fatigue in the reinforcement is the one that generate major concerns to engineers (ACI, 1997). Baroni (2010, p. 42) indicates that “the factors that influence the supporting capacity of steel bars to fatigue are: minimum stress”, diameter, curvature and seam of the bars and the type of beam. Therefore, fatigue service life in the steel bars reinforcement can be estimated by the equation (Santos, Pfeil, 2014, p. 41):

$$N = N_{fad} \cdot \left( \frac{\Delta\sigma_{fad}}{\Delta\sigma} \right)^m \tag{6}$$

$N_{fad}$  is equal to  $10^6$ ;  $\Delta\sigma_{fad}$  is equal to  $\Delta f_{sd,fad}$ ;  $m$  is the path slope, according to figure 2 (Junges, 2017), given by NBR 6118:2014. The values of  $\Delta f_{sd,fad}$  are given by Table 23.2 from NBR 6118:2014. The maximum and minimum stresses in the reinforcement steel bars can be determined using the following equations:

$$\sigma_{s,max} = \alpha_E \cdot \frac{M_{max} \cdot x_i}{I_{II}} \tag{7}$$

$$\sigma_{s,min} = \alpha_E \cdot \frac{M_{min} \cdot x_i}{I_{II}} \tag{8}$$

Where:  $\sigma_{s,max}$  is the maximum compression stress in the bar;  $\sigma_{s,min}$  is the minimum compression stress in the bar;  $x_i$  is the distance of neutral axis to the bottom of the beam;  $\alpha_E$  is the ratio between the modulus of elasticity of steel reinforcement bars and concrete.

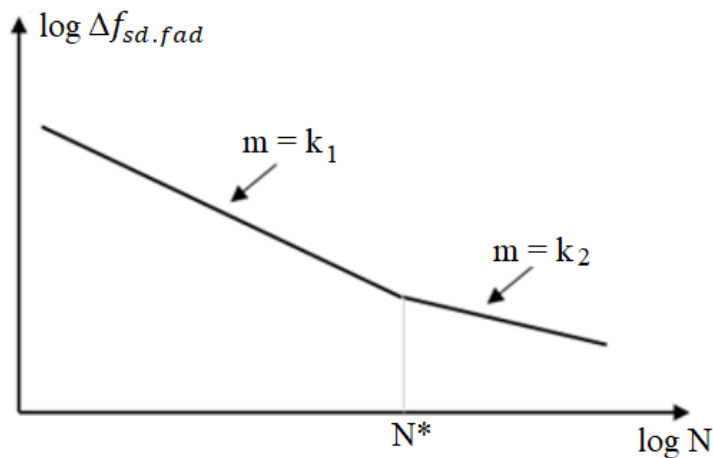


Figure 2. Fatigue characteristic resistance curves (S-N curves) for steel (Junges, 2017)

In this research it will be used passive reinforcement bars, the S-N curves can present two values,  $k_1 = 9$  e  $k_2 = 5$ . From this, the constants  $Const_1$  and  $Const_2$  can be determined for both curves through the following equations

$$Const_1 = (\Delta\sigma_{sd, fad})^5 \cdot N \tag{9}$$

$$Const_2 = (\Delta\sigma_{sd, fad})^9 \cdot N \tag{10}$$

For different values of  $\Delta f_{sd, fad}^f$ , to  $10^6$  cycles, the constants are given according to table 1.

Table 1. Values de  $\Delta f_{sd, fad}$

$\Delta f_{sd, fad, min}$ (MPa)	$Const_1$	$Const_2$	$\Delta f_{sd, fad}$ (MPa)
<b>190</b>	3.64E+17	6.45E+26	205.21
<b>185</b>	3.18E+17	5.08E+26	199.81
<b>180</b>	2.78E+17	3.97E+26	194.41
<b>175</b>	2.41E+17	3.08E+26	189.01
<b>165</b>	1.80E+17	1.81E+26	178.21
<b>150</b>	1.12E+17	7.69E+25	162.01

Source: Own Author (2019).

Hence, every time that  $\Delta\sigma_s$  is huger than  $\Delta f_{sd, fad}$ , the steel reinforcement areas must be multiplied by the fatigue coefficient k.

$$k = \frac{\Delta\sigma_s}{\Delta f_{sd, fad}} \quad (11)$$

### 2.3 Fatigue in reinforced concrete bridges

Zhang et al. (2012) state that the economic growth that China has passed in the last years has contributed directly to the significant increase in heavy vehicles traffic on the country's highways. This fact implies in the fatigue resistance of highway bridges and viaducts. Through the conducted studies, the authors obtained some conclusions. First, they claim that the Miner's rule is adequate and a "is a reasonable and practical method for determining the fatigue damage coefficient" of simply supported beams (Zhang et al., 2012, p. 793).

The authors also concluded that "it is recommended that the fatigue damage coefficient be updated to the new" Chinese road bridge moving load code for bridges with spans less than 20 m (Zhang et al., 2012, p. 793).

Rossigali et al. (2015, p. 124) claim that there is a growing concern and search for load models more compatible with reality "for highway bridge design in Brazil", and those models "are under development by assembling real traffic database, traffic simulations, analytical-numerical modeling of the dynamic interaction between vehicle and structure and statistical extrapolations". Considering this statement, the authors analyzed small span reinforced concrete bridges with two lanes single carriageway under different traffic scenarios.

The authors used structural reliability techniques and probability distributions to analyze the real flow of vehicles. At the end, they had concluded that the current live load model given in the current Brazilian code NBR 7188:2013 "is not appropriate to represent the actual traffic effects and may be, in some cases, non-conservative" (Rossigali et al., 2015, p. 124).

Alencar et al. (2016, p. 2) hold the position that "the imposition on the structure of new traffic conditions associated with material fatigue behavior can lead to structural damage with different levels of severity, and as the magnitude of the loads carried increases, the problem becomes even more relevant".

Wan et al. (2015) and Xin et al. (2017) also present arguments to emphasize that stating that the authorities and structural engineers have been paying more attention to the process of fatigue arising from the increase of heavy vehicles on the highways and their speed.

Almeida and Fortes (2016), Mota et al. (2018) and Camargo et al. (2018) demonstrate that the loads from the most recent actual vehicles commuting on Brazilian highways may be higher than those calculated by TB 450.

More recent researches such as that developed by Deng and Yang (2018) have dealt with the formulation of methods for determining the permission and legal weight limits for heavy vehicles considering the accumulated fatigue damage on bridges. The authors obtained results related to fatigue damage for different stress variations in their studies, and they indicate that those results "can be used to determine the weight limit for both new and existing bridges" (Deng; Yan, 2018, p. 7).

Braz et al. (2018, p. 1) analyzed "four models reinforced concrete bridge build with two beams based on the Brazilian and European codes", and the four bridges are "hyperstatic, with  $f_{ck}$  of 50 MPa, CA-50 steel and main spans of 20 m". Analyzing and comparing the results, the authors concluded that:

The European normative treatment proved to be more conservative than the Brazilian one regarding reinforcement fatigue and design. This behavior is a reflection of the European regulatory rigor that adopts design vehicles and load coefficients specific to the fatigue, as well, only one fatigue strength value for different reinforcement diameters (Braz et al., 2018, p. 10).



### 3. HEAVY VEHICLES DATABASE

In order to carry out the relevant assessments and calculations related to the fatigue process, the actual annual traffic volumes information between the years of 2009 to 2017 are used, and they were provided by CCR RodoAnel, which manages 29.30 kilometers of the western stretch of the highway Mario Covas, which integrates the Raposo Tavares, Castello Branco, Anhanguera, Bandeirantes and Régis Bittencourt highways” (CCR RODOANEL, 2018). The data collected refers to the annual number of road freight vehicles with 2 to 6 axes, according to the table 2.

Table 2. Annual Commercial Vehicle Traffic

Year	Vehicle of 2 axes	Vehicle of 3 axes	Vehicle of 4 axes	Vehicle of 5 axes	Vehicle of 6 axes
2009	5,531,774	3,306,437	1,180,226	663,505	889,091
2010	6,476,748	4,213,663	1,874,607	1,995,312	1,773,380
2011	3,820,060	4,652,486	2,169,154	2,170,282	2,109,843
2012	7,097,189	4,775,874	1,344,816	2,082,505	2,289,120
2013	6,208,545	5,072,068	1,792,046	2,492,961	3,194,281
2014	5,309,203	5,258,467	883,935	2,796,359	4,004,225
2015	5,008,912	2,540,180	856,232	2,487,752	4,076,946
2016	4,714,630	4,142,964	816,219	2,226,043	3,817,949
2017	4,718,774	3,941,475	988,906	2,205,195	3,898,191

Source: CCR RODOANEL (2018).

### 4. RESEARCH METHOD

For the calculations and verification due to fatigue, it is used a theoretical model with a structural system with a bridge with two simply supported beams with spans  $L$  by 10 m, 15 m and 20 m, respectively named V10, V15, V20. The choice for bridges made only with 2 beams is because Brazil still has a great number of old bridges and viaducts built with 2 beams. According to data from National Department of Transport Infrastructure (DNIT, 2017), 12.95% of the bridges and viaducts have spans up to 10 m and 16.40% from 10.01 to 20 m. Furthermore, 86.28% of the Brazilian bridges and viaducts have width up to 13 m (DNIT, 2017). The “Manual de Inspeção de Pontes Rodoviárias” (DNIT, 2004) states that bridges and viaducts build in Brazil after 1985 must have transverse section with total width of 12.80 m and lane width of 12.00 m. Based on this, the cross section of 12.80 m will be adopted for the three spans analyzed in this paper.

Two single carriageways are assumed for all analyzed bridges. Moreover, following the guidelines from “Manual de Projeto de Obras-de-Arte Especiais” (DNER, 1996), each carriageway will have adopted dimension of 3.60 m, totalizing 7.20 m of width, and 2.40 m to each shoulder. The figure 3 demonstrates the transverse cross section of the three bridges.

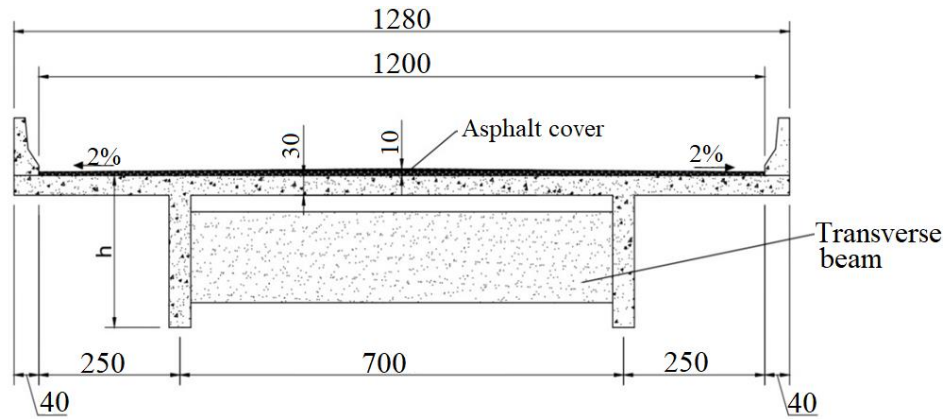


Figure 3. Cross section of the bridge (dimensions in centimeters) (Own Author, 2019).

There are intermediate transverse beams placed in each 5 m with constant width of 0.30 m and high of 0.80 m. The transverse beams are not connected to the slabs, so they have the locking function only. Due to the simplification of the calculations, the following hypotheses are adopted: the bridge slab is not usually of constant thickness, but in this research the slab thickness is adopted as constant; constant thickness is adopted for the 10 cm asphalt cover. The “T” section of the beams used is shown in figure 4.

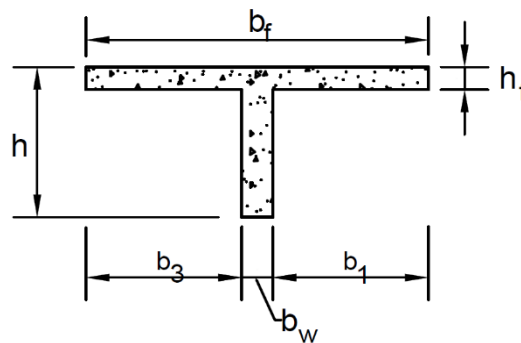


Figure 4. Cross section of the beams (Own Author, 2019).

The table 3 presents the adopted values to the transverse cross sections of the three studied bridges, and table 4 demonstrates the properties of the materials used.

Table 3. Bridge beam cross-sectional dimension values

Bridge	$b_1$ (cm)	$b_3$ (cm)	$b_w$ (cm)	$b_f$ (cm)	$h_f$ (cm)	$h$ (cm)
V10	100	100	35	235	30	100
V20	200	200	35	435	30	200
V30	300	300	35	635	30	300

Table 4. Properties of the materials

Concrete		Steel	
$f_{ck}$ (MPa)	$f_{yk}$ (MPa)	$f_{yk}$ (MPa)	$E_s$ (MPa)
35,0	500,0	500,0	210.000

#### 4.1 Brazilian load train

Regarding the positioning of the Brazilian load train, TB 450, the Brazilian Code NBR 7188:2013 clarifies that it can assume any position along the entire cross section of the bridge where there is a road lane, provided the wheels are in the most unfavorable position, “including shoulder and safety bands”. The distributed load must also be applied in the most unfavorable position, “regardless of the road lanes” (ABNT, 2013, p. 4). Figure 5 shows the TB 450 vehicle positioned in the most unfavorable section of the bridge cross section. The same position is assumed for the three bridges studied in the paper.

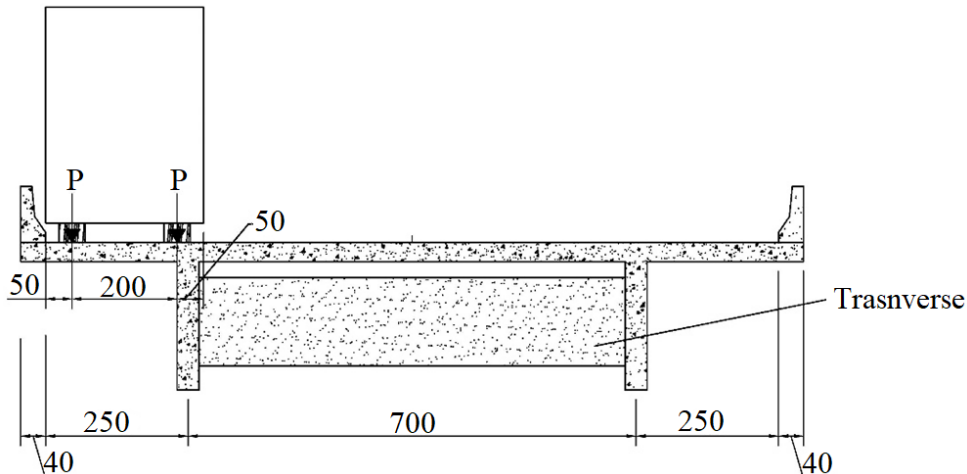


Figure 5. Load train vehicle TB 450 in cross-sectional for maximum stress on the left beam of the figure (dimensions in centimeters) (Own Author, 2019).

This critical position is determined using the technique of influence lines, and a simplified model already established that can be seen in numerous publications such as Carvalho (2017). In this case, the support reaction line of influence is used, thus, considering the load train (TB 450) in the position that leads to the greatest reaction of the studied beam, it is possible to determine the set of loads named longitudinal load train (“trem tipo longitudinal”, the original name is Brazilian Portuguese, TTL), which the bending moment forces of the beams will be determined with.

Regarding the determination of the moments, in this case the bending one, using the TB 450, the following considerations are made:

- a) Following the guidelines of NBR 6118 2014, item 23.5.3, the combination of actions to be considered will be frequent. Therefore, the maximum and minimum moments arising from the combinations of permanent and living loads in the middle of the beam span will be given by the frequent combination of actions;
- b) It is considered the diameter of the 25 mm of the steel reinforcement bar.

#### 4.2 Actual traffic

The vehicles that commute, over the bridge's lifetime, can assume various positions in its cross-section, which ultimately generate different internal stresses in the beams according to the position in which the moving loads are.

Toledo (2011) evaluated the positioning of real vehicles on highways in relation to traffic lanes. The author concluded that “the analysis with the vehicle on the centered lane is a good approximation for the calculation of the fatigue life of the structure, since the results obtained for this case were more unfavorable than for the vehicle in a eccentric position” (Toledo, p. 63, 2011). Eurocode 1: Actions on structures – Part 2: Traffic loads on bridges (2002) states that for the cross-sectional assessment of the vertical loads of real vehicles traveling on the highways, half of them

travel centered on the traffic lane and the others are distributed symmetrically along the lane, as shown by the frequency distribution of vehicle transverse positioning in a bridge shown in figure 6 (EUROCODE 1, 2002).

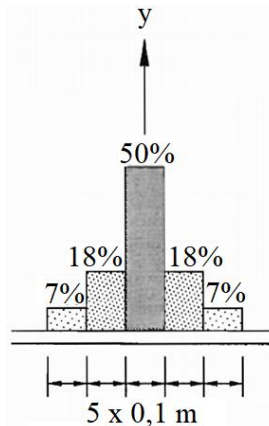


Figure 6. Frequency distribution of vehicle transverse positioning in the bridge

This research adopts the following considerations in the living load model of real vehicles:

- The procedure for determining the maximum TTL is the same as for the TB 450 vehicle; however, the actual freight vehicles are positioned as shown in figure 7;
- Crosswise the vehicles shall have the same dimensions as shown in Figure 7;
- 100% of the vehicles are positioned in the center of the traffic lane;
- It is considered to be only a freight vehicle traveling on the bridge;
- The bending moment and other calculations consider the loads due to the actual freight vehicles and the distributed loads according to NBR 7188 (ABNT, 2013), representing the small vehicles that can follow the passage of the freight vehicles;
- Moments arising from actual freight vehicles are not weighted by the Frequent Combination Reduction Factor for Service Limit State (ELS)  $\psi_1$  because NBR 6118 (ABNT, 2014) does not provide for such a procedure for actual loads.
- Each vehicle generates a stress cycle, which is used to determine the fatigue life by the Cumulative Damage Method.

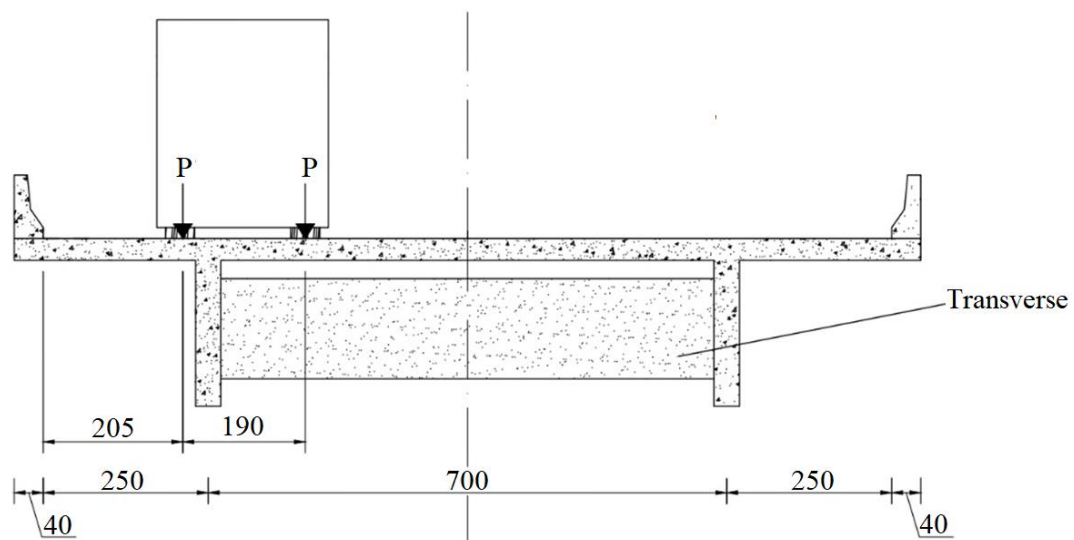


Figure 7. Transverse position adopted for the actual freight vehicles (dimensions in centimeters) (Own Author, 2019).

### 5. ANALYSIS OF RESULTS

Using the normative load train TB 450 and vehicles from 2 to 6 axes, the maximum bending moments in the middle of the beam span for the three types of bridges is calculated. It is important to mention that the values calculated for moving (living) loads are multiplied by the impact coefficient (CI), according to the Brazilian code, that varies according to the size of the span. Table 5 presents the bending moments calculated due to bridges own weight and the moving loads for the simply supported structures.

Table 5. Calculated bending moments for the simply supported beams

Bending moments in the middle of the span (kN.m)								
Beam	CI	Permanent load	TB 450	Vehicle of 2 exes	Vehicle of 3 exes	Vehicle of 4 exes	Vehicle of 5 exes	Vehicle of 6 exes
V10	1.35	1162.1	1251.3	443.1	541	563.9	632.1	585.9
V15	1.33	2725.5	2269	881.6	1051.2	1143	1261.1	1192.3
V20	1.27	5096	3130.1	1447.5	1688.8	1849.6	2037.9	2002.8

In determining the number of cycles N to fatigue in steel, it is necessary to determine the value of “m” of the S-N curve. As the calculated stress range in steel is less than the limit stress variation for the diameter of 25 mm, which is 17.5 kN/cm<sup>2</sup>, m is equal to 9.

The figure 8 presents the consumed life of each respective year analyzed for each bridge. In addition, in table 6 are presented the estimated fatigue service life of the longitudinal reinforcement steel bars, showing the consumption of fatigue resistance over the nine years considered, and the time required to reach 100% of consumption.

It is important to mention that the results presented do not consider the previous fatigue damage or any other previous damage, only during the 9 years of data considered; hence, the bridges are considered as new ones.

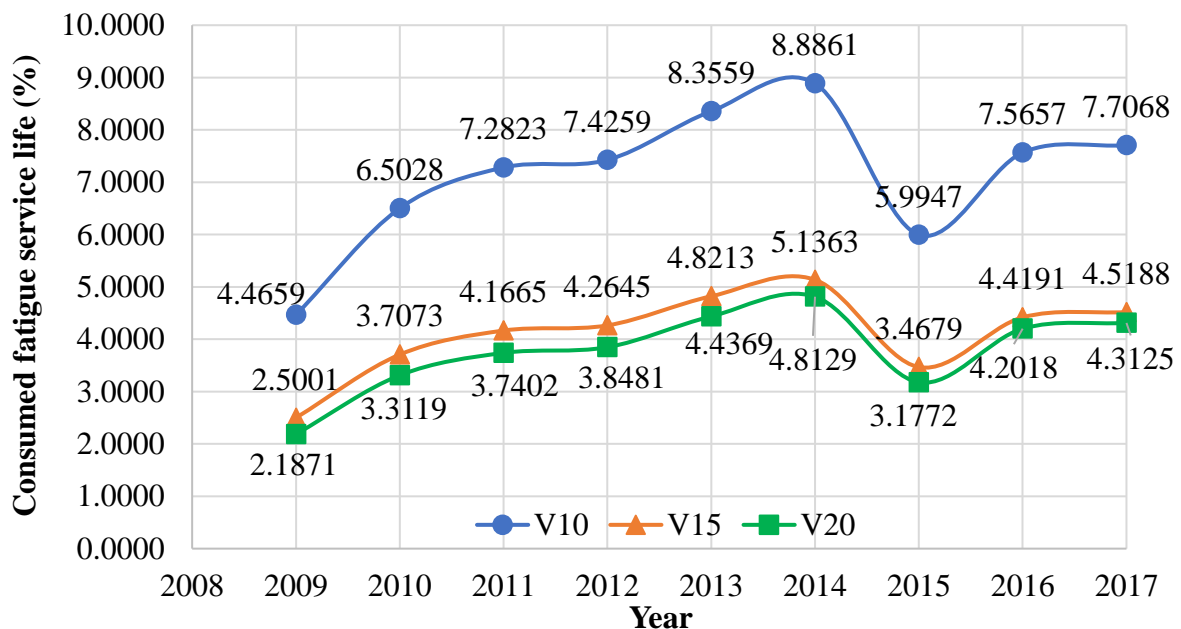


Figure 8. Consumption of longitudinal reinforcement fatigue service life (Own Author, 2019).

Table 6. Fatigue service life of the steel reinforcement

Bridge	Consume in 9 years (%)	100% of consume (years)
V10	64.19	14.02
V15	37.00	24.32
V20	34.03	26.45

Because it is a high vehicle flow per year, with an average annual traffic of 16,200,000, the three analyzed bridges presented fatigue service life of less than 30 years, to the longitudinal reinforcement. Moreover, it is verified that the consumption of 100% of the fatigue strength in the longitudinal reinforcement varies according to the span, and the smaller the span, shorter fatigue service life.

To increase the fatigue life of the steel reinforcement bars, one or some of the following possibilities are suggested: 1) Increase the number of beams; 2) Change the cross section of the analyzed bridges; 3) Modify the dimensions of the transverse profile of the beams; 4) Increase the compressive strength characteristic of concrete; 5) Review the procedures for verification and/or fatigue design of railway bridge beams present in Brazilian codes.

## 6. CONCLUSIONS

Based on the analyzes performed in this article, it is possible to conclude that although the normative vehicle TB 450 presents bending moments in the middle of the span greater than those presented for those actual vehicles considered here, in the bridges analyzed in this paper, the high number of vehicles in the analyzed section requires attention to the fast consumption of fatigue resistance.

The required times to achieve 100% of fatigue service life consumption in the longitudinal reinforcement bars on the three analyzed bridges have different values, but all would have fatigue life less than 30 years. This result is critical and worrisome, especially if it is considered a design service life from 50 to 80 years.

Therefore, it is necessary to adopt certain measures to increase the fatigue life of these reinforced concrete bridges simply supported, such as using a larger number of beams per deck of bridge and/or modifying the beam cross section.

Furthermore, the high age of Brazilian bridges and viaducts must be considered because the analyzes and calculations performed here consider that the bridges are new, whose damages are only those presented over the nine years analyzed. Hence, special attention should be given to these aged structures.

## 7. ACKNOWLEDGMENTS

The authors gratefully acknowledge Coordination for the Improvement of Higher Education Personnel (CAPES), associated to the Brazilian Ministry of Education, for its support through the scholarship granted to the corresponding author, allowing the most beneficial development of this research.

We are also grateful to CCR RodoAnel for its kindness in providing the data about the number of heavy vehicles, which were fundamental to the realization of this article, and to Civil Engineering Graduate Program (PPGECiv), of UFSCar, for all the support that has been provided.

## 8. REFERENCES




- Alencar, G., et al. (2016), “*Análise Dinâmica e Verificação à Fadiga dos Viadutos de Acesso da Nova Ponte Ferroviária Sobre o Rio Sado*” in: Iberian Latin American Congress in Computational Methods in Engineering, ABMEC, Brasília (Brasil), pp. 1-16.
- Almeida, E. P., Fortes, A. S. (2016), “*Análise da Carga Móvel em Pontes e Viadutos Rodoviários*” in: Congresso Brasileiro de Pontes e Estruturas, ABECE, Rio de Janeiro (Brasil), pp. 1-10.
- American Concrete Institute. (1997). *ACI 215R-74: Considerations for Design of Concrete Structures Subjected to Fatigue Loading*. Michigan.
- Associação Brasileira de Normas Técnicas. (2013), *NBR 7188: Carga Móvel Rodoviária e de Pedestres em Pontes, Viadutos, Passarelas e outras estruturas*. Rio de Janeiro.
- Associação Brasileira de Normas Técnicas (2014), *NBR 6118: Projetos de estruturas de concreto – Procedimento*. Rio de Janeiro.
- Baroni, H. J. M. et al. (2009), “*Vida Útil de Fadiga de Elementos Estruturais de Concreto Armado de Pontes Rodoviária*” in: Congresso Brasileiro do Concreto, IBRACON, Curitiba (Brasil), pp. 1-16.
- Baroni, H. J. M. (2010), “*Simulação da Vida Útil do Concreto em Vigas de Tabuleiro de Pontes em Função do Fluxo de Veículos Pesados*”. Tese de Doutorado, Universidade Federal do Rio Grande do Sul, p. 284;
- Bastidas-Arteaga, E. (2018), *Reliability of Reinforced Concrete Structures Subjected to Corrosion-Fatigue and Climate Change*. International Journal of Concrete Structures and Materials. 12(1):1-13. <https://doi.org/10.1186/s40069-018-0235-x>
- Branco, C. M. et al. (1999), “*Fadiga de Estruturas Soldadas*”, Editora Fundação Calouste Gulbenkian, Lisboa, Portugal.
- Branco, F., Paulo, P. (2012), *O projecto de pontes para vidas superiores a 100 anos*. Revista ALCONPAT, 2(1), 1 - 9. doi: <http://dx.doi.org/10.21041/ra.v2i1.20>.
- Branco, F. A. et al. *Boletín Técnico: Vida útil em la construcción civil*. ALCONPAT International. 2013. Disponível em: <<http://alconpat.org.br/wp-content/uploads/2012/09/B4-Vida-%C3%9Atil-na-Constru%C3%A7%C3%A3o-Civil.pdf>>. Access in 03 Apr. 2019.
- Braz, D. et al. (2018). “*Otimização da proporção entre balanço e vão de pontes de concreto armado de duas longarinas com base na fadiga das armaduras*” in: Congresso Brasileiro de Pontes e Estruturas, ABECE, Rio de Janeiro (Brasil), pp. 1-10.
- Camargo, M. V. et al. (2018), “*Análise comparativa entre comboios e o carregamento normativo da NBR 7188/2013 em tabuleiros de pontes rodoviárias de concreto*” in: Congresso Brasileiro de Pontes e Estruturas, ABECE, Rio de Janeiro (Brasil), pp. 1-10.
- Carvalho, R. C. (2017), *Introdução ao estudo de pontes*. Universidade Federal de São Carlos.
- CCR RODOANEL. “*Sobre a CCR RodoAnel*”. Disponível em: <<http://www.rodoaneloeste.com.br/institucional/>>. Access in 18 Ago. 2018.
- Confederação Nacional do Transporte (2018), “*Boletim Estatístico - CNT - Maio 2018*”. Brasília: CNT. Disponível em: < <http://www.cnt.org.br/Boletim/boletim-estatistico-cnt>>. Access in 18 Jul. 2018.
- Deng, L. et al. (2016), *State-of-the-art review on the causes and mechanisms of bridge collapse*. Journal of Performance of Constructed Facilities, ASCE, 30(2):1-13. <https://ascelibrary.org/doi/10.1061/%28ASCE%29CF.1943-5509.0000731>
- Deng, L., Yan, W. (2018), *Vehicle Weight Limits and Overload Permit Checking Considering the Cumulative Fatigue Damage of Bridges*. Journal of Bridge Engineering, 23(7):1-8. <https://ascelibrary.org/doi/10.1061/%28ASCE%29BE.1943-5592.0001267>
- Departamento Nacional de Estradas de Rodagem (DNER) (1996), *Manual de Projeto de Obras-de-Arte Especias*. Ministério dos Transportes. Rio de Janeiro. Disponível em: <

- [http://ipr.dnit.gov.br/normas-e-manuais/manuais/documentos/698\\_manual\\_de\\_projeto\\_de\\_obras\\_de\\_arte\\_especiais.pdf](http://ipr.dnit.gov.br/normas-e-manuais/manuais/documentos/698_manual_de_projeto_de_obras_de_arte_especiais.pdf)>. Access in 13 Apr. 2019.
- Departamento Nacional de Infraestrutura de Transportes (2017), *Base de Dados das OAE – BDOAE*. 2017. Disponível em: <<http://servicos.dnit.gov.br/dnitcloud/index.php/s/gkQB3SNPH7cwF5F>>. Access in 29 Oct. 2018.
- European Standard. (2002), *EN1991-2, Eurocode 1 - Actions on structures - Part 2: Traffic Loads on Bridges*. European Committee for Standardization, Brussels.
- Freitas, M. J. S. (2014), “*Verificação de Segurança à Fadiga de Pontes Rodoviárias*”. Dissertação de Mestrado, Universidade do Porto, p. 161.
- FTOOL (2018), “*A Graphical-Interactive Program for Teaching Structural Behavior*”. Disponível em: <<https://www.ftool.com.br/Ftool/>>. Access in 13 Sep. 2018.
- Habeeba, A et al. (2015), *Fatigue Evaluation of Reinforced Concrete Highway Bridge*. International Journal of Innovative Research in Science, Engineering and Technology, 4(4):2561-2569. <http://www.rroij.com/open-access/fatigue-evaluation-of-reinforced-concretehighway-bridge.pdf>
- Han, W. et al. (2015), *Characteristics and Dynamic Impact of Overloaded Extra Heavy Trucks on Typical Highway Bridges*. Journal of Bridge Engineering, 20(2):1-11. <http://ascelibrary.org/doi/10.1061/%28ASCE%29BE.1943-5592.0000666>
- Han, W. et al. (2017), *Dynamic Impact of Heavy Traffic Load on Typical T-Beam Bridges Based on WIM Data*. Journal of Performance of Constructed Facilities, 31(3):1-14. <http://ascelibrary.org/doi/10.1061/%28ASCE%29CF.1943-5509.0000991>
- Liu, F., Zhou, J. (2018), *Experimental Research on Fatigue Damage of Reinforced Concrete Rectangular Beam*. KSCE Journal of Civil Engineering, 22(9):3512–3523. <https://link.springer.com/article/10.1007/s12205-018-1767-y>
- Maggi, P. L. O. (2004), “*Comportamento de Pavimentos de Concreto Estruturalmente Armados sob Carregamentos Estáticos e Repetidos*”. Tese de Doutorado, Universidade de São Paulo, p. 219.
- Mota, H. C. et al. (2018), “*Estimativa de Esforços Extremos em Pontes Para Modelo Dinâmico de Cargas Móveis No Brasil*” in: Congresso Brasileiro de Pontes e Estruturas, ABECE, Rio de Janeiro (Brasil), pp. 1-10.
- Nowak, M., Fischer, O. (2016), *Traffic Parameter Sensitivity in the Development of Site-specific Load Models*. Procedia Engineering, 156:296–303. <https://doi.org/10.1016/j.proeng.2016.08.300>
- Pereira, H. F. S. G. (2006), “*Comportamento à Fadiga de Componentes Estruturais Sob a Acção de Solicitações de Amplitude Variável*”. Dissertação de Mestrado, Universidade do Porto, p. 292.
- Pimentel, M. et al. (2008), *Fatigue life of short-span reinforced concrete railway bridges*. Structural Concrete, 9(4): 215-222. <https://www.icevirtuallibrary.com/doi/abs/10.1680/stco.2008.9.4.215>
- Pircher, M. et al. (2011), *Damage due to heavy traffic on three RC road bridges*. Engineering Structures, 33(12): 3755–3761. <https://doi.org/10.1016/j.engstruct.2011.08.012>
- Ray, S., Kishen, J. M. (2014). *Analysis of fatigue crack growth in reinforced concrete beams*. Materials and Structures. 47(1):183-198. <https://link.springer.com/article/10.1617/s11527-013-0054-0>
- Rossigali, C. E. et al. (2015), *Towards actual Brazilian traffic load models for short span highway bridges*. Revista IBRACON de Estruturas e Materiais, 8(2):124-139. <http://dx.doi.org/10.1590/S1983-41952015000200005>
- Ruiz, M. F. et al. (2015), *Shear strength of concrete members without transverse reinforcement: A mechanical approach to consistently account for size and strain effects*. Engineering Structures, 99, 360-372. <https://doi.org/10.1016/j.engstruct.2015.05.007>



- Santos, L. F., Pfeil, M. S. (2014), *Desenvolvimento de Modelo de Cargas Móveis para Verificação de Fadiga em Pontes Rodoviárias*. Engenharia Estudo e Pesquisa, 14(1):40-47. [http://www.revistaeeep.com/imagens/volume14\\_01/cap05.pdf](http://www.revistaeeep.com/imagens/volume14_01/cap05.pdf)
- Schläfli, M., Brühwiler, EugEen. (1998), *Fatigue of existing reinforced concrete bridge deck slabs*. Engineering Structures, 20. 991-998. [https://doi.org/10.1016/S0141-0296\(97\)00194-6](https://doi.org/10.1016/S0141-0296(97)00194-6).
- Schneider, S., Marx, S. (2018), *Design of railway bridges for dynamic loads due to high-speed traffic*. Engineering Structures, 174(1):396–406. <https://doi.org/10.1016/j.engstruct.2018.07.030>
- Toledo, R. L. S. de. (2011), “*Avaliação da vida útil à fadiga em ponte mista aço-concreto considerando o espectro de veículos reais*”. Dissertação, Universidade Federal do Rio de Janeiro, p. 101.
- Wang, C-S. et al. (2013), “*Fatigue Safety Monitoring and Fatigue Life Evaluation for Existing Concrete Bridges*” in: International Conference on Fracture, ICF, Beijing (China), pp. 1-9
- Wang, C-S. et al. (2015), *Fatigue Service Life Evaluation of Existing Steel and Concrete Bridges*. Advanced Steel Construction, 11(3):305-321. [http://ascjournal.com/download/vol11no3/vol11no3\\_5.pdf](http://ascjournal.com/download/vol11no3/vol11no3_5.pdf)
- Xin, Q. et al. (2017), *Fatigue Behavior of Prestressed Concrete Beams under Overload*. Journal of Engineering Science and Technology Review, 10(4):124-131. <http://www.jestr.org/downloads/Volume10Issue4/fulltext171042017.pdf>
- Zanuy, C. et al. (2011), *Transverse fatigue behaviour of lightly reinforced concrete bridge decks*. Engineering Structures, 33(10): 2839–2849. <https://doi.org/10.1016/j.engstruct.2011.06.008>
- Zhang, Y., Xin, X., Cui, X. (2012), *Updating Fatigue Damage Coefficient in Railway Bridge Design Code in China*. Journal of Bridge Engineering, 17 (5): 788-793. <https://ascelibrary.org/doi/10.1061/%28ASCE%29BE.1943-5592.0000310>
- Zhou, Y., Chen, S. (2018), *Investigation of the Live-Load Effects on Long-Span Bridges under Traffic Flows*. Journal of Bridge Engineering, 23(5):1–18. <https://ascelibrary.org/doi/10.1061/%28ASCE%29BE.1943-5592.0001214>

## Application of GUT Matrix in the assessment of pathological manifestations in heritage constructions

I. C. Braga<sup>1</sup> , F. S. Brandão<sup>2\*</sup> , F. R. C. Ribeiro<sup>3</sup> , A. G. Diógenes<sup>4</sup> 

\*Contact author: [eng.fsbrandao@gmail.com](mailto:eng.fsbrandao@gmail.com)

DOI: <http://dx.doi.org/10.21041/ra.v9i3.400>

Reception: 25/03/2019 | Acceptance: 16/07/2019 | Publication: 30/08/2019

### ABSTRACT

The present paper presents the application of GUT (Gravity, Urgency, Tendency) Matrix methodology as a tool in the assessment of pathological manifestations in buildings. Three heritage constructions of the historic center of Sobral, Ceará, Brazil were studied through *in situ* inspections, photographic records and elaboration of the damage map. The GUT Matrix was used as a tool to rank, in each building, priority levels for each damage in order to define their order of treatment. Thus, it was possible to conclude that the applied method can be used as a useful tool to manage the maintenance of buildings through prioritization of the most significant problems and, to contribute directly to the preservation and safety of the built historical heritage.

**Keywords:** Heritage constructions; Sobral; Damage; GUT Matrix.

**Cite as:** Braga, I. C., Brandão, F. S., Ribeiro, F. R. C., Diógenes, A. G. (2019), “Application of GUT Matrix in the assessment of pathological manifestations in heritage constructions”, Revista ALCONPAT, 9(3), pp. 320 – 335, DOI: <http://dx.doi.org/10.21041/ra.v9i3.400>

<sup>1</sup> Department of Civil Engineering, UVA, Sobral, Brazil.

<sup>2</sup> Civil Engineering Graduate Program-PPGEC/UFRGS and LAREB/UFC, Porto Alegre, Brazil.

<sup>3</sup> Civil Engineering Graduate Program-PPGEC/UNISINOS and LAREB/UFC, São Leopoldo, Brasil.

<sup>4</sup> GEM/UVA, Department of Civil Engineering, UVA, Sobral, Brazil.

### Legal Information

Revista ALCONPAT is a quarterly publication by the Asociación Latinoamericana de Control de Calidad, Patología y Recuperación de la Construcción, Internacional, A.C., Km. 6 antigua carretera a Progreso, Mérida, Yucatán, 97310, Tel.5219997385893, [alconpat.int@gmail.com](mailto:alconpat.int@gmail.com), Website: [www.alconpat.org](http://www.alconpat.org)

Responsible editor: Pedro Castro Borges, Ph.D. Reservation of rights for exclusive use No.04-2013-011717330300-203, and eISSN 2007-6835, both granted by the Instituto Nacional de Derecho de Autor. Responsible for the last update of this issue, Informatics Unit ALCONPAT, Elizabeth Sabido Maldonado, Km. 6, antigua carretera a Progreso, Mérida, Yucatán, C.P. 97310.

The views of the authors do not necessarily reflect the position of the editor.

The total or partial reproduction of the contents and images of the publication is strictly prohibited without the previous authorization of ALCONPAT Internacional A.C.

Any dispute, including the replies of the authors, will be published in the second issue of 2020 provided that the information is received before the closing of the first issue of 2020.

## **Aplicação da Matriz GUT na análise de manifestações patológicas em construções históricas**

### **RESUMO**

O presente trabalho apresenta a aplicação da metodologia da Matriz GUT (Gravidade, Urgência, Tendência) na análise das manifestações patológicas em edificações, tomando como exemplares, três construções históricas do centro histórico de Sobral, Ceará, Brasil. O estudo foi conduzido com inspeções *in situ*, registro fotográfico, elaboração dos mapas de danos e aplicação do método, do qual foram gerados os gráficos de prioridades que representam a ordem para o tratamento de cada dano em cada edificação. Assim, foi possível concluir que o método aqui aplicado, pode ser utilizado como uma importante ferramenta de gestão da manutenção de edificações através da priorização da resolução dos problemas mais graves e também, contribui diretamente para a preservação e segurança do patrimônio histórico edificado.

**Palavras-chave:** Construções históricas; Sobral; Patologia; Matriz GUT.

## **Aplicación de la matriz GUT en el análisis de manifestaciones patológicas en construcciones históricas**

### **RESUMEN**

Este trabajo presenta la aplicación de la metodología de la Matriz GUT (Gravedad, Urgencia, Tendencia) en el análisis de las manifestaciones patológicas en edificaciones, teniendo como ejemplos tres construcciones históricas del centro histórico de Sobral, Ceará, Brasil. La investigación fue conducida con inspecciones *in situ*, registro fotográfico, elaboración de mapas de daños y aplicación del método. Los resultados generaron los gráficos de prioridades que representan el orden para el tratamiento de cada daño en cada edificación. Así, fue posible concluir que el método aplicado puede ser utilizado como una importante herramienta de gestión del mantenimiento de edificaciones a través de la priorización de resolución de los problemas más graves y contribuye directamente a la preservación y seguridad del patrimonio histórico.

**Palabras clave:** Construcciones históricas; Sobral; Patología; Matriz GUT.

## **1. INTRODUCTION**

Heritage constructions (HC) are material elements of the historical heritage with high documental, artistic, cultural and social value for a community, because the HC is part of its history. Therefore, these constructions have an immeasurable value for the society in which they are inserted. As highlighted by Roca et al. (2010), such other types of buildings, HC are also subject to several scenarios of degradation due to natural actions (physical and thermal effects, chemical attacks), anthropic actions (including alterations in the original building architecture, intentional destruction and inadequate interventions) and also dynamic actions (such as wind and earthquakes).

Differently contemporary constructions, where structural properties of their components and materials are already well studied and since majority scientific efforts currently are focused on the development of new materials and structural systems for applications in future construction, heritage constructions are still an unexplored field. Thus, to study this type of structure is very important, not only as a contribution to the valorization and preservation of the memory of a given society, but also allows the development of retrofitting techniques for these structures (MESQUITA et al., 2015).

Pathological manifestations in this type of structure can cause a decrease in their performance and

negative effects in the architectural aesthetics. In addition, these problems can also compromise the structural safety of the building. In general, the pathological manifestations tend to intensify over the time and if not correctly treated, they can cause many damages and, in severe cases, the structural collapse.

These problems can be exemplified by fissures, cracks, detachment of coatings, detachment of ceramic coatings, humidity stains, infiltrations, efflorescence, mold mildew, and others. Their origins may be related to lack of maintenance and/or exposure to environmental actions over a long period of time. Therefore, the role of building pathology is very important in order to know the state of degradation of these structures and provides subsidies for making-decisions focused on the repair and maintenance of structures.

In this perspective, it is necessary to have knowledge about the conditions of the structure and the severity of the pathological manifestations found. For this reason, the management tools are used to contribute to a better elaboration of a strategic planning regarding situations that require complex decisions. The GUT Matrix (Gravity, Urgency, Tendency), developed by Kepner and Tregoe in 1980, is a very useful and important tool that can contribute in this process. With the GUT Matrix it is possible to prioritize the problems and pay more attention to those that have more risks. This methodology, according to Brandão (2018), considers Gravity (G), Urgency (U) and Tendency (T) of the problems detected. For this evaluation, the method uses a quantitative classification for each damage inspected in order to define the degrees of criticality in relation to each problem found.

According to Martins et al. (2017), in the GUT method, Gravity (G) represents the importance of the problem to be examined and its potential of damage. Usually its study is carried out focusing on medium and long-time effects. Urgency (U) requires analysis of how significant the problem is, that is, the deadline for the damage to materialize; and the Tendency (T) consists of problem evolution in function of the time, that is, the probability of the problem to evolve negatively over the time.

In this context, the city of Sobral, located in the North region of Ceará State, in Brazil, preserves a large number of heritage constructions in its historic center with more than 1,200 buildings listed by the National Historic and Artistic Heritage Institute (IPHAN) and many of these buildings present several types of pathological manifestations. In this perspective, this study aims to show the application of the methodology of the GUT Matrix as a management tool in the assessment of pathological manifestations in buildings, taking three samples of heritage constructions of the historical center of Sobral as case study in order to obtain the prioritization of the solution for each damage in each construction.

## 2. METHODOLOGY

Initially, an extensive literature review was carried out about historical context of the historic center of Sobral and its buildings, and also, about the methodology of the GUT Matrix. Posteriorly, through *in situ* inspections, based on the technical recommendations of the scientific literature and Technical Bulletin Nº 11 of ALCONPAT: Characterization, evaluation and structural recovery of historical buildings by Mesquita et al. (2015), the three buildings were selected for the application of the GUT Matrix, taking into account their ages, cultural importance and historical context and degradation scenario. The three buildings selected were: Nossa Senhora do Rosário Church (18<sup>th</sup> Century), Nossa Senhora das Dores Church (19<sup>th</sup> Century) and Menino Deus Church (19<sup>th</sup> Century).

During *in situ* inspections, a photographic record of all pathological manifestations found in each construction was done and posteriorly used to prepare the building damage map. The check list of GUT Matrix, adapted from Verzola, Marchiori and Aragon (2014), was also completed during *in situ* inspections. The development of the GUT method was based on the work of Verzola, Marchiori and Aragon (2014) and according to those authors it is necessary a list of all pathological manifestations that could be found in each building, to do a check list and to fill it with numerical

values (weights) corresponding to the Gravity, Urgency and Tendency of each damage. When classifying Gravity, it is necessary to consider the possible risks and losses to users and the patrimony, where the definition of a problem considered critical was inserted in the degrees “Total” or “High”; the designation of the problem considered regular is inserted in the degree “Average”; and the definition of the problem considered as minimum, is inserted in the degrees “Low” or “None”, as shown in Table 1.

Table 1. GUT classification regarding the Gravity.

Degree	Definition of degree	Score
TOTAL	Risk of death, unrecoverable impact with excessive loss of performance, very high financial loss.	10
HIGH	Danger of lesion to users, recoverable damage to the environment and building.	8
AVERAGE	Risk to user’s health occasioned by degradation of systems, reversible environmental damage, average financial loss.	6
LOW	No health risk to users, low environmental degradation, necessity to substitute some systems, low financial loss.	3
NONE	No risk of health or physical, minimal deterioration of the environment, no financial damage.	1

Source: Adapted from Verzola, Marchiori e Aragon (2014).

Regarding Urgency, the definition of each degree is based on how significant the manifestation is at the time when the problem must be solved and how soon the adversity must be intervened. Table 2 represents the situation described.

Table 2. GUT classification regarding the Urgency.

Degree	Definition of degree	Score
TOTAL	Immediate event, necessity of interdiction of the property without extra deadlines.	10
HIGH	Event in the imminence of happening, urgent intervention.	8
AVERAGE	Adversity expected soon, necessity to intervene rapidly.	6
LOW	Initiation of an incident, intervention still in planning.	3
NONE	Unexpected adversity, but necessary monitoring for future maintenance.	1

Source: Adapted from Verzola, Marchiori e Aragon (2014).

For the Tendency, the degree is defined as a function of the possibility of the increasing, reduction or extinction of the problem over the time scale, as shown in Table 3.

Table 3. GUT classification regarding the Tendency.

Degree	Definition of degree	Score
TOTAL	Immediate progress of manifestation, could have worsening rapidly.	10
HIGH	Evolution of the situation about to occur.	8
AVERAGE	Medium-term evolution.	6
LOW	Possible long-term evolution. It may occur. Delay situation.	3
NONE	Situation stabilized, without evolution case.	1

Source: Adapted from Verzola, Marchiori e Aragon (2014).

After determined the weights for each topic (Gravity, Urgency and Tendency), the level of each problem in the three functions was classified and the product of their respective values (GxUxT) was calculated. The priorities were determined by descending order of the value calculated for each pathological manifestation of each building. Finally, to better visualize the results, the prioritization graphs of the damages of each church were developed. In these results, for a better elucidation of the GUT method, the classification of each observed damage (Total, High, Average, Low, None) according to its total scores in the prioritization graphs and based on each degree presented in Table 1, Table 2 and Table 3, is also commented.

### 3. ANALYZED STRUCTURES

#### 3.1. Nossa Senhora do Rosário Church

The Nossa Senhora do Rosário Church, shown in Figure 1, is the oldest church of the historic center of Sobral and therefore it has a very important role in the historical-social context of this city. Its construction, in vernacular masonry, occurred in the first half of 18<sup>th</sup> Century, approximately in the year of 1740. In the year of 1777, the church originated the “Pretinhos Church” and its architectural structure tending to baroque. This denomination was given by the Nossa Senhora do Rosário dos Homens Pretos de Sobral Brotherhood, founders of the church. In 1914, by request of Dom José, priest and later bishop of Sobral, a lateral expansion of the building was done. Later, in 1926, the floor (done of solid bricks) was changed for hydraulic ceramic floors.

Its floor plan, shown in Figure 1 (a), has two lateral naves and one main nave. In the same axis of the main nave, there is a main and two other secondary altars, and the sacristy can be seen in the middle of the main altar. The main entrance is in the main facade where, few meters from the main entrance, there is a metallic gate characterizing the environment as an anteroom that provides access to the sanctuary. There is also a coro-alto just behind the main facade, from which the altars can be seen, as shown by the Figure 1 (c).

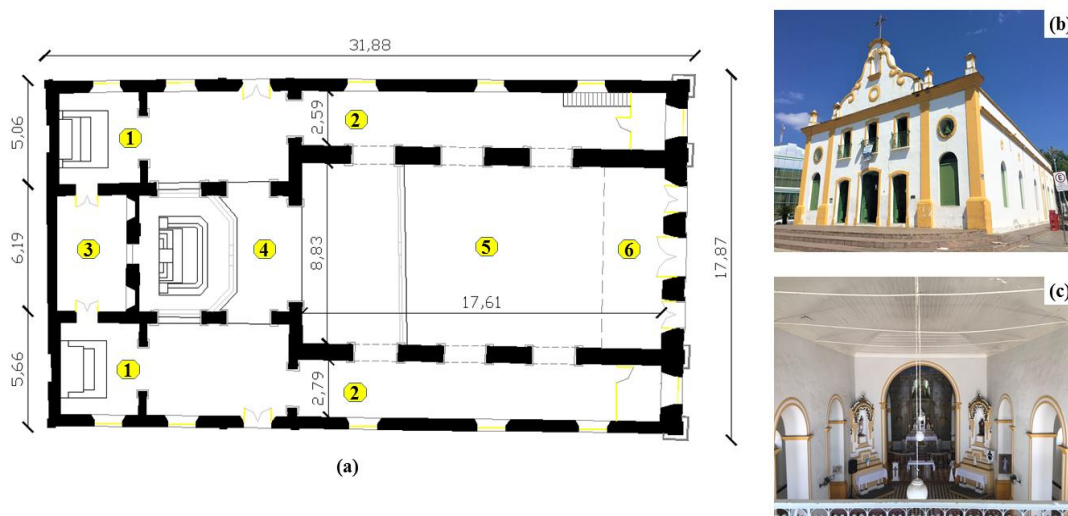


Figure 1. View of the Nossa Senhora do Rosário Church: (a) floor plan where (1) indicates the secondary altar, (2) lateral nave, (3) sacristy, (4) main altar, (5) central nave and (6) coro-alto; (b) main facade and (c) internal view of the central nave.

As highlighted by Santos et al. (2016) in Figure 1 (b), one of its most expressive characteristics is the pediment, which in much resembles baroque features, due to its curvilinear movements, creating an aperture in arc format, centrally arranged and enriched by the insertion of a cross.

### 3.2. Nossa Senhora das Dores Church

Considered one of the oldest churches in Sobral, the Nossa Senhora das Dores Church (Figure 2) was built near the Acaraú River, one of the few churches in the city which faces partially the river. The church, according to Pinto (2009), was built in 1818, although the date is not accurate. It has a neoclassical architecture, however, it has a single lateral tower, as shown in Figure 1 (b), posteriorly built, according to Mesquita et al. (2017) around 1924, not following the neoclassical rule. To build the church, constructive techniques of the period are used, being totally constructed in solid masonry bricks.

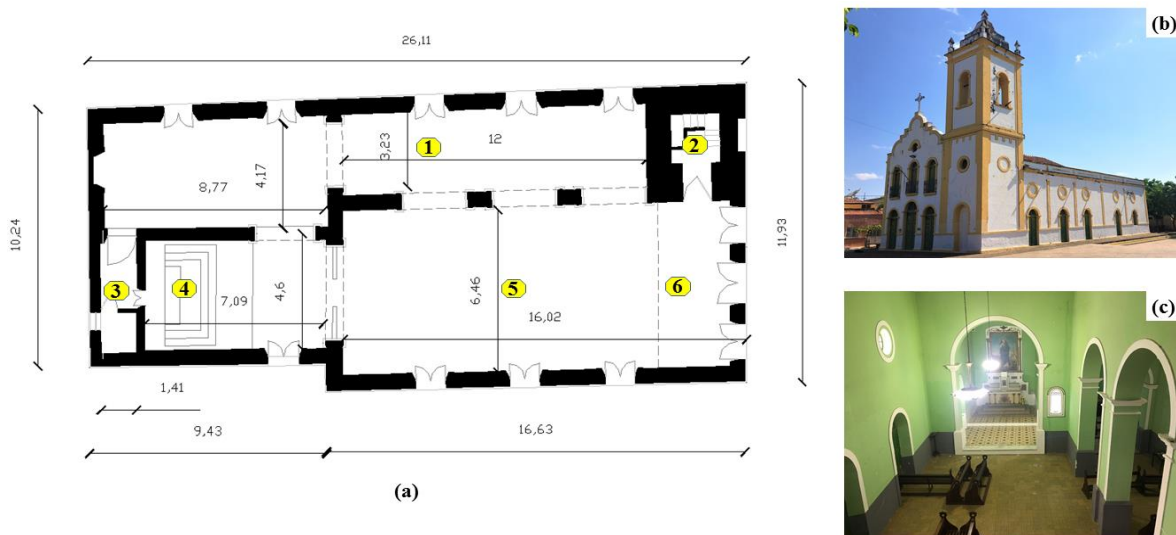


Figure 2. View of the Nossa Senhora das Dores Church: (a) Floor plan where (1) indicates the aisle, (2) lateral tower, (3) sacristy, (4) main altar, (5) central nave and (6) coro-alto; (b) main facade and (c) superior view of the main nave.

Its geometry is shown in Figure 2 (a), where can be observed that the church has a main nave, an aisle, a single lateral tower, a coro-alto, a single altar and, in the back of the main altar, a sacristy. Figure 1 (c) illustrates the interior view of the building, where it is observed that the church is little ornamented with only one picture located at the bottom of altar representing the image of Nossa Senhora das Dores, a wall with a large lateral arches separating the naves and a large arch located in front of altar.

### 3.3. Menino Deus Church

The Menino Deus Church (Figure 3), had its construction process started around the 1810 through the idea of two Carmelitas sisters arrived in Sobral in this same year with the nuns of the third order of the Carmelitas Emerenciana de Sant'Ana and Teresa de Jesus. According to the Inventário de Bens Arquitetônicos-IBA (IPHAN, 2005), a document that catalogs all the heritage constructions listed in Sobral, it is estimated that in 1820 the central part of the church was built. The towers were only got completed in 1940. The design clearly shows a correlation with the city's Cathedral, adopting the standard of the second half of the 18<sup>th</sup> century, with a distinctive characteristic of the cornice, which are elements constituents of facades of the period, generally located above the windows or main oculus of the building.

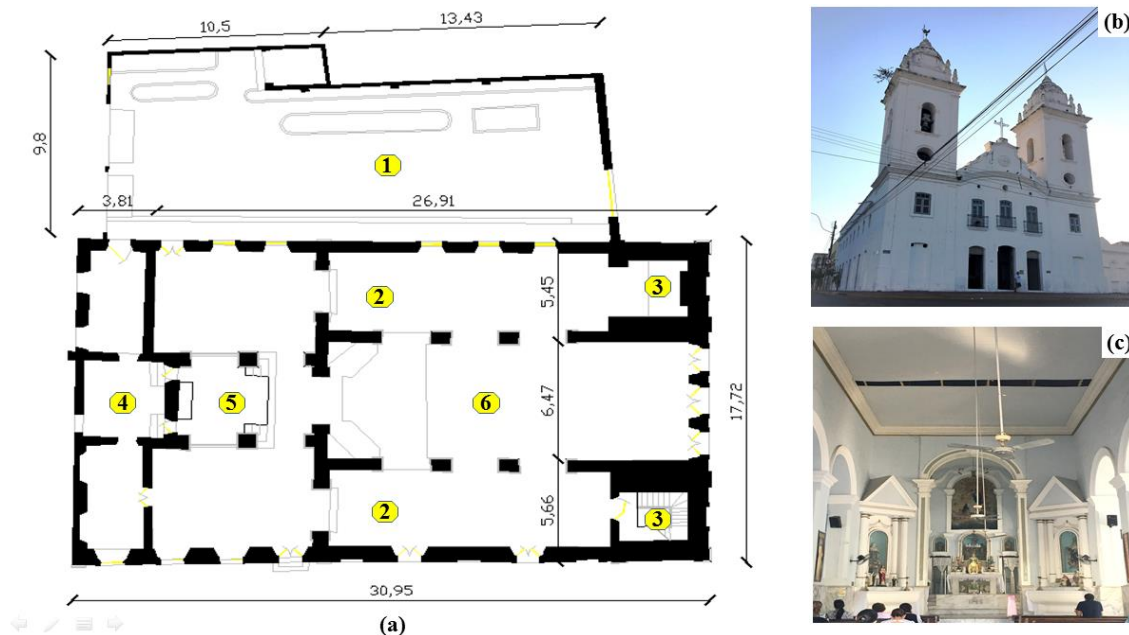


Figure 3. View of the Menino Deus Church: (a) Floor plan where (1) indicates the lateral courtyard, (2) aisles, (3) towers, (4) sacristy, (5) main altar and (6) central nave; (b) main facade and (c) internal view of the main nave.

Figure 3 (a) represents the floor plan of the church and shows that its geometry is divided in many parts, where in the side there is a large courtyard, in the internal part there are two aisles, each one in front of each tower, a large central nave that is located in front of the main altar and just behind this, the sacristy. In Figure 3 (c), it is observed that the degree of ornamentation of the church is also low.

## 4. RESULTS AND DISCUSSIONS

### 4.1 Pathological manifestations of the Nossa Senhora do Rosário Church

Visual inspection provides valuable data, being an important tool in the assessment and



identification of the damage of the structures. Moreover, combining the visual inspection with other control tools, as presented in this work through the GUT Matrix, enriches the results and contributes to their reliability. The inspection of this first church was carried out from the outside to the inside, where firstly the four facades and later the interior were inspected. During inspection the following pathological manifestations were identified: fissures and cracks, disintegration of lining elements, detachment of coating, humidity stains, atmospheric stains, mold/mildew. The main facade presented the biggest number of damages and it is represented by the damage map shown in Figure 4, where detachments are observed in the lower parts of the structure, in the openings and in the central door column some cracks are also visualized, and atmospheric stains can be seen on the top of the church.

The main reason for cracking may be associated with the vibrations existing in the place, because it is located in a central region of the Sobral city and there is a large flow of people and vehicles nearby, that can induce vibrations causing changes in the structure dynamic behavior, which often lead to fissures.

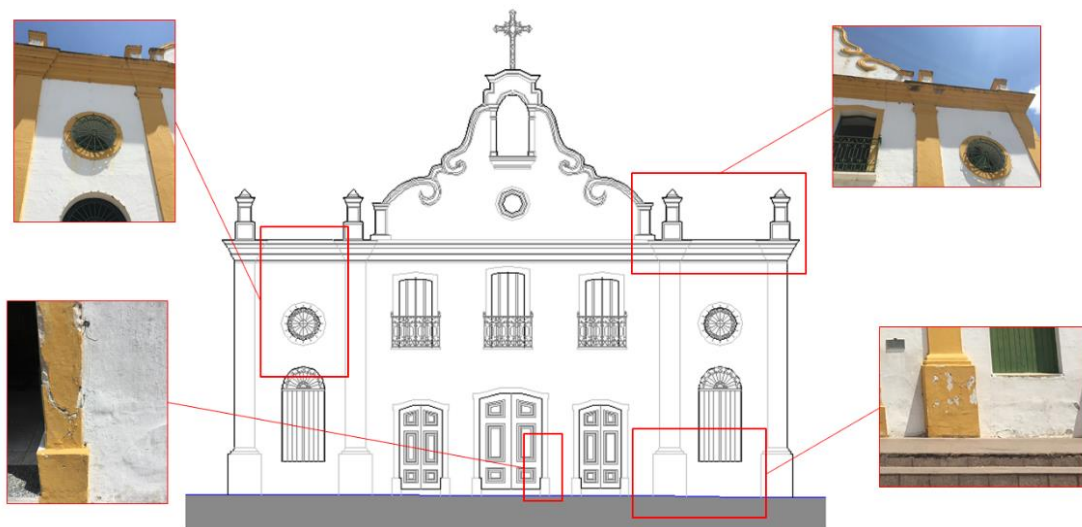


Figure 4. Damage map of the main facade of Nossa Senhora do Rosário Church.



Figure 5. Internal pathological manifestations of the Nossa Senhora do Rosário Church: (a) crack, (b) disintegration of lining elements, (c) detachment and (d) humidity stains.

In the internal part of the church the main, the following pathological manifestations were observed: crack, disintegration of lining elements, detachments and humidity stains, as illustrated by the Figure 5. The most serious situation was the crack located near the altar (Figure 5 (a)), because its presence may be associated with the movements adjacent to the building and new constructions in the vicinity of the sanctuary. These movements occasionally cause sinking of the soil and cracks and fissures in

some parts of the church.

For the Gravity in the application of the GUT methodology a score 8 was attributed to the crack located near the altar due its large opening. For the Urgency, a score 8 was also inserted due large area of commitment of this damage that requires urgent intervention. Regarding Tendency, a score 6 is attributed knowing that the problem is in a situation of average progression.

From the application of the checklist of the GUT Matrix in this building it was possible to elaborate the graph of priorities, which is represented by Figure 6, where it is possible to verify that priority pathological manifestations, that must be treated first, are fissures and cracks, in this case, in the main altar of the church, because it presents the highest scores, 384 scores, and represents a high priority damage, according to the descriptions in Tables 1, 2 and 3 of Section 2.

Second, in the order of priorities, it is the disintegration of lining elements with a total of 216 scores, being framed as an average damage. In the third position are the detachments of coating with 108 scores, being also framed in the degree of average damage. Humidity stains and atmospheric stains, both with 54 scores, are also identified as average damage. The damage with lowest severity, which is in the last position of the order of priorities, is mold /mildew, with 9 scores and low damage.

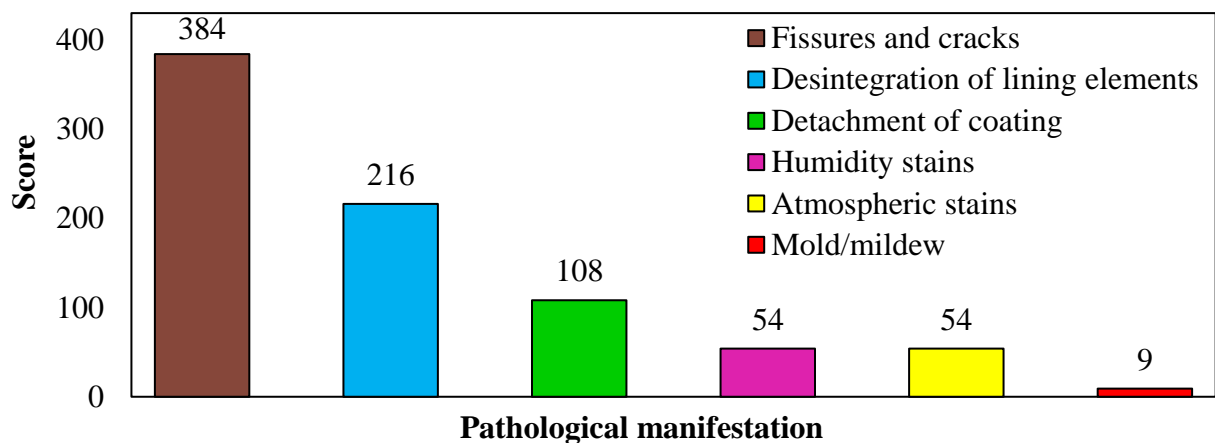


Figure 6. Priority graphic of the Nossa Senhora do Rosário Church.

In this building the number of pathological manifestations found was low, presenting as main and concern the cracks located on the sides of the altar, that can generate impacts that partially compromise the functionality of the structure. This little amount of damage found is related to periodic maintenance that is carried out by the administration of the church, because it is the oldest and most important cultural church for the city and it has a great contribution to the implementation of historical tourism to the city.

#### 4.2 Pathological manifestations of the Nossa Senhora das Dores Church

The pathological manifestations identified in the Nossa Senhora das Dores Church were the most numerous among the three churches analyzed. In many parts of the structure, several types of damages were found such as fissures, detachments and humidity stains and atmospheric stains. The damages observed were fissures and cracks, infiltrations, disintegration of lining elements, electrical system failures, mold/mildew, atmospheric stains, humidity stains, detachment of coating, disaggregation of roof elements, grouting inefficiency, frame failure, efflorescence and oxidation of metallic elements. The damage map of this building is presented through its facade with more incidence of pathological manifestations, the back facade, as illustrated by Figure 7.

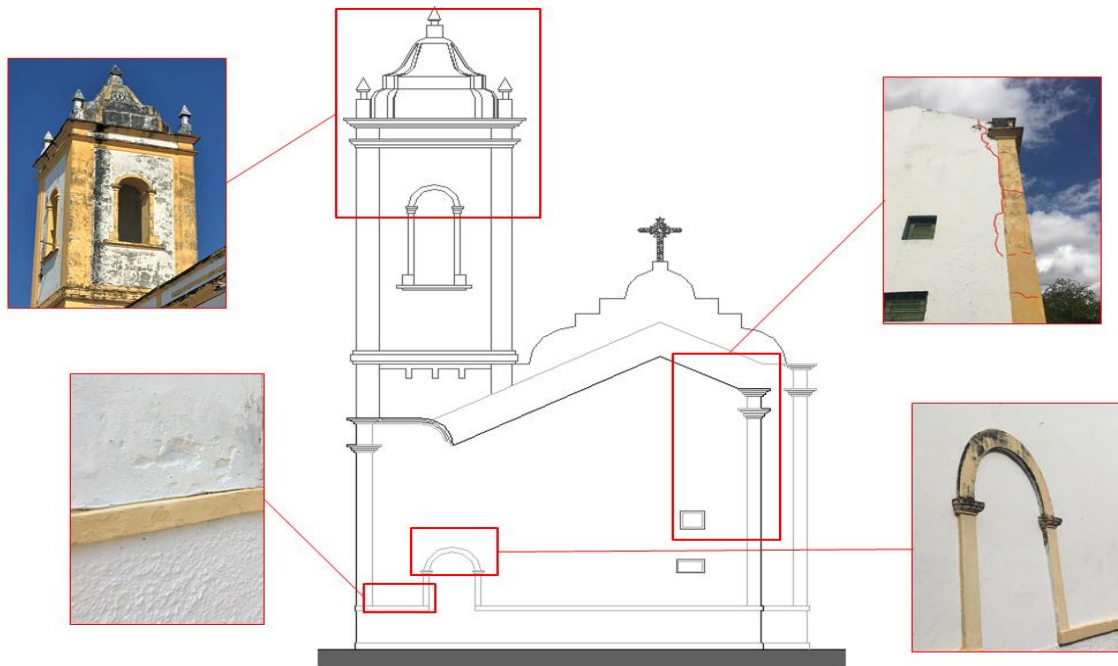


Figure 7. Damage map of the Nossa Senhora das Dores Church.

Figure 7 shows the incidence of a large amount of atmospheric stains in the lateral tower and also in the upper parts of the church. This type of damage was also evident in all other facades. A large crack in the right part of this figure, that starts from the mid height of the wall to the top, was observed. This anomaly is closely linked to a possible sinking of the soil, considering that the structure is located near of the Acaraú River and that over time was impacted by numerous new constructions in the vicinity. Besides this region, in the circular openings of the other facades, this type of damage is also evidenced. There are also detachments of coating in the lower part of this facade, which are also found in the other facades.

The main pathological manifestations observed in the internal part of the structure were: fissures and cracks, detachment of coating, humidity stains and detachment of coating with exposure of parts of the frame, which are illustrated in Figure 8. In Figure 8 (a), there is the most severe pathological manifestation for this building: a crack located in the central arch of the main nave. This anomaly is in a very aggravated situation, being its occurrence related to the incidence of soil movement of the foundation and to a possible overload in the arch, since many interventions with an increase of load were executed over time, as for example, the exchange of a lining that was previously made of PVC by a slab of reinforced concrete. Thus, to Gravity, a score 10 was attributed, that is, the maximum score of the method here used, which causes a high impairment of the performance of the building. Regarding Urgency, a score 10 was also inserted, due to the large area of commitment of this manifestation, requiring urgent intervention. And for Tendency it was also chosen a score 10, corresponding to the large possibility of evolution of the situation.

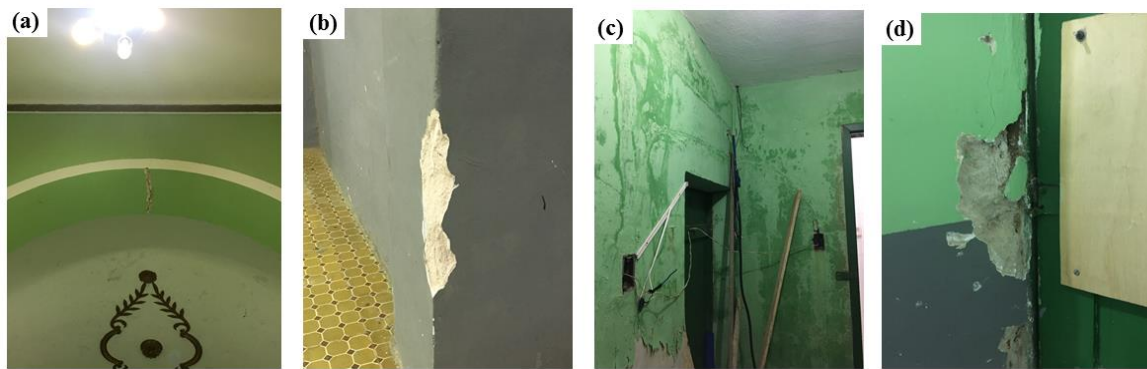


Figure 8. Internal pathological manifestations of the Nossa Senhora das Dores Church: (a) crack in the central arch, (b) detachment of coating, (c) humidity stains and (d) detachment of coating with exposure of the frame parts.

The data obtained from the application of the GUT Matrix in this building were organized in the priority graph shown in Figure 9, where it is verified that the pathological manifestation of highest priority is the crack in the central arch of the main nave, with a total of 1000 scores, which classifies it as a total damage, that is, of extreme gravity, urgency of solution and fast tendency of evolution. In addition, the difference between this damage and the two other (infiltration and disintegration of lining elements, both with 216 scores each) is very high, that corresponds to 784 scores, which show the severity of this crack.

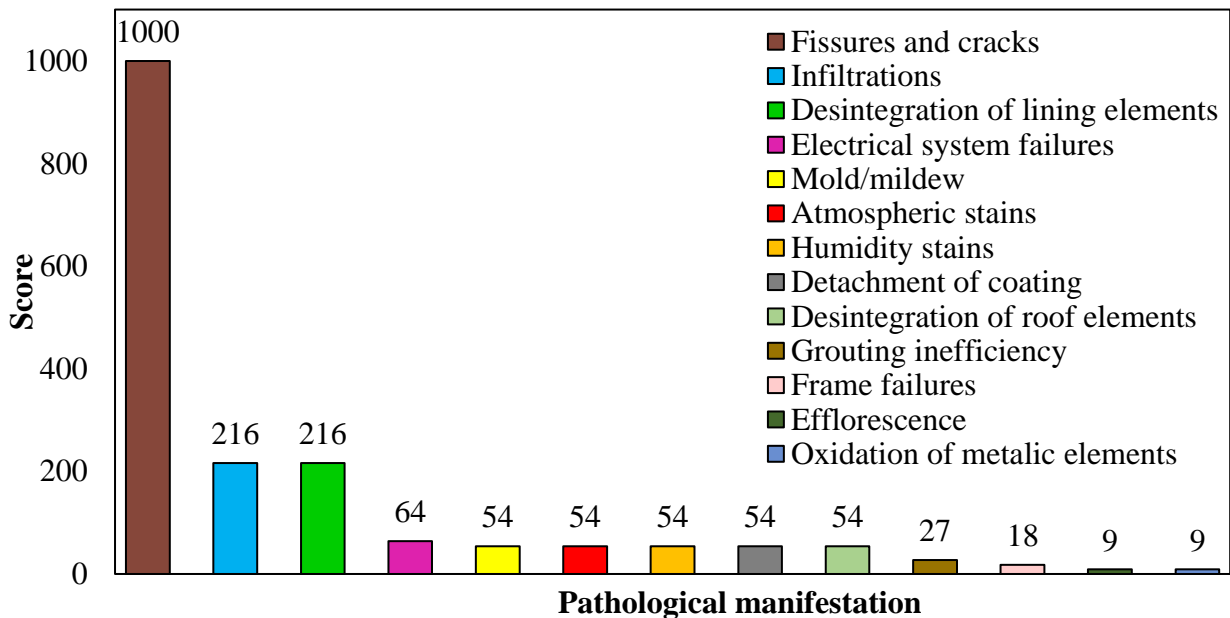


Figure 9. Priority graphic of the Nossa Senhora das Dores Church.

Four pathological manifestations presented the same scores (54 scores): mold/ mildew, atmospheric stains, humidity stains, detachment of coating, which evidences pathological manifestations of average damage. The damages: grouting inefficiency (27 scores), frame failure (18 scores), efflorescence (9 scores) and oxidation of metallic elements (9 scores) correspond to category of low potential damages, the latter two occupying the final position of the order of prioritization. This building presented the largest number of pathological manifestations and this fact is connected to the lack of maintenance of the structure, moreover this church is now interdicted. The existing

damages, if left untreated, can evolve into more severe problems that can seriously compromise the stability and safety of the structure.

### 4.3 Pathological Manifestations of the Menino Deus Church

The right lateral facade (connected to the lateral courtyard) and the back facade of the Menino Deus Church were not analyzed because these two facades are linked to the adjacent buildings. However, the other facades as well the internal area were thoroughly inspected, and the main facade presented the most severe damages, which can be observed in Figure 10, where the most evident were: atmospheric stains, located in many regions of the structure mainly on top of the two towers; fissures in the vicinity of circular openings of all doors and windows and in the lower part the columns of a tower, which is accompanied by detachment of coating; and rooting of shrubs, located at the top of the left lateral tower.

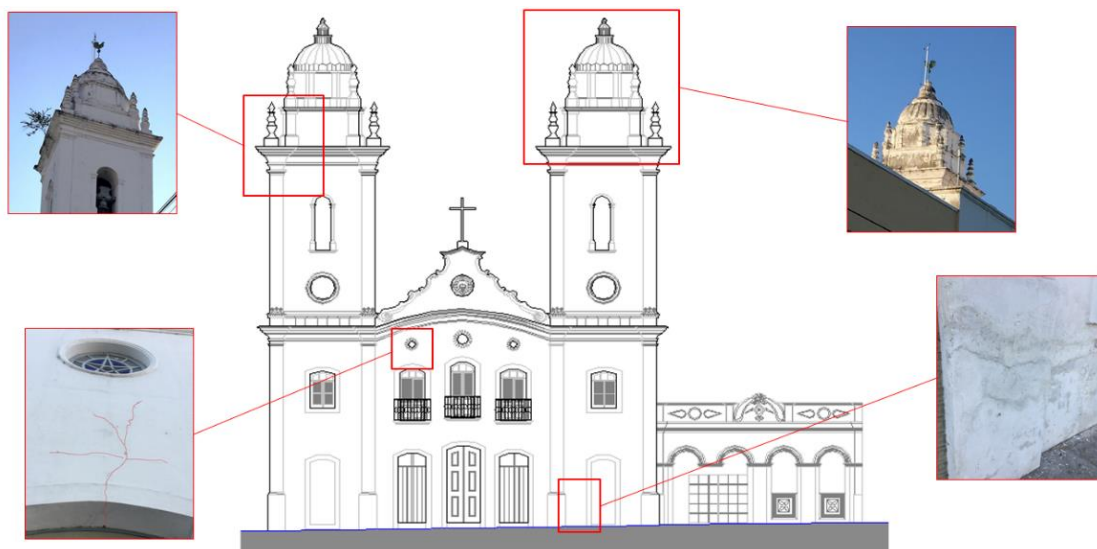


Figure 10. Pathological manifestations of the Menino Deus Church.

In the internal part of the church the main damages observed were fissures and cracks, disintegration of lining elements and disintegration of floor elements, as shown in Figure 11. Disintegration of lining elements was observed in many parts of the roof, as well as fissures.

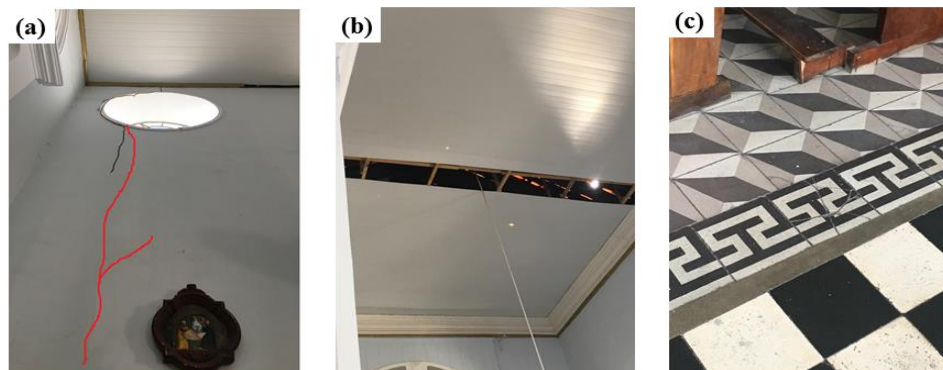


Figure 11. Pathological manifestations in the internal part of the Menino Deus Church: (a) Fissures, (b) disintegration of lining elements and (c) disaggregation of floor elements.

With the results of the checklist of GUT Matrix applied in this building, the graph of priorities was constructed and it is illustrated in Figure 12, where it is verified that the most prioritized pathological manifestation are the fissures, which can be observed in the upper opening of the front facade door (Figure 10) and also in an internal wall of the left lateral facade (Figure 11 (a)). The scores of this anomaly corresponds to 216 and are obtained by applying to the Severity, Urgency and Tendency 6 scores per each one, being therefore an average priority damage. In second position is the detachment of coating that presents a total of 108 scores, being also an average damage. In third and fourth positions are the disaggregation of lining elements and atmospheric stains, with 36 and 27 scores each one, being classified as average and low damage, respectively. In the final positions in the order of priorities, are the rooting of shrubs and the disintegration of floor elements, with 18 scores each, classified as low damage.

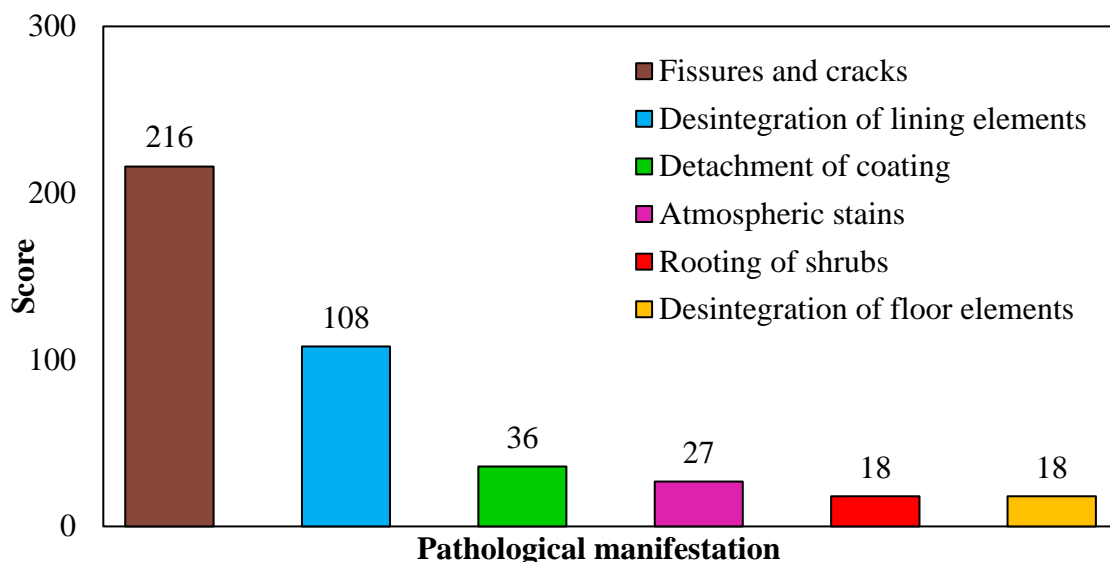


Figure 12. Priority graphic of the Menino Deus Church.

The Menino Deus Church presented few pathological manifestations and among the three inspected, it was the one that also presented the lowest scores in its most severe damage. This may also be related to the good level of maintenance that is performed by its managers.

#### 4.4 Comparison among the obtained results

By the comparative analysis of the pathological manifestations listed in first position for each church and having as parameter its total score, among the three buildings studied, the Nossa Senhora das Dores Church presented the most severe damage with a total of 1000 scores for the crack in the central arch of the main nave. The second most severe was the Nossa Senhora do Rosário Church with a total of 384 scores also for a crack in the main altar. And finally, the third most severe damages were the fissures present in the main facade near the opening of the upper window, in the lower part of one of the columns of a tower and in walls of the internal part of the Menino Deus Church with a total of 216 scores. Figure 13 shows the comparison between the most severe damages of these churches.

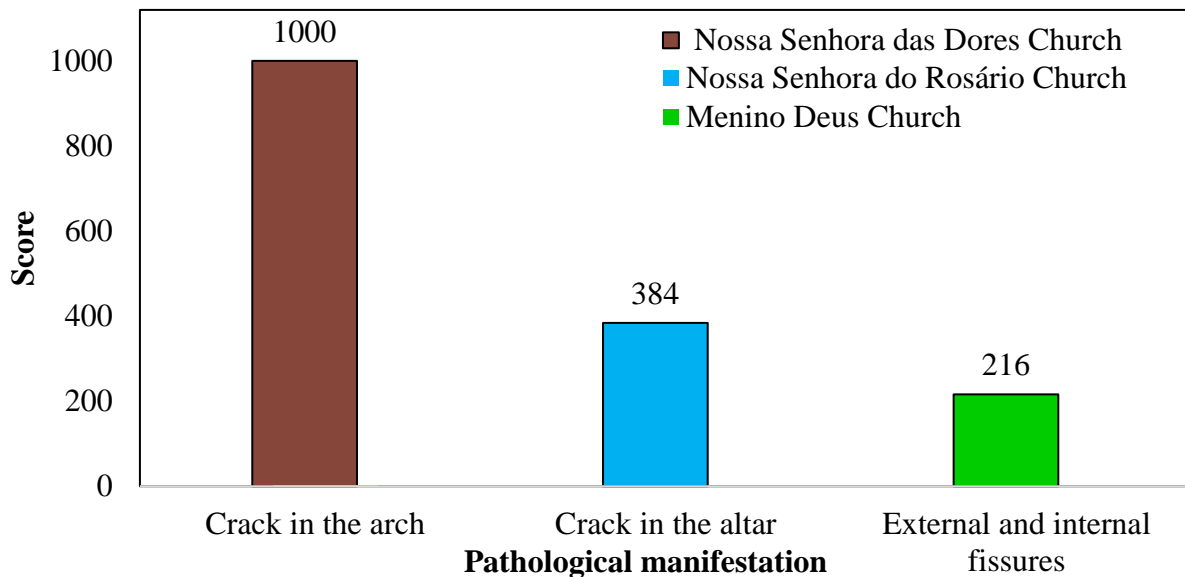


Figure 13. Comparative graphic between the most severe pathological manifestations for each church.

The analysis of the pathological manifestations through GUT Matrix can help the manager in the decision process about interventions that may contribute to the preservation and safety of the building. In this study, it was observed that the newest building among the three analyzed (Nossa Senhora das Dores Church) was the one that presented the largest number and severity of pathological manifestations, thus, it is highlighted that the characteristic factors of the deterioration associated to the lack maintenance, are elements of large influence in the conservation and protection of the historical good.

#### 4.5 Limitations of GUT Matrix

From these results, it can be verified that the GUT Matrix method is a very useful strategic planning tool that, through visual inspections, contributes to the making-decision process on possible interventions that may be implemented in the structures, aiming the repair of the observed damages. However, being a visual inspection, this tool has some restrictions and is very important that the inspectors involved have knowledge and experience about building pathology, which allows the evaluations to be coherent and reflect the reality of the damages observed in the structures.

For the heritage constructions, usually protected by preservation organism, therefore they cannot be damaged, the visual inspection, even providing qualitative data, is an important tool in the process of assessing and diagnosing of the state of structural damage, because it is not an invasive tool and does not cause damage to the good. When combined with non-destructive tests, the information from visual inspection also contributes to the efficiency of the results which collaborate for a better knowledge about the conservation status and severity of damage of these structures.

An example of the application of visual inspection in heritage structures can be found in Santos and Silva (2017) that identified the damages in the facade of the Block A of the Polytechnic School of the University of Pernambuco, a building of the 19<sup>th</sup> century in Recife, Brazil. The following pathological manifestations were identified: disaggregation, cracking, spurious element, chromatic alterations, superficial spots, partial loss, presence of vegetation, cracks and contamination. The results showed that the state of conservation of the structure, considering that the building is more than 100 years old, is regular. However, the authors emphasize that the identification of these damages was very important for the elaboration of an efficient restoration plan and that the maintenance activities, if executed correctly and at adequate intervals, guarantee a good

performance of the building.

Another important example of the use of the visual inspections can be found in work developed by Rocha et al. (2018) that through this technique combined with Damage Identification Lists (DIL), that registered the pathological problems in the building, it was possible to draw a damages map of the Igreja do Carmo, in Olinda, Pernambuco, Brazil, a very important structure of the 16<sup>th</sup> century. The results allowed to show the location of the problems found and their dimensions, more accuracy in the correct diagnosis and in the preventive measures for the anomalies. The authors concluded that the use of this technique in the elaboration of damage map provides subsidies that facilitate the analysis of the symptomatology and the correct diagnostic of the pathologies found, guaranteeing a more reliable proposal for the treatment of these problems.

Therefore, visual inspection combined with GUT Matrix, for an initial diagnosis of the problems, is efficient in the identification of damages in heritage constructions, their gravity and possibilities of evolution over time, because it is a not invasive technique. However, it can still be complemented with non-destructive tests.

## 5. CONCLUSIONS

Identification and assessment of the pathological manifestations of heritage constructions has essential importance to the preservation of these types of structures. Sobral is one of the few Brazilian cities that presents in its urban structure a historic center with many heritage constructions, which denotes the importance of studies directed to the conservation of these structures. This study aimed to demonstrate the application of GUT Matrix for an initial diagnostic of the pathological manifestations in heritage constructions and in the development of a prioritization order, regarding the solution of the damages found in these constructions, showing that it can be a very useful tool for the management of maintenance of buildings.

The Nossa Senhora das Dores Church, among the three buildings studied, presented the largest degree of deterioration, especially as regards to a crack in the arch in front of the altar. In the Nossa Senhora do Rosário Church, the number of damages found was low, presenting as the main and worrisome the cracks located on the sides of the main altar. For Menino Deus Church, the main aggravating factor was the cracks in the main facade and some internal walls.

In this perspective, it was possible to conclude that the GUT Matrix can be an important support tool in the management of the maintenance of buildings, contributing to the preservation and safety of structures, especially when applied to the heritage constructions.

## 6. ACKNOWLEDGMENTS

The authors would like to acknowledge the National Historic and Artistic Heritage Institute (IPHAN), the Paróquia de Nossa Senhora da Conceição, in Sobral, and the Laboratory of Rehabilitation and Buildings Durability - LAREB/UFC in Campus Russas, for all support and useful information for development of this work.

## 7. REFERENCES

- Brandão, F. S. (2018), “*Aplicação da Matriz GUT como ferramenta de suporte na gestão da manutenção de edificações*”, Trabalho de Conclusão de Curso de Especialização em Engenharia e Gerenciamento de Manutenção, Faculdade Única de Ipatinga, p. 08.
- Instituto do Patrimônio Histórico e Artístico Nacional- IPHAN. (2005), “*Inventário Nacional de Bens Arquitetônicos – IBA*”. IPHAN, Sobral, Brasil, p. 42.



- Martins, N., Pessoa, R., Nascimento, R. (2017), Priorização na Resolução de Manifestações Patológicas em Estruturas de Concreto Armado: Método GUT, *Revista de Engenharia e Pesquisa Aplicada*, 2 (3): 139-147. <http://dx.doi.org/10.25286/repa.v2i3.707>
- Mesquita, E., Brandão, F., Diógenes, A., Antunes, P., Varum, H. (2017), Ambient vibrational characterization of the Nossa Senhora das Dores Church, *Engineering Structures and Technologies*, 9 (4): 170-182. <https://doi.org/10.3846/2029882X.2017.1416311>
- Mesquita, E., Paupério, E., Arêde, A., Varum, H. (2015), “*Boletim Técnico nº 11: Caracterização, avaliação e recuperação estrutural de construções históricas*”. ALCONPAT-BRASIL, p. 18.
- Pinto, J. J. de S (2009), “*Os novos palácios da velha princesa: Intervenções arquitetônicas contemporâneas no sítio histórico de Sobral*”, Dissertação de Mestrado em Arquitetura e Urbanismo, Universidade Federal do Rio Grande do Norte, p. 129.
- Rocha, E. A., Macedo, J. V. S., Correa, P., Monteiro, C. B. (2018), Adaptation of a damage map to historical buildings with pathological problems: Case study at the Church of Carmo in Olinda, Pernambuco, *Revista ALCONPAT*, 8 (1): 51-63. <http://dx.doi.org/10.21041/ra.v8i1.198>
- Roca, P., Cervera, M., Gariup, J., Pela', L. (2010), Structural Analysis of Masonry Historical Constructions. Classical and Advanced Approaches, *Archives of Computational Methods in Engineering*, 17(3): 299–325. <https://doi.org/10.1007/s11831-010-9046-1>
- Santos, C. L. L., Silva, A. J. C. (2017). “*Conservação de edifício histórico do século XIX – análise de patologias na fachada do Bloco A da Escola Politécnica da Universidade de Pernambuco*”. In: Conferência Nacional de Patologia e Recuperação de Estruturas, CONPAR 2017, Recife: Pernambuco (Brasil), pp. 1-12.
- Santos, F., Alves, A., Brandão, F., Mesquita, E., Diógenes, A., Varum, H. (2016). “*Análise estrutural de uma edificação histórica do Século XVIII*”. In: Congresso Brasileiro de Patologia das Construções, CBPAT 2016, Belém: Pará (Brasil), pp. 317-327.
- Verzola, S. N., Marchiori, F. F., Aragon, J. O. (2014). “*Proposta de lista de verificação para inspeção predial x urgência das manutenções*”. In: Encontro Nacional de Tecnologia do Ambiente Construído, XV ENTAC, Maceió: Alagoas (Brasil), pp. 1226-1235. <http://doi.org/10.17012/entac2014.300>

## Diagnostic of damage in a building of the early twentieth century in Havana. Case study

A. H. Oroza<sup>1\*</sup> , R. G. Hernández<sup>1</sup> 

\*Contact author: [ahernandez@proyectos.ohc.cu](mailto:ahernandez@proyectos.ohc.cu)

DOI: <http://dx.doi.org/10.21041/ra.v9i3.327>

Reception: 04/07/2018 | Acceptance: 22/05/2019 | Publication: 30/08/2019

### ABSTRACT

The objective of this work is to diagnostic the existing deterioration in a reinforced concrete building located in Old Havana, Cuba, built in 1906. Due to the years of exploitation and lack of maintenance, the property began to show detachment of concrete and cracks in almost all structural elements. To evaluate the service life, electrical resistivity studies of the concrete were carried out, chemical tests to quantify the levels of free chloride and sulphate, corrosion potential tests, section losses of the reinforcement bars, extractions of concrete specimens and visual analysis of the present damages. The results obtained showed that although the building presents an advanced deterioration, it can be rehabilitated, and it is possible to extend its service lifetime.

**Keywords:** diagnostic, corrosion, resistivity, service life, durability.

**Cite as:** Oroza, A. H., Hernández, R. G. (2019), “*Diagnostic of damage in a building of the early twentieth century in Havana. Case study*”, Revista ALCONPAT, 9 (3), pp. 335 – 349, DOI: <http://dx.doi.org/10.21041/ra.v9i3.327>

<sup>1</sup>Departamento de Diagnóstico y Levantamiento. UEB Restaura. Empresa de Restauración del Patrimonio. Oficina del Historiador. La Habana. Cuba.

### Legal Information

Revista ALCONPAT is a quarterly publication by the Asociación Latinoamericana de Control de Calidad, Patología y Recuperación de la Construcción, Internacional, A.C., Km. 6 antigua carretera a Progreso, Mérida, Yucatán, 97310, Tel.5219997385893, [alconpat.int@gmail.com](mailto:alconpat.int@gmail.com), Website: [www.alconpat.org](http://www.alconpat.org)

Responsible editor: Pedro Castro Borges, Ph.D. Reservation of rights for exclusive use No.04-2013-011717330300-203, and ISSN 2007-6835, both granted by the Instituto Nacional de Derecho de Autor. Responsible for the last update of this issue, Informatics Unit ALCONPAT, Elizabeth Sabido Maldonado, Km. 6, antigua carretera a Progreso, Mérida, Yucatán, C.P. 97310.

The views of the authors do not necessarily reflect the position of the editor.

The total or partial reproduction of the contents and images of the publication is strictly prohibited without the previous authorization of ALCONPAT Internacional A.C.

Any dispute, including the replies of the authors, will be published in the second issue of 2020 provided that the information is received before the closing of the first issue of 2019.

## **Diagnóstico de daños en una edificación de principios del siglo XX en La Habana. Caso de estudio**

### **RESUMEN**

El objetivo del trabajo es hacer un diagnóstico del deterioro de una edificación de hormigón armado ubicada en La Habana Vieja, Cuba, construida en el año 1906. Debido a los años de explotación y falta de mantenimiento, el inmueble presenta desprendimientos de hormigón y grietas en casi todos los elementos estructurales. Para evaluar la vida de servicio se realizaron estudios de resistividad aparente del hormigón, ensayos químicos para cuantificar los niveles de cloruro libre y sulfato, ensayos de potenciales, pérdidas de sección de las barras, extracciones de probetas de hormigón y análisis visual de las lesiones presentes. Los resultados obtenidos demostraron que, aunque el inmueble presenta un avanzado deterioro, este puede ser rehabilitado siendo posible extender su tiempo de vida de servicio.

**Palabras clave:** diagnóstico, corrosión, resistividad, vida de servicio, durabilidad.

## **Diagnóstico de danos em um edifício do início do século XX em Havana. Caso de estudo**

### **RESUMO**

O objetivo deste trabalho é diagnosticar a deterioração atual em um edifício de concreto armado localizado em Havana Velha, Cuba, construído em 1906. Devido aos anos de exploração e falta de manutenção, a propriedade começou a apresentar deslizamentos de concreto e rachaduras em quase todos os elementos estruturais. Para avaliar a vida útil, estudos de resistividade elétrica do concreto foram realizados, testes químicos para quantificar os níveis de cloreto e sulfato livres, ensaios potenciais, perdas de seção das barras de reforço, extrações de amostras de concreto e análise visual dos ferimentos presentes. Os resultados obtidos mostraram que, embora a propriedade apresente uma deterioração avançada, ela pode ser reabilitada e é possível estender sua vida útil.

**Palavras-chave:** diagnóstico, corrosão, resistividade, vida útil, durabilidade.

## **1. INTRODUCTION**

Since the use of reinforced concrete in the nineteenth century in the field of construction, this material has shown great performance and durability, even when exposed to different levels of corrosive aggressiveness (Castañeda et al., 2018; Howland, 2012; Vera et al., 2009). The first time a concrete plant was installed in Cuba was in June 1895, making Havana the first city in Latin America to manufacture Portland cement concrete (Toraya, 2001).

Despite this national technological advancement, many of the buildings erected with reinforced concrete showed poor performance and the need for recurrent repair actions. This was largely due to the lack of knowledge about the negative effect of the use of unwashed sea sand in the preparation of the concrete mix, inefficient urban planning, changes in use, modernizations and erroneous estimates of environmental effects. As a consequence, many buildings reached the service life or the residual life in the first 50 years of operation (Castro-Borges and Helene, 2007; Howland, 2012). The damages caused by the corrosion of reinforcing steels due to the entry of chlorides, sulfates or carbonation of concrete have been deeply studied by several researchers in different regions of the world (Andrade and Dal Molin, 2000; Castañeda et al., 2012; Chávez et al., 2013; Helene and Castro-Borges, 2009), where the significant loss of the bearing capacity of the affected structural element has been demonstrated.

Once the material detachments begin due to the corrosion stresses of the reinforcement bars and the loss of adhesion, the risks to the life of the property's residents also appear, and repair and maintenance costs are drastically increased (Castañeda and Rodríguez, 2014). The deepening of knowledge of these aspects is the key to the design and execution of durable structures, as well as the rational rehabilitation of them (Costa and Appleton, 2002).

This paper aims to discuss the results of the diagnosis made to a reinforced concrete building erected between 1900 and 1906 for the firm Casteleiro & Vizoso (Figure 1). Eclectic style and seven levels high, it was projected so that all levels had 4 m high struts, except for the ground floor with 6.3 m. The building was erected on a steel structure, covered in hydraulic concrete with foundations and reinforced concrete roof. The foundations consisted of support rafts calculated to support an average load of 3 Kg/cm<sup>2</sup>. The concrete prepared to form all the midlevel and stairs was dosed in proportion to 1 volume of cement, 3 of sand and 5 of gravel. The calculation of the accidental load of the floors was estimated for 366 Kg/m<sup>2</sup> and a safety factor of 4 was applied to the metal structure.

The property is located two kilometers away from the bay of Havana and less than 50 m from the Avenida del Puerto, in an urban-coastal environment. Since its construction and until today it has had different uses, the first being a commercial building for the firm's negotiations. After 1960 it became a post office, sometime after school and finally for two decades, real estate for renting apartments to foreign investors. To meet the needs of modern times, the hydraulic system was updated by installing a hot water line in each apartment, in the kitchen and bathroom areas.



Figure 1. Studied building

## 2. RESEARCH METHODOLOGY

### 2.1 Research procedure

For the selection of the diagnostic tests to be used, a two-stage research methodology was applied (Geocisa, 2002). The first one aims to carry out a detailed photographic survey of each of the visible lesions, and the second one of an experimental type, based on the analysis of the organoleptic results obtained and conclusions reached in the first stage (Oroza and Bouza, 2015).

The corrosion assessment was carried out according to the standard procedure described by (NACE SP0390, 2009) which sets out as fundamental objectives the definition of the nature of the environment in which the structure is located, the inspection of physical conditions, the establishment of the extension, the nature of the corrosion and the historical data of the present structure.

## 2.2 Corrosion potential ( $E_{corr}$ )

The method of evaluating corrosion by means of the half-cell potential is a technique that allows measuring the possible corrosive activity from the  $E_{corr}$  value obtained, however it does not offer information about the kinetics of the process or the resulting  $i_{corr}$  (Yu et al., 2017). When  $E_{corr} < 350$  mV vs. CSE, indicates that there is a probability greater than 90% of active corrosion on that the rebar. On the contrary, if the  $E_{corr} > -250$  mV vs. CSE, the probability is less than 10% (ASTM C876, 2009). The equipment used for the measurements was Proceq Canin<sup>+</sup>. For the application of the potential map on the slabs, work areas of 2x2 m were established and the fixed grid was 50x50 cm.

## 2.3 Measurement of apparent resistivity ( $\rho$ ) of concrete

To estimate the risk of corrosion presented by reinforcing steels, the Proceq Resipod equipment was used, which works based on the Wenner method (Gowers and Millard, 1999). This technique consists in evaluating the risk of corrosion presented by reinforcing bars depending on the level of saturation of the concrete pores. It is closely related to the quality of concrete (microstructure, water/cement ratio, porosity, curing, compressive strength), and therefore its durability (Andrade and D'Andrea, 2011; Azarsa and Gupta, 2017; D'Andréa and Andrade, 2009; Sanchez et al., 2017). The equipment works by applying a current on the surface of the material through the two external probes, measuring the resulting potential between the interior probes. The moisture content (water or water vapor) present in the pores of the concrete can transport the current between the probes, which makes it possible to obtain the resistivity of the material, as well as calculate the corrosion rate ( $i_{corr}$ ). Surface preparation and measurements were executed according to the manufacturer's instructions. To avoid interference in the reading due to the effect of the bars (Presuel Moreno et al., 2009), they were located and identified using a Proceq Profoscope rebar detector. For the evaluation of the  $i_{corr}$ , the equation proposed by RILEM was applied (Andrade and Alonso, 2004) where:

$$I_{corr} = \frac{3 \times 10^4}{\rho} \quad (1)$$

## 2.4 Extraction of concrete probes

In order to know the compressive strength ( $R_c$ ) of the concrete of the slabs, concrete probes were extracted at all levels. The equipment used was a Hilti DD-160E and a concrete press model Controls Automax 5 of 2000 KN was used. Five concrete probes were extracted per level for a total of 35.

## 2.5 Chemical assays of chloride and sulfate

Eight samples were extracted in the reinforced concrete slabs of each level, except for the ground floor, for a total of 48 samples. The method used for sample extractions was the indicated by ASTM C-1152 (C1152/C1152M-04, 2004). The chemical analysis procedure used was in accordance to (Oroza et al., 2016).

# 3. RESULTS

## 3.1 Diagnostic of reinforced concrete slabs

### 3.1.1 Results of the visual inspection

Slabs with loss of concrete coating, exposed steels and longitudinal cracks in the direction of reinforcement bars were identified (Figure 2a). The roof slab of the seventh level, in addition to

the previously indicated lesions, efflorescence and leaching spots were detected due to rainwater seepage from the roof.

On the ceiling of all the apartments it was observed that the slabs had been previously repaired. The material used for the restoration was a cement-based structural mortar. During the inspection it was possible to verify that in these previous repairs, the original slab thickness was never recovered. Also, no anticorrosive treatment was applied to the reinforcing steel bars and as a consequence, most of the applied restoration mortar already showed cracks, slapping and loosening in various areas (Figure 2b)

The most affected spaces were those destined for cooking and bathing due to the steam generated by to the use of hot water. The reinforcement steels in the slabs of these areas had severe atmospheric corrosion effects. Some of the existing bars were found fractured or with a very advanced localized section loss (Figure 2c), jeopardizing the structural stability of the element due to possible flexural failure. The measured carbonation depth ranged between 5-6 cm, with a calculated  $K_{CO_2}$  of 5.2 mm/year. The coating thicknesses (ec) were within 1-2 cm.

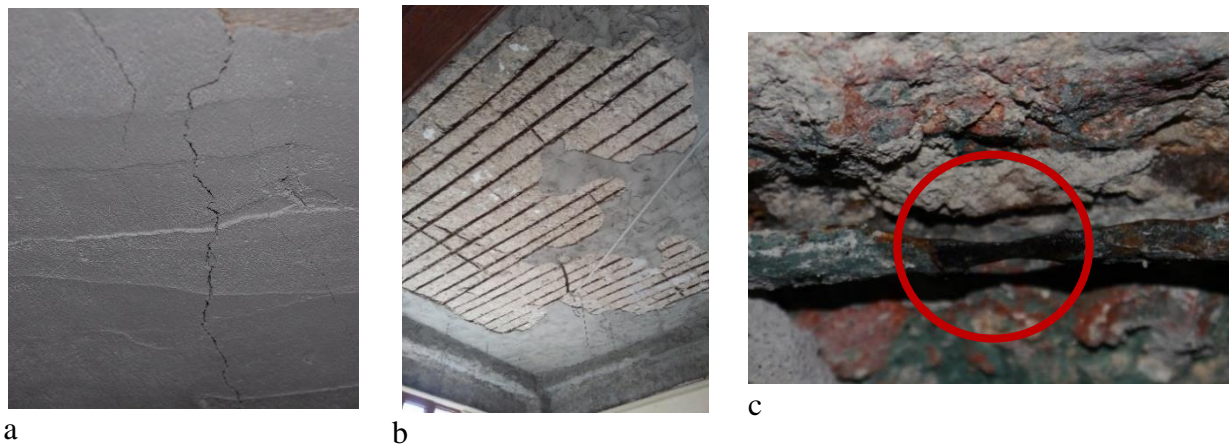


Figure 2. Damages identified in the roof slabs. a) Longitudinal cracks in the direction of the steel bars resulting from corrosion. b) Loss of repair mortar on the ceiling slabs in large areas of the living room. c) Localized corrosion at reinforcement bar

### 3.1.2 Results of the diagnostics assays

Based on the results of the visual assessment, two areas with different lesion manifestations were identified. One located in the first axes destined to hall and bedrooms, and another to the bottom with bathrooms and kitchens. The use of hot water in these areas increases the humidity of the environment and produces condensation of the steam on the surface of the concrete slabs. As a consequence of the increase of the water content in the concrete mass, the transport mechanisms and ionic mobility between the capillary pores are increased, accelerating the corrosion of the steel reinforcements of the slabs. To assess the risk of corrosion of the bars,  $E_{corr}$  measurements were made, potential maps were constructed and the  $\rho$  was measured in each zone separately. Figures 3 and 4 show the  $E_{corr}$  mapping obtained in the third level, as well as Figures 5 and 6 show the levels of  $\rho$  corresponding to the spaces prepared for  $E_{corr}$  measurements.

The results between both techniques demonstrate that there is a correspondence between the values of  $E_{corr}$  and  $\rho$ . In areas with hot water use, the diffusion of oxygen is increased, as well as its availability at the level of reinforcements. In reinforced concrete elements where there is no primary protection due to the advance of carbonation and the presence of chloride salts, the established corrosion rate ( $i_{corr}$ ) becomes the main parameter that determines the reason for deterioration of the structure. In the drier areas, more positive  $E_{corr}$  values are recorded with resistivity levels greater than 80 K $\Omega$ -cm.

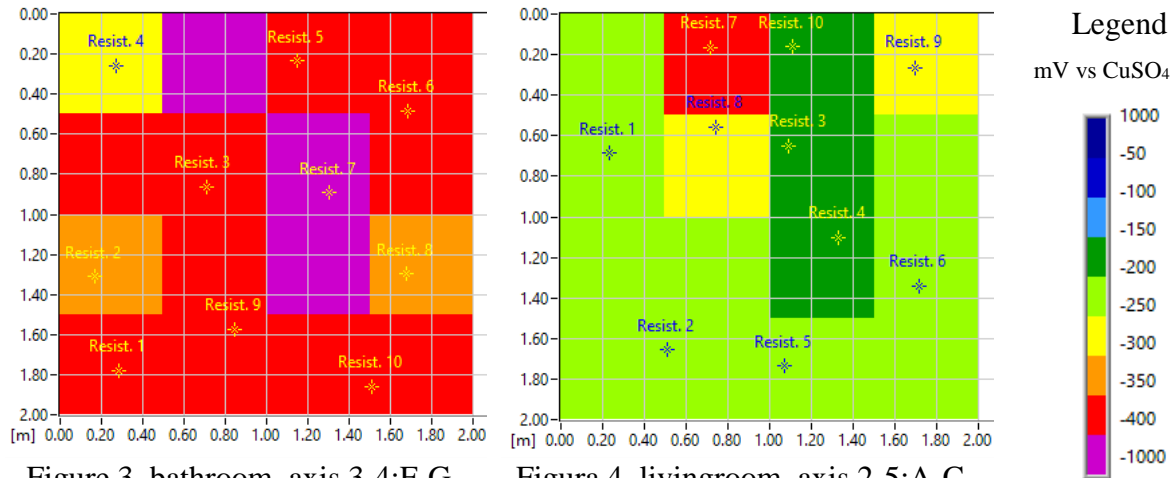


Figure 3. bathroom, axis 3-4:F-G

Figura 4. livingroom, axis 2-5:A-C

Figure 3 and figure 4. Mapping of Ecorr on the reinforced concrete slabs of the third level

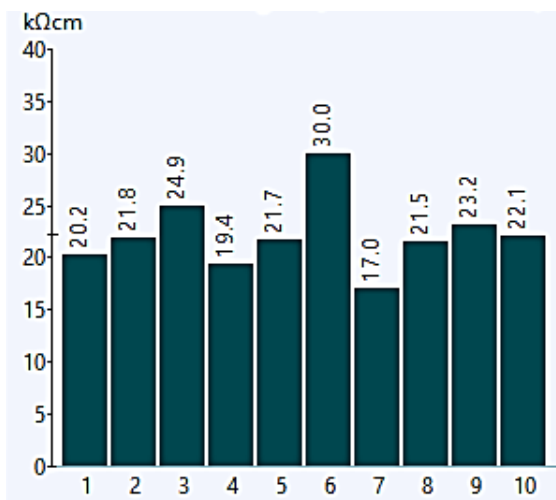


Figure 5. bathroom, axis 3-4:F-G

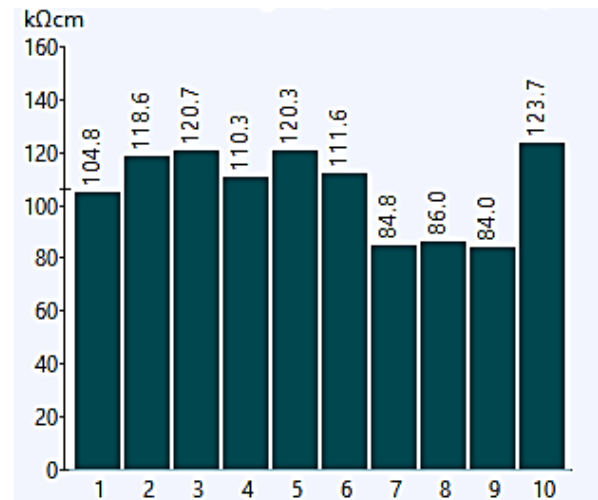


Figure 6. livingroom, axis 2-5:A-C

Figure 5 and figure 6. Results of the apparent resistivity on the reinforced concrete slabs of the third level

Table 1 shows the average results obtained where the resistivity,  $i_{corr}$  and chemical tests are correlated to the concrete samples, at each level of the property.

Table 1. Resume of the average results obtained by levels

Nivel	$\rho$ (K $\Omega$ -cm)	$i_{corr}$ ( $\mu$ A/cm <sup>2</sup> )	Cl <sup>-</sup> (% weight of concrete)	SO <sub>4</sub> (mg/L)
2do	17,0	1,76	0.11	<100
3ro	21,1	1,42	0.12	107
4to	36.7	0,82	0.14	<100
5to	30.1	1,00	0.11	118
6to	43.2	0,69	0.12	<100
7mo	12.6	2,38	0.13	<100

The lowest values of  $\rho$  were obtained in the 7th level roof slab as a result of rainwater leakage. This leads to the roof slab being exposed to wet-drying cycles, with leaching processes that decrease the alkalinity of the material and increase the porosity. This result in  $i_{\text{corr}}$  values greater than  $2 \mu\text{A}/\text{cm}^2$ . The chemical analysis of the concrete samples reflects a high concentration of  $\text{Cl}^-$  ions, which is in correspondence with the  $\rho$  and  $i_{\text{corr}}$  obtained at each level. The use of unwashed sea sand was a common practice in the buildings of the first half of the 20th century, where the negative effect of this anion on reinforcing steel was yet unknown. In relation to the  $\text{SO}_4$  concentrations obtained, these are not sufficient to promote a significant formation of late ettringite capable of causing cracks in the concrete (Howland, 2012).

To determine the section losses of the steel reinforcements in the slabs, measurements were made at all levels. The reinforcement was discovered by removing the concrete coating between 5-8 bars per work area. As an example, the values obtained in the 5th level are shown in Table 2. All the main steels found were of 16 mm square section (crooked squares) with a nominal area of  $256 \text{ mm}^2$  and spaced between 12-16 cm. The second layer of steels are of square section of 10 mm.

Table 2. Loss section values measured in the 5th level

Location	Bar No.	Measured side (mm)	Residual area ( $\text{mm}^2$ )	Nominal side (mm)	Nominal area ( $\text{mm}^2$ )	Section loss (%)
Living room	1	14,15	200,22	16,00	256,00	21,8
	2	15,04	226,20			11,6
	3	14,38	206,78			19,2
	4	15,28	233,48			8,8
	5	15,17	230,13			10,1
	6	15,1	228,01			10,9
	7	14,9	222,01			13,3
	8	14,67	215,21			15,9
Kitchen	1	1,73	2,99	16,00	256,00	98,8
	2	7,62	58,06			77,3
	3	2,61	6,81			97,3
	4	7,03	49,42			80,7
Bathroom	1	12,13	147,14	16,00	256,00	42,5
	2	12,4	153,76			39,9
	3	12,6	158,76			38,0
	4	11,9	141,61			44,7
	5	11,6	134,56			47,4

The greatest losses of steel were registered in the spaces destined for kitchen and bathroom. The result obtained is the decrease in section in some bars of up to 99% in the kitchen area, close to the location of the water heater. In the rest of the areas of the apartments, although the measurements of  $\rho$  and  $E_{\text{corr}}$  show a more “dry” material, the amount of steel losses ranges between 10-20%, being necessary a structural recalculation, to assess the feasibility in terms of replacement or splicing of new steel bars in their repair. The respective recalculation is not part of this work. However, the structure in question is rigidly framed, with columns made with I-sections where in specific cases there columns with an additional reinforcement of ordinary steel and other columns with complete reinforcement of ordinary steel are. This structure is covered with concrete, which protects the steel that forms them. The slabs are reinforced with ordinary steel bars and they support the loads of use, as well as their own weight and are transmitted to the structure provided, so it is inferred that the



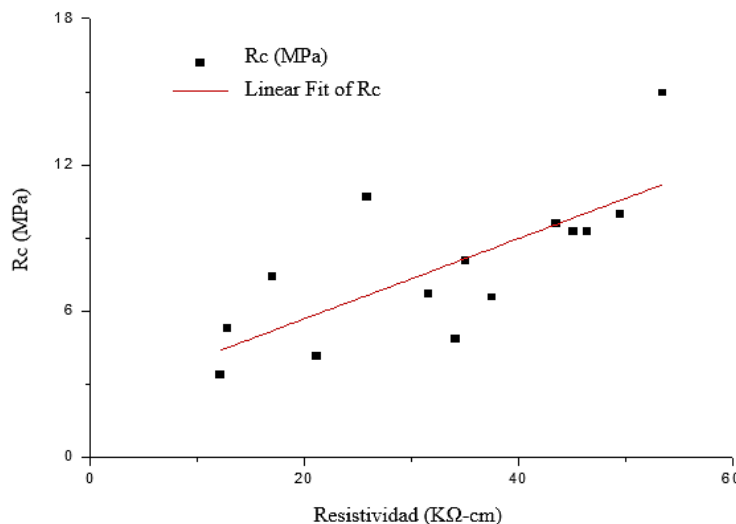
work is done by both elements. The results obtained proved that the current strength of the concrete is very affected.

In reinforced concrete structures, damages (cracks and fissures) caused by the phenomenon of atmospheric corrosion of reinforcing steel, chemical transformations caused by carbonation, chlorides and years of exposure, significantly influence the strength of concrete. Additionally, the charges that have acted during the lifetime of the property, which also cause a decrease in the  $R_c$  due to a phenomenon similar to relaxation, known as the Rüsçh effect, should be considered (Couto et al., 2015). The results of the concrete witnesses extracted in the slabs are shown in Table 3. The highest strengths obtained were at the 5th level with average values of 8.71 MPa. The standard (ACI:562M-16, 2016) establishes as an evaluation tool that the reinforced concrete elements constructed between 1900-1919 should have a compressive strength between 7-14 MPa. This criterion is still met in the building for almost all levels, except for the third and fourth which may be due to some of the causes previously discussed.

Table 3. Average values of  $R_c$  from the concrete samples extracted from the slabs.

Levels	$R_c$ (MPa)
2do	7.40
3ro	4.11
4to	6.91
5to	8.71
6to	8,03
7mo	7.13

Other authors (Ramezaniapour et al., 2011) demonstrated that for the same cement mix design, there is a linear relationship between compressive strength and  $\rho$  due to the chemical similarity of the pore solution. To assess the correspondence between the concrete permeability of reinforced concrete slabs and the  $\rho$  measured directly on the slabs, both results were correlated based on the strengths of the extracted probes. Figure 7 shows the graph obtained regarding the correlation between the  $R_c$  and  $\rho$  for the mid-level slabs of the studied property.



<b>Rc</b>	<b>Intercept</b>	Value 2,38046	Error 1,56301
	<b>Slope</b>	0,16484	0,04373
	<b>Statistics R-Square</b>	R <sup>2</sup> 0,50396	

Figure 7. Relationship obtained between  $R_c$  and  $\rho$  of the slabs

As a summary of the measurements in the slabs, the following table is presented:

Table 4. Summary of the results obtained by levels

Level	$\rho$ ( $K\Omega\text{-cm}$ )	$i_{\text{corr}}$ ( $\mu\text{A}/\text{cm}^2$ )	Cl <sup>-</sup> (%weight of concrete)	SO <sub>4</sub> (mg/L)	Rc (MPa)	Bars diameter (AP- main bar AT- second layer bar)	Section loss (%)	Main bar spacing (cm)
2nd	17,0	1,76	0.11	<100	7.40	AP- Ø16 AT- Ø10	42.9	12-16
3th	21,1	1,42	0.12	107	4.11		25.1	
4th	36.7	0,82	0.14	<100	6.91		27.7	
5th	30.1	1,00	0.11	118	8.71		45.1	
6th	43.2	0,69	0.12	<100	8.03		30.2	
7th	12.6	2,38	0.13	<100	7.13		65.1	

### 3.2 Damages present in columns

The visual inspection was carried out in the columns located in the last, penultimate and intermediate corridor. For the construction of the columns, I-sections and Ø16 steel bars were used interchangeably. It was identified that the vast majority of these had been previously intervened and still have a state of deterioration marked mainly by longitudinal cracks (Figures 8 and 9), as a consequence of the corrosion of the reinforcements. In general, both the I-sections and the bars that make up the columns showed a high level of corrosion with loss of section.



Figure 8



Figure 9

Figure 8 and figure 9. Current deterioration state of columns.

In the particular case of the second level, a high degree of corrosion with loss of section in the different reinforcements of the columns was widely observed. All the elements studied are made up of type I profiles. The coves were made in the columns indicated in Figure 10. Next, in table 5 the numbers of the coves made, and the measured wing thicknesses are presented.

Table 5. Specifications of the coves made in columns.

Coves	Axis	Location	Measurement (mm)
C1	1':H	edge of the flange	22,07
C2	3:D-E	edge of the flange	15,25
C3	6:H'	edge of the flange	20,40
C4	4:G	edge of the flange	22,90
C5	H: 1'-2	edge of the flange	5,49
C6	1':J	bar diameter	16,00
C7	4: E-F	edge of the flange	20,00
C8	6: D-E	edge of the flange	7,38

In the case of cove C1, the profile is accompanied by a ladder type reinforcement with 10 mm diameter bars that also presents corrosion. In the fifth level, when executing the coves (Figure 11) it was observed that the reinforcement of the column corresponding to the C6 is an ordinary steel reinforcement that still retains its metallic gray color. In coves C5, C7 and C8, corrosion was observed with loss of section in reinforcements consisting of type I-sections.

On the seventh level the reinforcement of the columns corresponding to the C9 and C10, is an ordinary steel armor that shows good state of preservation. In the case of C9 and C10, they have corrosion with very little section loss. In coves C11 and C12, the reinforcement is constituted by I-sections, with a high level of corrosion with loss of section. Table 6 shows the results obtained from the measured elements:

Table 6. Loss of section of reinforcement measured in columns

Coves	Axis	Location	Measurement (mm)	Section loss (%)
C9	1':H	bar diameter	16,00	0,0
C10	3:F	bar diameter	15,37	7,7
		bar diameter	9,36	12,4
C11	4:H'	edge of the flange	9,99	Undetermined
C12	4:C	edge of the flange	8,57	Undetermined

It should be noted that in the case of cove C9, as previously explained, the reinforcing steel has a metallic gray color, however, in the column there is a longitudinal crack that runs along its entire height. This lesion originated as a result of a flexo-compression effort that was not able to support the concrete due to its low mechanical strength and eccentricity of the reinforcement.

On the other hand, in the case of columns with ordinary steel bars, the loss of section was calculated from the nominal diameter of the bars that make up the reinforcement. For columns whose reinforcement is an I-section, it was not possible to calculate the percentage of loss because the nominal measurements are not known.

It is important to note that the concrete that makes up the columns presented very low mechanical resistance, because in the process of executing the coves it did not offer resistance to cutting, crumbling with great ease. To the extent that it descends in the levels, from the seventh to the second, there is evidence of a decrease in resistance, the latter being the most vulnerable to the cut.

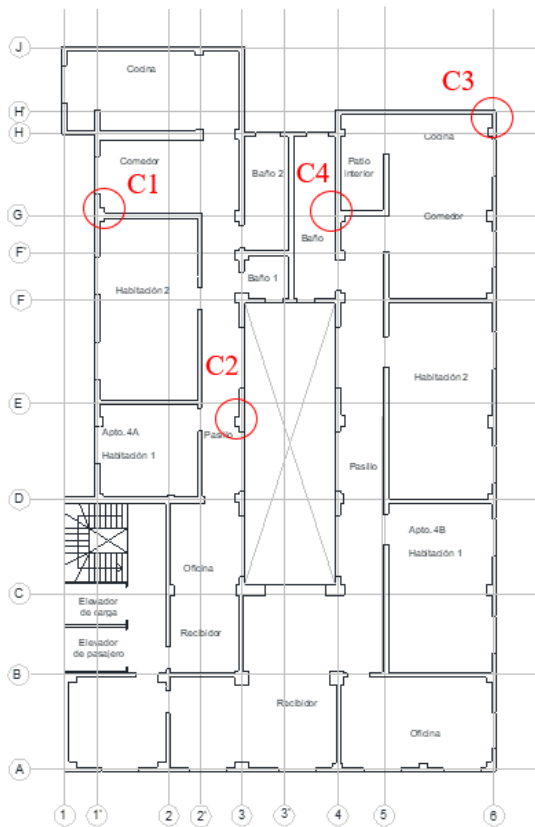


Figure 10. Cove's location at the 2nd level

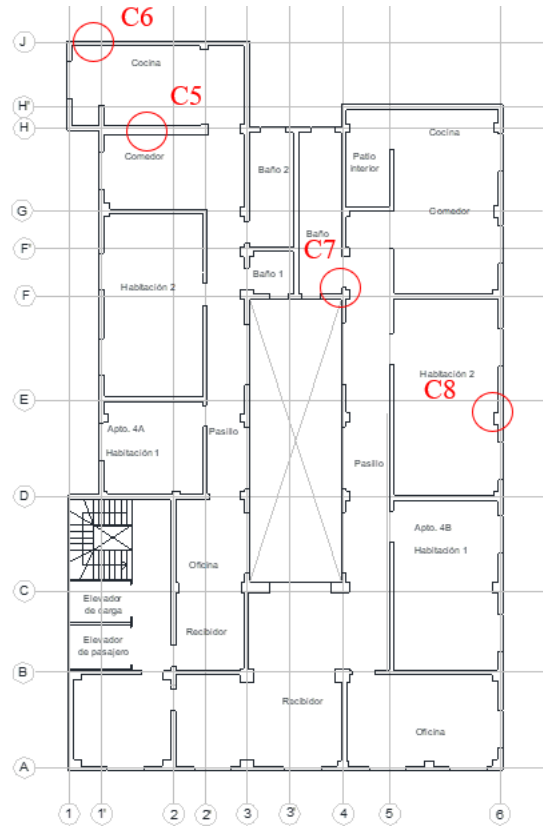


Figure 11. Cove's location at the 5th level

### 3.3 Evaluation of the service life

Figure 12 shows a graphical representation of the service life of a structure proposed by (Castro-Borges and Helene, 2007).

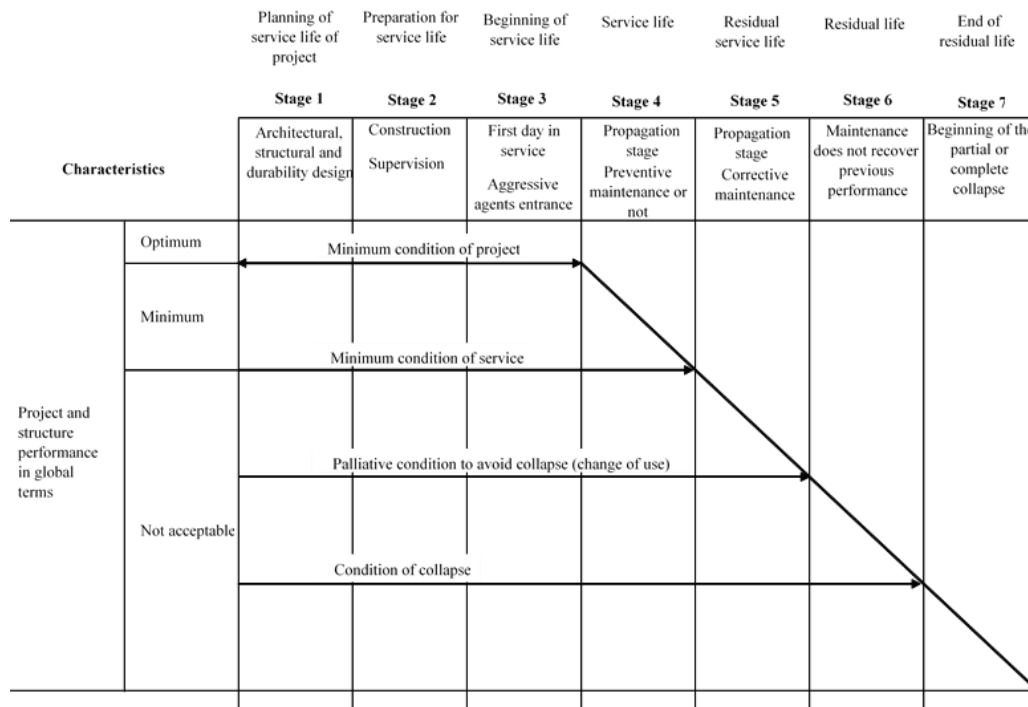


Figure 12. Conceptual model of the service life of a structure (Castro-Borges and Helene, 2018)

The results of the diagnosis of the slabs and columns show an advanced deterioration that extends to all levels of the building. The extent, magnitude and severity of the lesions show that they have been developing for a prolonged period of time, without the application of adequate maintenance in the time of service, on a scheduled or systematic basis. Based on all the previously presented analysis, it is to be considered in accordance with the proposed service life model, that the building is in the “state 5” in transit to its residual life, where the deteriorations will continue of no corrective measures for repair and maintenance are taken in time.

#### 4. CONCLUSIONS

The damages of a building of the early twentieth century in Havana were diagnosed. In general, damage caused primarily by corrosion of reinforcement steels was recorded throughout the structure. In the case of mid-level and roof slabs, the magnitude of the lesions present in the kitchens and bathrooms areas does not allow their rehabilitation through routine maintenance, because the bars have lost more than 90% of their section.

Considering that the structure is based on a rigidly frame system, these slabs can be demolished and replaced by new systems that lighten the loads of the columns and the structure in general, such as joist and vault, or other techniques. With respect to the columns, many of them are cracked as a result of the corrosion of the bars and I-sections, however the damages are not so significant and can be properly rehabilitated.

The current state of conservation of the property does not present acceptable safety conditions to continue with its exploitation, being necessary to perform various repair actions and the development of a corrective maintenance plan that allows extending the life of the structure.

#### 5. REFERENCES

- ACI:562M-16. (2016). *Code Requirements for Assessment, Repair, and Rehabilitation of Existing Concrete Structures and Commentary*.
- Andrade, C. and Alonso, C. (2004), *Test methods for on-site corrosion rate measurement of steel reinforcement in concrete by means of the polarization resistance method*. RILEM TC 154-EMC: Electrochemical Techniques for Measuring Metallic Corrosion.
- Andrade, C. and D’Andrea, R. (2011), *La resistividad eléctrica como parámetro de control del hormigón y de su durabilidad*. Revista ALCONPAT, 1(2): 93-101, DOI: <http://dx.doi.org/10.21041/ra.v1i2.8>
- Andrade, J. and Dal Molin, D. (2000), *A Case Study about Degradation of Reinforced Concrete Structures in a Marine Macro environment in Brazil*. NDT.net, <http://www.ndt.net/article/v05n02/andrade/andrade.htm>.
- ASTM C876 (2009). *Standard Test Method for Corrosion Potentials of Uncoated Reinforcing Steel in Concrete*.
- ASTM C1152/C1152M-04 (2004), *Standard Test Method for Acid-Soluble Chloride in Mortar and Concrete*.
- Azarsa, P. and Gupta, R. (2017), *Electrical resistivity of concrete for durability evaluation: a review*. Advances in Materials Science and Engineering, 2017. <https://doi.org/10.1155/2017/8453095>
- Castañeda, A., Howland, J. J., Corvo, F. and Pérez, T. (2013), *Corrosion of steel reinforced concrete in the tropical coastal atmosphere of Havana City, Cuba*. Quimica Nova, 36: 220-229.
- Castañeda, A. and Rodriguez, M. R. (2014), *Las pérdidas económicas causadas por el fenómeno de la corrosión atmosférica del acero de refuerzo embebido en el hormigón armado*. Revista CENIC Ciencias Químicas, 45: 52-59.

- Castañeda, A., Valdés, C. and Corvo, F. (2018), *Atmospheric corrosion study in a harbor located in a tropical island*. Materials and Corrosion, 1-16. <http://dx.doi.org/10.1002/maco.201810161>
- Castro-Borges, P. and Helene, P. (2007), *Service Life of Reinforced Concrete Structures: New Approach*. ECS Transactions, 9(13): 9-14. <http://dx.doi.org/10.1149/1.2721426>
- Castro-Borges, P., and Helene, P. (2018). *Un enfoque conceptual holístico para la vida de servicio del concreto: división en diferentes etapas de tiempo*. Revista ALCONPAT, 8(3), 280 - 287. doi: <http://dx.doi.org/10.21041/ra.v8i3.324>
- Chávez, E., Chab, R. C., Baz, M. S., Castro-Borges, P. and López, T. P. (2013), *Corrosion Process of Reinforced Concrete by Carbonation in a Natural Environment and an Accelerated Test Chamber*. International Journal of Electrochemical Science, 8: 9015-9029.
- Costa, A. and Appleton, J. (2002), *Case studies of concrete deterioration in a marine environment in Portugal*. Cement and Concrete Composite, 24: 169-179.
- Couto, D., Carvalho, M., Cintra, A. and Helene, P. (2015), *Concrete structures. Contribution to the safety assessment of existing structures*. IBRACON Structures and Materials Journal, 8(3): 365-389. <http://dx.doi.org/10.1590/S1983-41952015000300007>
- CYTED (2003), *Manual de rehabilitación de estructuras de hormigón, reparación, refuerzo y protección*, Red temática XV.B.
- D'Andréa, R. and Andrade, C. (2009), *Predicción de la vida útil de las estructuras mediante el uso de la resistividad como indicador de durabilidad*. In: IETCC (Editor), Aplicaciones prácticas de seguridad y durabilidad de estructuras de hormigón, Buenos Aires. Argentina, pp. 1-31.
- GEOCISA S. A. (2002), *Manual de evaluación de estructuras afectadas por corrosión de la armadura*. In: Geocisa (J. Rodríguez y J. Aragoncillo). Y por el Instituto de Ciencias de la Construcción "Eduardo Torroja" del CSIC (C. Andrade y D Iquierdo) dentro del proyecto de Innovación CONTECVET-IN 309021, pp. 152.
- Gowers, K. R. and Millard, S. G. (1999), *Measurement of Concrete Resistivity for Assessment of Corrosion Severity of Steel Using Wenner Technique*, American Concrete Institute.
- Helene, P. and Castro-Borges, P. (2009), *A novel method to predict concrete carbonation*. Concreto y Cemento. Investigación y Desarrollo, 1(1): 25-35.
- Howland, J. J. (2012), *"Desempeño por durabilidad de las estructuras de hormigón armado"*. Instituto Politécnico de La Habana, Departamento de Ingeniería Civil, 196 pp.
- NACE SP0390 (2009), *Maintenance and rehabilitation considerations for corrosion control of atmospherically exposed existing steel-reinforced concrete structures*.
- Oroza, A. H. and Bouza, D. G., (2015), *Influencia del micro-ambiente en el interior de una edificación sobre la corrosión del acero de refuerzo*. Revista CENIC Ciencias Químicas, 46: 45-55.
- Oroza, A. H., Pimentel, F. R., Parrab, E. P., León, L. M. D. and Amorós, Y. G. (2016), *Development of two analytical methods for determination of water-soluble chlorides and sulfates in the conservation of concrete heritage buildings*. Journal of Building Chemistry, 1: 61-68. <http://dx.doi.org/10.17461/j.buildchem.2016.201>
- Presuel Moreno, F., Liu, Y. and Paredes, M. (2009), *Understanding the Effect of Rebar Presence and/or Multilayered Concrete Resistivity on the Apparent Surface Resistivity Measured via the Four Point Wenner Method*. NACE International.
- Ramezaniapour, A. A., Pilvar, A., Mahdikhani, M. and Moodi, F. (2011), *Practical evaluation of relationship between concrete resistivity, water penetration, rapid chloride penetration and compressive strength*. Construction and Building Materials, 25: 2472-2479. <http://dx.doi.org/10.1016/j.conbuildmat.2010.11.069>
- Sanchez, J., Andrade, C., Torres, J., Rebolledo, N. and Fullera, J. (2017), *Determination of reinforced concrete durability with on-site resistivity measurements*. Materials and Structures, 50(41): 1-9. <http://dx.doi.org/10.1617/s11527-016-0884-7>

- Toraya, J. C. (2001), "*500 Años de construcciones en Cuba*". D.V. Chavín, Servicios Gráficos y Editoriales, S.L., Madrid, 557 pp.
- Vera, R., Villarroel, M., Delgado, D., Carvajal, A. M., De Barbieri, F. and Troconis, O. (2009), *Influencia de la Acción del Medio Ambiente en la Durabilidad del Concreto. Parte 2*. Revista de la Construcción, 8(1): 13-23.
- Yu, B., Liu, J. and Chen, Z. (2017), *Probabilistic evaluation method for corrosion risk of steel reinforcement based on concrete resistivity*. Construction and Building Materials, 138: 101–113. <http://dx.doi.org/10.1016/j.conbuildmat.2017.01.100>

## Inspection and evaluation of roofing systems: a case study

L.M.A. Santos<sup>1\*</sup> , L.F. Andrade<sup>2</sup> , C.H.A.F. Pereira<sup>1</sup> 

\*Contact author: [laramonalisa.arq@gmail.com](mailto:laramonalisa.arq@gmail.com)

DOI: <http://dx.doi.org/10.21041/ra.v9i3.413>

Reception: 30/04/2019 | Acceptance: 24/07/2019 | Publication: 30/08/2019

### ABSTRACT

The roof system of one of the buildings of the University of Brasília - DF is characterized and evaluated. The main existing anomalies in the roof systems are analyzed and the intervention priority is systematized, in order to correlate them with the corrective measures. The limiting factors for the inspection of the structures were accessibility as well as the lack of intervention projects. The results obtained reported that the main anomalies found in the systems are related to the lack of maintenance. The study also brings, as a contribution, indications and technical recommendations for the resolution of situations.

**Keywords:** roofing systems; roof inspection; roofing pathologies; anomalies.

**Cite as:** Santos, L.M.A., Andrade, L.F., Pereira, C.H.A.F. (2019), “*Inspection and evaluation of roofing systems: a case study*”, Revista ALCONPAT, 9 (3), pp. 350 – 363, DOI: <http://dx.doi.org/10.21041/ra.v9i3.413>

<sup>1</sup> Structures and Civil Construction Graduate Program - Universidade de Brasília, Brasília, Brazil.

<sup>2</sup> Civil Engineering Department – Universidade de Brasília, Brasília, Brazil.

### Legal Information

Revista ALCONPAT is a quarterly publication by the Asociación Latinoamericana de Control de Calidad, Patología y Recuperación de la Construcción, Internacional, A.C., Km. 6 antigua carretera a Progreso, Mérida, Yucatán, 97310, Tel.5219997385893, [alconpat.int@gmail.com](mailto:alconpat.int@gmail.com), Website: [www.alconpat.org](http://www.alconpat.org)

Responsible editor: Pedro Castro Borges, Ph.D. Reservation of rights for exclusive use No.04-2013-011717330300-203, and ISSN 2007-6835, both granted by the Instituto Nacional de Derecho de Autor. Responsible for the last update of this issue, Informatics Unit ALCONPAT, Elizabeth Sabido Maldonado, Km. 6, antigua carretera a Progreso, Mérida, Yucatán, C.P. 97310.

The views of the authors do not necessarily reflect the position of the editor.

The total or partial reproduction of the contents and images of the publication is strictly prohibited without the previous authorization of ALCONPAT Internacional A.C.

Any dispute, including the replies of the authors, will be published in the second issue of 2020 provided that the information is received before the closing of the first issue of 2020.



## **Inspeção e avaliação dos sistemas de cobertura: um estudo de caso**

### **RESUMO**

O sistema de cobertura de um dos prédios da Universidade de Brasília - DF é caracterizado e avaliado. As principais anomalias existentes nos sistemas de telhado são analisadas e a prioridade de intervenção é sistematizada, a fim de correlacioná-las com as medidas corretivas. Os fatores limitantes para a inspeção das estruturas foram a acessibilidade, bem como a falta de projetos de intervenção. Os resultados obtidos relataram que as principais anomalias encontradas nos sistemas estão relacionadas à falta de manutenção. O estudo traz também, como contribuição, indicações e recomendações técnicas para a resolução de situações.

**Palavras-chave:** sistemas de cobertura; inspeção de coberturas; patologias de coberturas; anomalias.

## **Presentación y Evaluación de los Sistemas de Cubiertas: Estudio de Caso**

### **RESUMEN**

Se caracteriza y evalúa el sistema de cubierta de una de las edificaciones de la Universidad de Brasília - DF. Se analizan las principales anomalías existentes en los sistemas de cubiertas y se sistematiza la prioridad de intervención, con el propósito de correlacionarlas con las medidas correctivas. Los factores limitantes para la inspección de las estructuras fueron la accesibilidad así como la falta de proyectos de intervención. Los resultados obtenidos reportaron que las principales anomalías encontradas en los sistemas están relacionadas con la falta de mantenimiento. El estudio trae además, como contribución, indicaciones y recomendaciones técnicas para la resolución de las situaciones.

**Palabras clave:** sistemas de cubierta; inspección de cubiertas; patologías de cubiertas; anomalías.

## **1. INTRODUCTION**

The building roofing systems are most affected by atmospheric factors, including the constitution of their parts, designed to resist and define a barrier to these actions. Thus, it is coherent to define that the pathological manifestations resulting from these processes are the most common in roofs. Studies and analysis by Rocha (2008) in Portugal, Azeredo (1997), Ambrozewicz (2015, p.203), and ASTM D1079 (2016, p.8) also describe this element as an integral part of environmental control systems, i.e. responsible for thermal and hygroscopic adaptations for environments.

The main function of a roof is to insulate a building to create a sealed and protected indoor environment through a barrier against external agents such as temperature, humidity, rain, wind, and noise. There are also indirect actions, such as incorrect design or poor execution, which are currently the most prominent threats to roof performance (Rato, 2003). For Lopes (2010), these actions, despite the emergence of new and better waterproofing materials, are closely related to the lack of training of installation workers and are a frequent source of problems, such as water leakage to the underlying layers.

According to Ferraz et al. (2016), rehabilitation and maintenance activities are key factors for building sustainability. It is essential to develop a correct interpretation of defects, supported by diagnostic means, with the aim of significantly increasing quality standards of buildings and their useful life. Therefore, the identification, classification, and planning of all stages of the inspection processes are indispensable for diagnosis.

The use of flat roofs has gained strength in the construction sector, and there is few information on the correlation among the most common types of anomalies, the most likely causes, applicable diagnostic tests, and the most appropriate rehabilitation techniques. Inspections aim to identify the causes and prerequisites of each anomaly, allowing, during the use phase, greater ability to detect the need for inspection reducing, thus, the risk of unexpected anomalies (Conceição et al., 2019). The justification that led to the research was that the problems in the roofing systems constitute one of the most elementary components of a building, since those systems are characterized, along with the vertical sealing, as the main barrier against bad weathering forces. Thus, a study of the current state of the roofing system is carried out, by defining the existing anomalies and solving problems present in these elements, to ensure the proper functioning of the buildings and, consequently, their activities.

## 2. OBJECTIVE

The main objective is to characterize the current state and to evaluate the roofing systems in specific areas, with the description and classification of anomalies for a building located at the University of Brasilia in the Federal District, Brazil.

## 3. LITERATURE REVIEW

As any other system of a building, the roofing system is also likely to suffer from the pathological manifestations that arise during the building useful life. That compromises the building required level of performance. Infiltration may occur when the roofing system does not have its waterproofing done correctly or when, for some reason, it stopped acting and made room for water percolation (Frazão, 2015).

For these reasons and similar to other materials and building elements, they should be the target of a systematic routine inspection process in which a diagnosis is developed (Walter et al., 2005).

The scientific community has devoted more attention to the vast field of building inspection, diagnosis, maintenance, and rehabilitation, including systems to support the inspection of anomalies (Ferraz, G.T. et al., 2016). In order to provide good results, this inspection and diagnostic process must be planned and standardized. Therefore, in addition to a schedule, the inspector must follow a set of standard procedures for reliable results.

Data analysis by Conceição et al., (2019), from an inspection in 105 flat roofs, determined that the use of the inspection, diagnosis, and rehabilitation system increases the objectivity and effectiveness of an inspection. The author also emphasizes that inspection sheets are necessary for proper characterization of anomalies, besides using one of the recommended methods during inspections, which is the use of mapping. The mapping determines the incidence of each anomaly, as well as its severity, allowing the creation of its repair project and other building elements.

Conceição et al. (2017) proposes a system with classification techniques to diagnose anomalies in associated flat roofs through a correlation matrix, stating that during inspection, all anomalies must be identified and classified. The author characterizes diagnostic techniques and describes that visual aspects were the only criterion used to classify anomalies.

### 3.1 Building inspection regulations

The standard ABNT NBR 5674: 2012 Building Maintenance - Requirements for the maintenance management system is available in Brazil, with the purpose of assisting professionals in the field. General procedures establish by the standard must be implemented. Therefore, maintenance procedures on building elements are necessary during their useful life; prior to this phase, inspections for the assessment and correct prescription of maintenance should be carried out.

ABNT NBR 5674: 2012 defines that inspections should be carried out under a defined guide for the systems of a building, taking into account the degradation pattern and expected manifestations for each element, as well as user complaints.

The Brazilian Institute of Engineering Assessment and Expertise (IBAPE) is another reference institution in Brazil, regarding inspection and evaluation of engineering structures, which is also a National Building Inspection Standard. IBAPE defines building inspection procedures with a view to what is required by ABNT NBR 5674: 2012 and ABNT NBR 15575-1: 2013, regarding building maintenance and general performance requirements of housing buildings, respectively. This normative specifies that the inspections performed must be classified into three levels of complexity. Then, all systems and elements to be inspected are listed, through a systematic and logical sequence that takes into consideration the relationship among the components.

After that, the inspection is carried out. It is the phase of in situ obtaining the real conditions, anomalies, and failures that may occur in pathological manifestations. In addition, the priorities for treatment of anomalies and failures are established based on defined methodologies appropriate to the elements. Such priorities will determine the need for total or partial possible interdictions in the structure (Ibape, 2012).

Technical recommendations for problems should also be defined, i.e., how anomalies and failures can be corrected to recover the minimum performance demands and requirements that the structure must attend.

## 4. METHODS

In order to achieve the objectives of this paper, the method used for the inspection will be as required by the IBAPE National Inspection Standard, which defines the building inspection procedures, and by the ABNT NBR 5674: 2012 standard, under the inspection and definition of building criteria for intervention priorities proposed by Morgado (2012), in Portugal. The method is applied in a case study: one of the buildings of the University of Brasilia (UnB).

### 4.1 Definição do critério para prioridade de intervenção

In a simplified way, in the methodology presented by Morgado (2012), with regard to inspection, the elements of a covering under the perspective of maintenance and inspection, called Maintenance Source Elements (MSE), are identified so that pathologies and causes can be registered and systematized, and intervention may be proposed. The MSEs can be found in Tables 4.1 and 4.2 in Morgado (2012).

Each MSE is associated with the possible anomalies for each element; Tables 4.3; 4.4; 4.5 and 4.6 were used for the demonstrations present in Morgado (2012).

Each of the identified anomalies has 4 criteria to characterize it. The environment aggressiveness, the extent of the anomaly (relative to the MSE area), the MSE degradation level, and the severity of the anomaly. Each of these criteria has a score for each degradation level and a multiplier factor for it (Table 1).

Table 1. Proposed MSE anomaly classification for building roofs (Adapted from Morgado, 2012).

Criterion	Level	Description	Score	Multiplier Factor
Environment Aggressiveness	Reduced	Rural Area	1	1
	Medium	Urban Area	2	
	High	Coastal Zone	3	
Anomaly Extent	Reduced	≤ 20%	1	2
	Medium	21 a 70%	2	
	High	≥ 70%	3	
MSE Degradation Level	0	No relevant degradation	1	3
	1	Superficial Degradation	2	
	2	Moderate Degradation	3	
	3	Sharped degradation	4	
Anomaly Severity	A	Negative influence on aesthetic aspect	1	4
	B	Considerable increase in charges for subsequent maintenance actions	2	
	C	Decreased element durability	3	
	D	Impaired building functionality	4	
	E	Danger to user safety	5	

The indicator for the scaling of intervention priorities developed by Morgado (2012) is calculated taking into account the weight of each anomaly with the worst-case scenario. Each manifestation has its weight calculated (Equation 1) according to the values presented in Table 2.

$$P_{\text{anomaly}} = 1 \times A + 2 \times E + 3 \times D + 4 \times S \quad (1)$$

Where:

$P_{\text{anomaly}}$  = weight of each anomaly in analysis;

A = Environment Aggressiveness;

E = Anomaly Extent;

D = Degradation Level;

S = Anomaly Severity.

To determine the intervention priority indicator, the  $P_{\text{anomaly}}$  is weighted with the worst-case value according to Equation 2.

$$P_{\text{intervention}} = \frac{P_{\text{anomaly}}}{\text{Max}(P_{\text{anomaly}})} \times 100 = \frac{1xA + 2xE + 3xD + 4xS}{41} \times 100 \quad (2)$$

Where:

$P_{\text{intervention}}$  = indicator for the scaling of intervention priority;

$P_{\text{anomaly}}$  = weight of each anomaly under analysis;

By applying these calculations, it is possible to determine various values and percentages and, thus, rank the urgency of corrective maintenance actions.

Finally, after possession of the  $P_{weighted}$ , it must be corrected to a percentage index indicating the speed required to correct the problem, called  $P_{intervention}$ , where the intervals are present in Table 2, with a scale divided into four levels.

Table 2. Proposed priority classification of intervention in roofing MSEs. (Adapted de MORGADO, 2012)

Level	Intervention Priority	$P_{intervention}$
1	Actions without urgency	$24\% \leq P_{intervention} \leq 40\%$
2	Medium term actions (2 to 5 years) needing to be monitored	$40\% \leq P_{intervention} \leq 60\%$
3	Short term actions (1-2 years)	$61\% \leq P_{intervention} \leq 80\%$
4	Immediate Priority Actions (6 months)	$P_{intervention} \geq 80\%$

#### 4.2 Case Study Description, Structure and Sealing

For this paper it is proposed the inspection and evaluation of the roofing systems of Building C - Department of Civil and Environmental Engineering (ENC) of the College of Technology (FT) of the University of Brasilia (UnB) that has a total area of 17,500m<sup>2</sup> located in Darcy Ribeiro University Campus, North Wing (Asa Norte), on the banks of the L3 road. The identification of Building C, in FT, is highlighted in red in Figure 1:

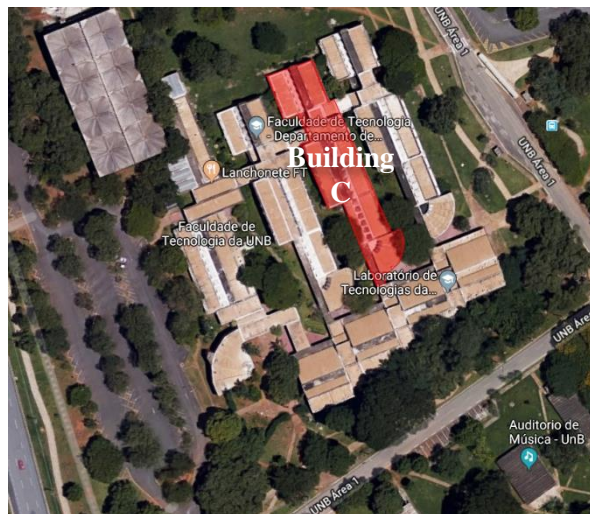


Figure 1. Building C highlighted, at College of Technology, University of Brasilia; - 15.763476° Latitude and -47.872465° Longitude (Adapted from Google Maps, 2019).

These structures are in a medium complexity building, with specific facilities, such as high-power electricity and pumps, not having a fully defined maintenance plan. It is a level 2 inspection, according to the IBAPE standard.

The design of Building C roofing system consists of waterproof ribbed reinforced concrete slabs in areas where there is no roof. In regions where this element is present, ribbed slabs protected by roof tiles are used.

The shed modules for zenith lighting, the thresholds, and the auditorium entrance hall roofing are in the waterproofed slab areas. The roofs are responsible for transporting rainwater to rectangular perimeter gutters, built in the concrete itself and waterproofed.

From consultations carried out at the Campus City Hall (PRC) and department, it was found that there isn't a maintenance plan for Building C. The IBAPE standard establishes that consulting users and those responsible for information and complaints about the surroundings should be a preliminary inspection phase.

The problems listed by users served as a guide for defining focus areas in surveys. From this, ENC students and staff showed great discomfort related to the roofing system during the rainy season in the Federal District, Brazil, from September to April.

### 4.3 Survey

It was used a sheet with general information of the building proposed by Morgado (2012), identified in his paper in Annex A.4.1. During the visit, a second sheet was used, with the characterization of the roofing according to the typology (flat or sloping roof according to Morgado (2012)) and maintenance source elements.

#### 4.3.1 Description of survey focus areas

Based on the projects provided by the Oscar Niemeyer Planning Center (CEPLAN), the current Building C roofing system is highlighted in Figure 2, the Department of Civil and Environmental Engineering - ENC, and the focus areas represented.



Figure 2. Highlight in the site plan for the built area (Adapted from CEPLAN, 1973).

Complaints focus on infiltrations in the ENC classroom corridor (focus area 1, 2, and 3) shown in Figure 3 in the CT 25/15 classroom (focus area 4) with water spilling into the wall, which, according to users, comes from the connection between the beam supporting the roof and the masonry, figure 4. Finally, in Building C - ENC, there are complaints about the Auditorium of the Department of Civil and Environmental Engineering, in the center of the room, also near beams supporting the roof (focus area 5) Figure 5.

#### 4.3.2 Identified issues

The evaluated roofing system of Building C - Department of Civil and Environmental Engineering is generally dirty, with fungal formations, especially near the trees that line the building. Such manifestations originate from factors of the dynamic nature of the envelope. It should be noted that

the causes and manifestations presented are only probable hypotheses and determined from the visual tactile inspection that occurred during the on-site visit.

*a) Focus Areas 1, 2 and 3*

In the internal visit held on 10/30/2018 in the morning, after a rainy season, leaks were observed in the ceiling of the classroom corridor (area 1, 2 and 3), even after rain had ceased, as shown in Figure 3 and Figure 4. The gutters are multiple and are spread over a wide area of the ceiling.



Figure 3. Gutters in the ceiling of the hallway with mold, humidity stains, and peeling of the coating.



Figure 4. Deformed roof with water accumulation and debris.

*b) Focus Area 4*

Another major problem related by complaints in Building C is the infiltrations in the CT 25/15 (area 4) classroom of the Department of Civil and Environmental Engineering. The images provided were taken on the morning of 10/29/2018 after a rainy night. Through Figure 5 and Figure 6, it is observed that the infiltrations have water flow originating from the beam-masonry transition inside the room, and at the end of the survey zone, near the focus zone 4, there is a structural joint without signs of sealant to prevent water passage.



Figure 5. Water dripping on the beam-masonry interface



Figure 6. Structural joint without sealant

*c) Focus Area 5*

Another place with expressed discomfort related to loss of roof tightness performance was the ENC auditorium (area 5). The internal inspection was performed on 11/13/2018 for the verification of

reported infiltrations. In the auditorium ceiling, it is possible to see marks of freshly dried gutters near a beam, including the puddles on the floor. Figure 7 and Figure 8 below illustrate such spots that indicate the water path and the formation of puddles.



Figure 7. Spotlight humidity on ceiling



Figure 8. Water puddles formed by dripping

#### *d) Areas that influence system performance*

These areas were discovered from the on-site external inspection. Such areas influence the system performance by the appearance of anomalies.

The sheds and the covering of the auditorium entrance hall have no roof: they are made of solid waterproofed slabs, figure 9, figure 10 and figure 11. The sheds present in the roof are from a structural point of view. The performance of the roofing system elements is in good condition, with only fouled surface dirt.

In the support structure, there are no signs that indicate waterproofing after the removal of the roof. Shrinkage cracks were found mostly throughout the slab and, in some places, there are small concrete disintegration. The joints along the length of the slab, as well as between the slabs and rails, are very degraded, with no sign of filler elements and sealant, with water accumulation.



Figure 9, Figure 10 and Figure 11. Support structure without roof/skylight.

## 5. RESULTS AND DISCUSSION

### 5.1 Intervention priority for anomalies in Building C

Table 3 is presented with the anomalies in Building C, indicating the acronym and description, according to Tables 4.3, Table 4.4, Table 4.5 and Table 4.6 presented in the methodology described by Morgado (2012).



Table 3. Identification of Building C anomalies for intervention priority (Author, 2018).

MFE	Anomaly Acronym	Description
Coating (Roof)	A-R 1	Sharp deformation
	A-R 4	Surface dirt and debris accumulation
	A-R 7	Parasitic vegetation development
Support structure (bare slab only)	A-E 2	Cracking
	A-E 3	Surface dirt and debris accumulation
	A-E 4	Biological degradation by fungal effect, xylophagous insects
	A-E 5	Disintegration
	A-E 10	Humidity
Skylights	A-V 1	Surface dirt and debris accumulation
Drainage system (gutters and drop pipes)	A-D 1	Surface dirt and debris accumulation
	A-D 2	Water stains
	A-D 3	Water accumulation
	A-D 5	Gutter fractures or cracks
	A-D 9	No drains

Table 4 and Table 5 present the procedure for the definition of anomaly intervention priority.

Table 4. procedure for the definition of intervention priority in Building C (Author, 2018).

MSE	Anomaly	Environment Aggressiveness		Extent	
		Level	Score	Level	Score
Coating (Roof)	A-R 1	Medium	2	Medium	2
	A-R 4	Medium	2	High	3
	A-R 7	Medium	2	Medium	2
Support structure (bare slab only)	A-E 2	Medium	2	Medium	2
	A-E 3	Medium	2	High	3
	A-E 4	Medium	2	Reduced	1
	A-E 5	Medium	2	Reduced	1
	A-E 10	Medium	2	High	3
Skylights	A-V 1	Medium	2	High	3
Drainage system (gutters and drop pipes)	A-D 1	Medium	2	High	3
	A-D 2	Medium	2	High	3
	A-D 3	Medium	2	Medium	2
	A-D 5	Medium	2	Reduced	1
	A-D 9	Medium	2	High	3

Table 5. Continuation (Author, 2018).

Anomaly	Degradation Level		Severity of anomalies		P <sub>weighted</sub>	P <sub>intervention</sub>	Intervention Priority
	Level	Score	Level	Score			Level
A-R 1	2	3	B	2	23	56%	2
A-R 4	1	2	A	1	18	44%	2
A-R 7	1	2	B	2	20	49%	2
A-E 2	2	3	D	4	31	76%	3
A-E 3	1	2	B	2	22	54%	2
A-E 4	1	2	B	2	18	44%	2
A-E 5	2	3	D	4	29	71%	3
A-E 10	1	2	A	1	18	44%	2
A-V 1	0	1	A	1	15	37%	1
A-D 1	2	3	D	4	33	80%	4
A-D 2	1	2	A	1	18	44%	2
A-D 3	2	3	B	2	23	56%	2
A-D 5	2	3	D	4	29	71%	3
A-D 9	2	3	D	4	33	80%	4

It is noteworthy that the criteria of environment aggressiveness, extent, degradation level, and severity of anomalies were attributed to each of the anomalies as observed in the external survey. It is clear from the priority levels found that most problems are at level 2, i.e., without immediate repair, with medium term actions (2 to 5 years), but with constant monitoring of the situation to verify the evolution of anomalies. The skylight, for example, is in good condition and with intervention level 1, i.e., it has no urgent actions.

Consideration should be given to manifestations with level 3 intervention priority criteria, such as cracks in the slab, small cracks in the concrete, and cracks in the gutters and their joints, which require short-term actions within 1 to 2 years at most.

The accumulation of debris and dirt in the gutters certainly demand immediate action, within a period of up to 6 months and is classified in level 4, indicating a need for immediate cleaning, which is verified by the huge amount of leaves in the elements, obstructing the passage of water.

User-verified infiltrations are probably related to joints and cracks in the supporting slab. In the intervention priority criterion, such manifestations were level 3, which requires short-term actions, not level 4 – immediate, as one might think –, which is explained by the fact that these problems do not reach large parts and are not so severe, without representing serious risks to users. Even so, it is recommended that these problems be analyzed and solved by maintenance teams as soon as possible, as they may represent major inconvenience to the academic community, if indeed they are the sources of infiltration.

In addition to the tables and solutions presented, anomalies that obtained higher levels of intervention priority were also analyzed. Figure 12 shows the relative contribution of each anomaly to the total sample of anomalies detected in the flat cover and allows to measure the intervention priority level of the anomalies through the MSE.

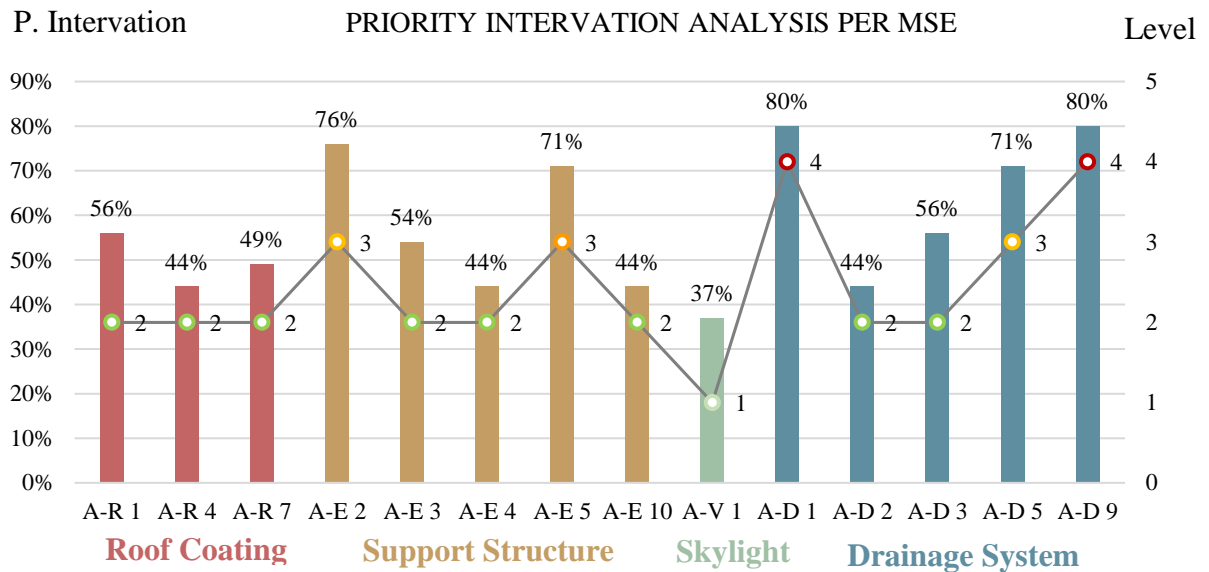


Figure 12. Intervention priority per MSE (Author, 2018).

It is noticed that the Support Structure and Drainage System obtained the highest Intervention Priority Levels. This means that for levels 3 and 4 found in the MSE resulted in an Intervention Priority in the range of 70% to 80%.

Figure 13 shows the distribution of intervention priority levels. It is worth noting that level 3 requires short-term actions, and concentrate a total of 27% of the anomalies, while for level 4, with an immediate priority action, a total of 20% was obtained. Thus, the priority intervention given at level 3 and level 4 corresponds to almost 50% of the total observed anomalies, concentrated in cracks, disintegration, surface dirt, and no-drain points.

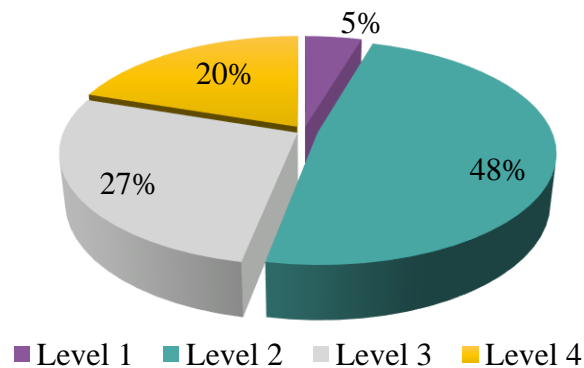


Figure 13. Distribution of priority intervention levels for detected anomalies (Author, 2018).

Morgado (2012) presents the application of the method in flat roofs in Portugal, and obtained results with higher levels of anomalies for level 2 and level 3, justifying with two aspects: (1) the fact that the most common anomalies were aesthetic anomalies and loss of adhesion and fixation (superficial dirt, accumulation of debris, and parasitic vegetation/biological colonization, differences in shade and small spots of corrosion), and that, (2) when anomalies are not aesthetic, they may be punctual, with reduced levels of degradation and severity. The aesthetic anomalies are associated with the visual aspect and not the safety or cracking of the maintenance source elements, which gives them lower values in the multicriteria analysis in question.

This fact is presented in the study by Poça (2015), where the main anomalies detected through inspections are related to debris accumulation, biological colonization, and surface detrition, accounting for over 50% of anomalies. Results found by Conceição et al. (2019) also show that the main anomalies detected were due to lack of maintenance resulting in the development of debris accumulation and biological growth.

An interesting approach to highlight is the development of integrated building management systems. Authors such as Ferraz, G.T. et al., (2005), provide a framework of methods for assessing pathology in non-structural elements of buildings. The authors point out that, in the rehabilitation of buildings, most occurrences of anomalies in non-structural elements can be solved systemically. Using inspection data and cross-checking information in an integrated building management system, an inspector can diagnose the anomaly and define the best repair technique, thereby extending the expected life of the building.

Therefore, when anomalies that may affect the proper functioning of a roofing occur, diagnostic techniques should be used to locate the source of the anomaly in order to assess the most appropriate intervention technique and possible repairs to the structure.

## 6. CONCLUSIONS

The inspection and evaluation of the roofing systems in this case study (Department of Civil and Environmental Engineering, University of Brasilia) were able to characterize, evaluate, and satisfactorily identify one of the main anomalies affecting building users and related to this part of the building: the infiltrations.

These roofing systems had part of the support slab with disintegrations, cracks, and no signs of waterproofing (which should have been done after the arbitrary removal of part of the roof), in addition to very dirty rails, debris accumulation, and movement joints with no sealant filling, impairing the tightness of the elements.

Situations that require rapid resolution in Building C are concentrated in: dirt and debris build-up in the rails as well as installation of protective elements at the inlet of the fall pipes; resolutions for joints and cracks in the bare slab are also recommended. Ventilation and lighting systems (sheds) are in good condition.

Infiltration is very uncomfortable during rainy seasons, directly impacting academic life, whether in the comfort of classrooms, in interdictions in locomotion spaces, or during research and assays procedures.

It was noticed that the anomalies obtained by the intervention priority criterion, level 3 and level 4, should be immediately solved, and these actions, when summed, represent values of approximately 50% of the total anomalies observed. The Supporting Structure and Drainage System presented the highest indices and the largest number of anomalies, being, thus, the main focuses of the intervention.

Maintenance management responsible for buildings needs to adapt to ABNT NBR 5674: 2012, in order to implement a periodic maintenance plan that can identify problems and solve them more effectively, avoiding recurring inconveniences to the academic community. As anomalies are quickly identified, in early stages, they are usually less expensive to repair.

It is noteworthy that the focus of this paper was not the explanation of causes and attribution of responsibilities, which would configure an expertise. The objective was only the characterization of the current state of the roofing systems that were under inspection, focusing on identifying problems and proposing technical recommendation.

## 7. REFERENCES

- Ambrozewicz, P. H L (2015), “*Construção de edifícios do início ao fim da obra*”. 1ª Edição. São Paulo: PINI.
- ASTM D1079 - American Society for Testing and Materials (2016). *Standard Terminology Relating to Roofing and Waterproofing*. Pensilvânia.
- ABNT - Associação Brasileira de Normas Técnicas (2012). *NBR 5674: Manutenção de edificações – Requisitos para o Sistema de gestão de manutenção*. Rio de Janeiro.
- Azeredo, H. A (1997), “*O Edifício até sua Cobertura*”. 2ª Edição. São Paulo: Edgard Blücher.
- Conceição, J. et al (2019), *Data Analysis of Inspection, Diagnosis, and Rehabilitation of Flat Roofs*. Journal Of Performance Of Constructed Facilities, [s.l.], v. 33, n. 1, p.04018100-0401810014, American Society of Civil Engineers (ASCE). [http://dx.doi.org/10.1061/\(asce\)cf.1943-5509.0001252](http://dx.doi.org/10.1061/(asce)cf.1943-5509.0001252).
- Conceição, J. et al (2017), *Inspection, Diagnosis, and Rehabilitation System for Flat Roofs*. Journal Of Performance Of Constructed Facilities, [s.l.], v. 31, n. 6, p.137-148. American Society of Civil Engineers (ASCE). [http://dx.doi.org/10.1061/\(asce\)cf.1943-5509.0001094](http://dx.doi.org/10.1061/(asce)cf.1943-5509.0001094).
- Ferraz, G. T. et al (2016), *State-of-the-Art Review of Building Inspection Systems*. Journal Of Performance Of Constructed Facilities, [s.l.], v. 30, n. 5, p.04016018-04010188. American Society of Civil Engineers (ASCE). [http://dx.doi.org/10.1061/\(asce\)cf.1943-5509.0000839](http://dx.doi.org/10.1061/(asce)cf.1943-5509.0000839).
- Ferraz, G. T. et al (2015), *Integrated management systems building technique: inspection and repair of non-structural elements*. Revista Alconpat, [s.l.], v. 5, n. 2, p.137-148. Revista ALCONPAT. <http://dx.doi.org/10.21041/ra.v5i2.83>.
- Frazão, Julie Cristie Faria (2015), “*Patologias Relacionadas às Coberturas: Estudo de caso em edificações unifamiliares de interesse social na cidade de Campo Mourão*” - PR. 2015. 53 f. TCC (Graduação) - Curso de Engenharia Civil, Departamento Acadêmico de Construção Civil, Universidade Tecnológica Federal do Paraná, Campo Mourão.
- Google Maps. Disponível em: <<http://mapas.google.com>> Acesso em 12 jan. 2019.
- IBAPE - Instituto Brasileiro de Avaliações e Perícias de Engenharia (2012). *Norma de inspeção predial nacional*. São Paulo.
- Lopes, G. (2010). “*Waterproofing coatings on flat roofs*”, LNEC, Lisbon, Portugal.
- Morgado, João Nicolau Pires Lopes Veiga (2012), “*Plano de inspeção e manutenção de coberturas de edifícios correntes*”. 267f. Dissertação de Mestrado – Universidade Técnica de Lisboa, Lisboa.
- NBR 15575-1 (2013). *Edificações habitacionais – Desempenho Parte 1: Requisitos gerais*. Rio de Janeiro.
- Poça, Bruno João Fernandes (2015), “*Recuperação do edificado afeto ao Exército. Tecnologia e reabilitação de coberturas em terraço*”. 2015. 129 f. Dissertação (Mestrado) - Curso de Engenharia Militar, Técnico Lisboa, Portugal.
- Walter, Ana; BRITO, Jorge de; LOPES, Jorge Grandão (2005), *Current flat roof bituminous membranes waterproofing systems – inspection, diagnosis and pathology classification*. Construction And Building Materials, [s.l.], v. 19, n. 3, p.233-242. Elsevier BV. <http://dx.doi.org/10.1016/j.conbuildmat.2004.05.008>.
- Rato, Vasco; BRITO, Jorge de (2003), *Exigências Funcionais das Coberturas Inclinadas*. Disponível em: <<https://www.researchgate.net/publication/282251188>>. Acesso em: 29 abr. 2019.
- Rocha, Pedro Tomé da (2008), “*Anomalias em coberturas de terraço e inclinadas*”. 179f. Dissertação de Mestrado – Universidade Técnica de Lisboa, Lisboa.